UNIVERSIDADE DE LISBOA

Faculdade de Farmácia

Biopharmaceutical formulations for dry powder inhalers

Diana Alexandra Santana da Silva Fernandes

Orientador(es): Doutora Maria Luísa Teixeira de Azevedo Rodrigues Corvo
Doutora Eunice Margarida Santos Costa

Tese especialmente elaborada para obtenção do grau de Doutor no ramo de conhecimento de Farmácia, especialidade de Tecnologia Farmacêutica

2021

UNIVERSIDADE DE LISBOA

Faculdade de Farmácia

Biopharmaceutical formulations for dry powder inhalers

Diana Alexandra Santana da Silva Fernandes

Orientador(es): Doutora Maria Luísa Teixeira de Azevedo Rodrigues Corvo
Doutora Eunice Margarida Santos Costa

Tese especialmente elaborada para obtenção do grau de Doutor no ramo de Farmácia e especialidade em Tecnologia Farmacêutica

Júri:

Presidente: Doutor António José Leitão das Neves Almeida, Professor Catedrático e Presidente do Conselho Científico da Faculdade de Farmácia da Universidade de Lisboa

Vogais:

- Doutora Ana Isabel Nobre Martins Aguiar-Ricardo, Professora Catedrática, Faculdade de Ciências e Tecnologia da Universidade Nova de Lisboa;
- Doutora Ana Margarida Moutinho Grenha, Professora Auxiliar, Faculdade de Ciências e Tecnologia da Universidade do Algarve;
- Doutora Helena Maria Cabral Marques, Professora Associada com Agregação, Faculdade de Farmácia da Universidade de Lisboa;
- Doutora Ana Paula Costa dos Santos Peralta Leandro, Professora Auxiliar com Agregação, Faculdade de Farmácia da Universidade de Lisboa;
- Doutora Maria Luísa Teixeira de Azevedo Rodrigues Corvo, Investigadora Auxiliar Faculdade de Farmácia da Universidade de Lisboa, Orientadora;

2021

The research presented in this thesis was conducted at BioNanoSciences – Drug Delivery and Immunotherapy (BioNanoSci), Research Institute of Medicines (iMed.Ulisboa), Faculty of Pharmacy, University of Lisbon, Portugal, under the scientific supervision of Maria Luísa Teixeira de Azevedo Rodrigues Corvo, PhD, and at the Inhalation and Advanced Drug Delivery, Drug Product Development Research and Development Group at Hovione Farmaciência SA, Loures under the scientific supervision of Eunice Margarida Santos Costa, PhD. The research was funded by Fundação para a Ciência e a Tecnologia, IP (FCT project UID/DTP/04138/2020) and Hovione Farmaciência SA.

AGRADECIMENTOS

Recebo um email reencaminhado aos mestrandos recém-formados com duas propostas de Doutoramento. Ao ler, lembrei-me da minha Avó Vita que tinha asma e do meu Avô Genaro que tinha Doença Pulmonar Obstrutiva Crónica do pulmão (DPOC). Candidatei-me. Uma destas propostas de Doutoramento, felizmente, acabou por se tornar na minha.

Embora presentes de outro modo, começo por agradecer aos meus Avós, com saudade, a motivação que me fez bater à porta deste projeto, e de o desenvolver ao longo destes anos.

Foi uma caminhada dinâmica, sempre povoada de pessoas a quem estarei para sempre grata por a terem enriquecido e tornado mais ligeira.

Professora Luísa (Corvo), agradeço-lhe o apoio firme, sempre prático e eficaz, assertivo e de poucas palavras, dentro e fora do laboratório, de perto ou à distância.

Professora Paula (Leandro), agradeço-lhe a disponibilidade para, com toda a paciência, ensinar, explicar, ouvir, aconselhar, debater resultados e tantas outras questões de forma incansável e rigorosa.

Eunice (Costa), agradeço-te os compromissos, as reflexões, os desafios e oportunidades que me permitiram expandir a minha forma de ver e, assim, de ser.

Estimo-as como Pessoas, Líderes e Cientistas que são e agradeço a motivação com que me cobriram em alturas mais desafiantes.

Sofia (Rodrigues), agradeço-te o apoio a este projeto através das diversas oportunidades de formação que desbloqueaste.

João (Henriques), tenho a agradecer-te a paciência e o cuidado. Também a lembrança do que é equilíbrio na vida e essencial no trabalho.

Grupos BioNanoSciences, Metabolomics & Genetics, Faculdade de Farmácia da Universidade de Lisboa: Margarida (Silva)**, Nago** (da Silva)**, Jacinta** (Pinho)**, Hanna** (Pereira)**, Daniela** (Peixoto)**, Raquel** (Lopes) **e Catarina** (Miranda) agradeço a boa

companhia no Lumiar ou na FFUL, o apoio técnico sempre que algum ensaio experimental extra era necessário e os *after-lab* com as caipirinhas de maracujá.

Grupo Drug Product Development e amigos, Hovione: **António** (Eloy), **Norberto** (Pardelha), **André** (Gaspar), **Carlos** (Calixto), **Djemila** (Monteiro), **Miguel** (Cardoso), **Pedro** (Machado) e **Ricardo** (Dias), obrigada pela formação, auxílio e tempo no laboratório que permitiram conduzir esta investigação partindo, sempre, de uma base robusta e sem fugas.

Ameessa (Tulcidas), **Ana** (Prates), **André** (Cruz), **Artur** (Saramago), **Beatriz** (Fernandes), **Cláudia** (Moura), **Clara** (Sá Couto), **Helena** (Mota), **Inês** (Matos), **Inês** (Ramos), **João** (Pires), **João** (Vicente), **João** (Sá), **Nuno** (Branco), **Patrícia** (Henriques), **Patrícia** (Nunes), **Paulo** (Francisco), **Paulo** (Lino), **Pedro** (Monteiro), **Ricardo** (Sousa), **Rita** (Laires), **Rui** (Churro), **Rui** (Cruz), **Slavomira** (Doktorovova), **Susana** (Farinha) e **Tiago** (Porfírio), obrigada pelas refeições com ou sem lotes a decorrer, por me ensinarem a jogar à sueca, pelas partilhas sobre os mais diversos e exóticos assuntos, pelas pausas à porta do Edifício S, pelo pedestrianismo no campus do Lumiar, pelos *quizzs* e pelo *team building online* em tempos de pandemia.

Equipa AT06: **Joana** (Cristóvão), **Faissen** (Lordeiro), **Mafalda** (Rodrigues), **Sofia** (Riboira), **Nuno** (Águas), assim como antigos e novos membros, agradeço-vos o apoio e compreensão, durante esta altura. Que bom foi pertencer a esta equipa de alto rendimento que muito me fez evoluir.

Cristina (Abascal Ruiz) e **Mariana** (Fernandes), obrigada por me desafiarem e me permitirem crescer noutro papel enquanto vossa orientadora/co-orientadora. Aprendi muito convosco, também sobre mim mesma.

Cohort Hovione Academy: **Beatriz** (Anacleto), **Beatriz** (Fernandes), **Bruno** (Capiche Ladeira), **Cláudia** (Moura), **Iris** (Duarte), **Lúcia** (Volta e Sousa), **Maria Inês** (Lopes), **Marianna** (Katz), **Marina** (Ciriani), **Nuno** (Enes), **Susana** (Gomez) e **Tiago** (Porfírio) fico muito feliz que nos tenhamos cruzado naquele que foi um grupo tão heterogéneo a nível de vivências. As melhores recordações que levo deste Doutoramento incluem-vos a todos. Desde os *sprints* que fazíamos para não falhar os pequenos-almoços no antigo bar de Sete

Casas, a companhia que fazíamos uns aos outros, dentro e fora do laboratório durante longas horas, as conversas filosóficas de almoço a jantar, os concertos a que íamos de quando em vez, as viagens ao Gerês, a Sever do Vouga e a Edimburgo, felizmente, entre tantas outras. Um valente obrigada.

Grupo Alumni de Engenharia Biológica IST: **Leonor** (Guedes da Silva), **Elsa** (Requeixa), **Pedro** (Grilo), **Rita** (Almeida), **Gonçalo** (Forjaz), **Cátia** (Carias) e **Daniel** (Guedelha) obrigada por esta *community of practice* tão valiosa que me trouxe alento e inspiração em momentos mais exigentes, dando-me oportunidade de descobrir outras valências que se revelaram tão úteis a este projeto.

Korf Lx Project, Clube de Corfebol: A toda a equipa, agradeço-vos o companheirismo, os bons momentos, os valores e também um lema de vida: All the way up.

Flo (Ka Ying Florence Lip), **Ivette** (Parera Olm), **Lucia** (Cabas Rodriguez), **Txema** (Jose Gutierrez) and **Muli** (Murali Kumar), grateful for this Wageningen family that still managed to be around. Thank you, regardless of where in this world we happen to be.

Filipa (Faustino), **Joana** (Cadete), **Lisanne** (Esthuis), **João** (Rosa) e **Catarina** (Gonçalves), obrigada por despertarem e desenvolverem em mim um olhar alternativo sobre um mesmo assunto tornando-me consciente da minha voz, fosse através de orientação, do yoga, do Vedanta, do Teatro ou da vossa amizade.

Carla (Cardeira), **Patrícia** (Barroca) e **Silvia** (Sousa), grata ao Teatro por nos ter unido. Agradeço o vosso apoio consistente durante esta última fase da jornada.

Iris Dani (Iris Duarte), agradeço-te a amizade a que também deste voz nos áudios de apoio e que tão importantes foram para *plot twists* de humor, ao aproximar-me da meta.

Mommy Lu (Lúcia Volta e Sousa), obrigada por me encorajares sempre de forma franca e fraterna e de me lembrares do que às vezes me esqueço de ser capaz.

Mari (Marina Ciriani), obrigada pelo teu apoio, energia leve e solar de carioca que me faz esboçar um sorriso em qualquer dia do ano.

Btrizinha (Beatriz Anacleto) de San Joã, obrigada pela amizade cuidada, por ouvires, pela força que sempre me dás e pelo “Louvado!”.

B (Beatriz Fernandes), meu lado B da vida, do vinil. Companheiras desde o começo ao fim e *beyond*. Agradeço-te esta bela viagem e que assim continue, de feição.

Babi (Marianna Katz), so many emotions. Thank you, my dear friend, for all your blind support, honest and practical feedback with the wittiest sense of humour. For the countless especial moments, we shared during this journey, sitting in front or next to each other. Also, for the Hungarian words, paramount to know my way around in Hungary and, of course, in life.

Cláudia (Cordeiro), minha querida amiga, 10 anos de uma sólida amizade que brotou de um aceso arrufo num grupo de laboratório no IST. Obrigada, Anja, por todo o amparo e por me trazeres a casa quando il faut.

Mariana (Romão), do infantário, das esmolas da Disney Paris à porta dos Piratas das Caraíbas até às traseiras da Aula Magna, mesmo que online. Agradeço-te a presença, minha querida amiga, mesmo que moldada às circunstâncias de cada uma.

Ben-Hur (Bernardo Figueiredo), obrigada pelo dim-sum, chacuti, couve pak-choi, salada de bulgur e néctar Muralha sempre acompanhados de conselhos bem temperados de sabedoria. Seguimos, agora a norte.

Família, **Tia Ivone**, **Tia Sónia**, **Tio Almiro**, **(A)Vó (A)Lice**, **João**, **Mãe** e **Pai**, agradeço-vos toda a gestão dos meus estados emocionais, todo o amor e paciência com que sempre o fizeram e fazem.

Filipa, Irmã, meu par, obrigada por me ouvires, compreenderes e motivares. Feliz, por voltarmos a ser vizinhas.

Rasmus, jolly one, grateful to partner with you. Thank you for supporting me in these last yards with love, light, and lightness.

Por fim, um agradecimento é também devido à Faculdade de Farmácia da Universidade de Lisboa e Hovione pelo financiamento deste projeto.

ABSTRACT

Significant advances on recombinant DNA technology and the repurpose of chemical synthesis, coupled with the rising capacity of large-scale production of biologics, are paving the way towards the cumulative increase of macromolecules in the pharmaceutical industry pipeline able to treat respiratory diseases, such as Asthma and Chronic Obstructive Pulmonary disease (COPD) and systemic diseases like Diabetes. More specifically, inhaled formulations are increasingly attractive given the large and highly vascularized lungs surface for absorption, the rapid onset of the drug action, reducing the required drug load and minimizing adverse side effects, whilst improving patient compliance over injectables. However, the efficient delivery of biopharmaceuticals to the lungs still presents a significant challenge: the generation of a stable aerosol with adequate aerodynamic properties while preserving the integrity of the biologic. Hitherto, there have been aqueous solutions of biopharmaceutical formulations approved for human use with nebulizers. Nonetheless, these fail to provide the desired efficiency and patient compliance. Hence, the present research aims to tackle these bottlenecks by developing dry powder inhaler biopharmaceutical formulations, using spray drying as an alternative particle engineering technology. An integrated methodology is thus proposed, combining the analytical techniques of high-throughput Isothermal Denaturation Fluorimetry and Andersen Cascade Impaction, to expedite the formulation of protein-based biologics, using therapeutic enzymes as the subject of study.

Keywords: Spray drying, Dry powder inhalers, Biologics, high-throughput Isothermal Denaturation Fluorimetry, Andersen Cascade Impaction

RESUMO

O avanço significativo da tecnologia recombinante de DNA e o *repurposing* da síntese química, aliados à crescente capacidade de produção em larga escala de produtos biológicos, tem repercutido num efeito cumulativo do número de macromoléculas presentes no pipeline da indústria farmacêutica capazes de tratar doenças respiratórias, como a Asma e a Doença Pulmonar Obstrutiva Crónica (DPOC) mas também doenças sistémicas, como a Diabetes. Em particular, as formulações inaláveis são cada vez mais atraentes para o tratamento destas doenças, dada a área de superfície do pulmão altamente vascularizada, a ação imediata do fármaco *in locu*, reduzindo a sua quantidade terapêutica necessária e minimizando possíveis efeitos secundários adversos. Adicionalmente, a via de administração pulmonar reúne uma maior adesão do paciente na medida em que permite um tratamento menos invasivo do que o da via injetável. Contudo, a administração eficiente de produtos biológicos por esta via ainda enfrenta um desafio: a produção de um aerossol estável com propriedades aerodinâmicas que permitam que se deposite no pulmão, preservando, em simultâneo, a conformação do biológico. Até ao momento já foram aprovadas formulações aquosas de produtos biológicos para uso humano com nebulizadores. No entanto, estas formulações não têm conseguido proporcionar a eficácia desejada assim como a adesão do paciente. A presente investigação teve assim como objetivo o desenvolvimento de formulações para inaladores de pó seco de produtos biológicos em pó, em alternativa às aquosas, utilizando secagem por atomização como a principal tecnologia de engenharia de partículas. Uma metodologia integrada é proposta, fazendo o uso combinatório das técnicas analíticas de *high-throuput Isothermal Denaturation Fluorimetry* e de *Andersen Cascade Impaction,* para conduzir a formulação de biológicos de base proteica, utilizando enzimas terapêuticas como objeto de estudo.

Palavras-chave: Secagem por atomização, inaladores de pó seco, biológicos, *High-throughput Isothermal Denaturation Fluorimetry, Andersen Cascade Impaction*

TABLE OF CONTENTS

LIST OF FIGURES

LIST OF TABLES

LIST OF ABBREVIATIONS

2F	Two-fluid
ACI	Andersen cascade impaction
Alt_SD	Alternative spray drying set-up
API	Active pharmaceutical ingredient
aPSD	Aerodynamic particle size distribution
ASO	Anti-sense oligonucleotide
BP	Biopharmaceutical
Cat	Catalase
CFC	Chlorofluorocarbons
COPD	Chronic obstructive pulmonary disease
C_{solids}	Solids concentration
Cu,Zn-SOD	Copper, Zinc superoxide dismutase
DNA	deoxyribonucleic acid
DP	Dry powder
DPI	Dry powder inhaler
Dv10	Size below which there is 10% of the volume of the sample
Dv50	Size below which there is 50% of the volume of the sample
Dv90	Size below which there is 90% of the volume of the sample
EAR	Enzymatic activity retention
EMA	European Medicines Agency
FD	Freeze drying
FDA	U.S. Food and Drug Administration
F_{drying}	Drying flow rate
F_{feed}	Feed flow rate
FIB-SEM	Focused ion beam-scanning electron microscopy
FPF	Fine particle fraction

GI	Gastrointestinal
GOx	Glucose oxidase
GSD	Geometric standard deviation
HPMC	Hydroxypropyl methylcellulose
HT	High-throughput
HT-DSF	High-throughput differential scanning fluorimetry
HT-ITDF	High-throughput isothermal denaturation fluorimetry
IBC	International Biotech Center
MMAD	Mass median aerodynamic diameter
OI	Oral inhalation
pDNA	Plasmid deoxyribonucleic acid
PLGA	Poly(lactic-co-glycolic acid)
PLS	Partial least squares
pMDIs	Pressurized meter dose inhalers
PS	Particle size
RNA	Ribonucleic acid
Rot_{atom}	Atomization flow rate
$scCO_2$	Supercritical carbon dioxide
SCF	Supercritical fluid
SD	Spray drying
SEM	Scanning electron microscopy
T_g	Glass transition temperature
T_m	Melting temperature
T_{out}	Outlet temperature
US	Ultrasonic

CHAPTER 1

Introduction

1.1 MOTIVATION

The development of recombinant DNA technology and the repurpose of chemical synthesis coupled with the rising capacity of large-scale production of therapeutic biologics are paving the way towards the cumulative increase of macromolecules in the pharmaceutical pipeline. In particular, dry powder (DP) dosage forms of orally inhaled biologics have been gaining momentum given their extended shelf-life when compared to liquid dosage forms, more prone to undergo liquid-mediated chemical reaction, aggregation or contamination. In addition, the pulmonary delivery route has its own advantages. The lungs display a large and highly vascularized surface area for drug absorption, thus allowing for local and systemic treatment while avoiding first pass metabolism. This ultimately translates into a rapid onset of the drug action, reducing the required drug load and minimizing adverse side effects, whilst improving patient compliance of DP dosage forms over injectables.

Lyophilization or Freeze Drying (FD), has been the gold standard drying technology to produce biopharmaceutical DP dosage forms. However, FD is a lengthy process, low energy efficient entailing a high cost of purchase and maintenance. Spray Drying (SD), on the other hand, emerges as an alternative candidate to FD, given its lower cycle time, higher solids throughputs, flexible and easier to scale. In addition, SD allows for an increased control over DP key features like particle size (PS), conversely to FD, that render it a suitable particle engineering technology to produce DP dosage forms intended for different routes of administration: oral (PS~100 μm to enable a direct compressible dosage form), nasal (PS> 10 μm) and pulmonary (1 μm < PS < 5 μm). Despite previous work concerning spray dried biologics has already been described in the literature, an integrated formulation methodology for the choice of the better operational parameters to achieve biopharmaceutical stabilization and powder adequate aerodynamic and solid-state properties is still not available. Considering the great number of possible excipients and range of process parameters, this integrated methodology would be advantageous to shorten sample requirements and development time, lowering the optimization costs while reducing the gap between production to market and

patient. This PhD thesis aims to tackle this, choosing as study subject the class of therapeutic enzymes.

1.2 RESEARCH AIMS AND OBJECTIVES

This project aims at producing dry powder inhaler formulations featuring therapeutic enzymes as active pharmaceutical ingredient (API), while preserving their conformational stability. Hence, the proposed research can be further translated into the following objectives:

i) Evaluation and optimization of biopharmaceutical dry powder-based formulations by developing and resorting to dry powder and biological advanced analytical tools.

ii) Establishment of an integrated methodology for biopharmaceutical formulation and spray drying process development.

1.3 THESIS OUTLINE

This thesis is structured into 7 main chapters.

Chapter 1 conveyed the framework and research focus of this thesis. Motivation, aims, and objectives were shared, herein.

Chapter 2 presents the state-of-the-art supporting this work. The oral inhalation outlook of therapeutic enzymes is overviewed and the scope for dry powder inhaler (DPI) formulation of these molecules introduced. The challenges associated to DPI formulation of therapeutic enzymes are thus showcased, from a patient and drug product development standpoints. Patient-wise, the anatomy and physiology of the lungs are reviewed, and the underlying mechanisms of particle deposition, absorption and clearance explored. Drug product development-wise, considerations on the biopharmaceutical nature of the API, formulation, particle engineering technologies employed in carrier-free DPI formulation, with especial emphasis on the spray drying, DPI delivery platforms and analytical characterization are presented.

Chapter 3 describes a proof-of-concept study to investigate the effect of spray drying (SD) process parameters on a fixed DPI formulation featuring a model enzyme, Cu-Zn Superoxide Dismutase (Cu,Zn-SOD), as API. Powder properties (particle morphology and aerodynamic performance), enzyme activity and protein conformational stability of the enzyme are assessed.

Chapter 4 features the work developed to render the spray drying process milder and more efficient to produce dry powder inhaler formulations intended for biopharmaceutical delivery. Nozzle type, length and surface area of the drying chamber and implementation of a mesh as gas distributor were studied as potential sources of improvement in reducing the shear stress to which the biopharmaceutical may be exposed during atomization on the spray drying process, as well as limiting the loss of powder to the drying chamber walls.

In Chapter 5, focus is given to high-throughput formulation screening, namely, Differential Scanning Fluorimetry (HT-DSF) to downsize the formulation conditions leading to an increased biopharmaceutical stabilization prior to SD. Three enzymes of increasing molecular mass and structural complexity belonging to the oxidoreductase class and often implicated in oxidative stress, were selected as models: Cu,Zn-SOD (previously tested in Chapter 3), Glucose Oxidase (GOx) and Catalase (Cat). Their conformational stability was analysed under a range of different conditions comprising pH, NaCl concentration, single and combo excipients (non-reducing sugars, hydrophobic and hydrophilic amino acids), using HT-DSF.

Based on the outcomes of the previous chapters, Chapter 6 presents an integrated methodology combining high throughput Isothermal Denaturation Fluorimetry (HT-ITDF) and Andersen Cascade Impaction (ACI) testing to expedite the selection of the best dry powder inhaler formulation to embed Cu,Zn-SOD, GOx and Cat.

Finally, Chapter 7 presents the main conclusions of this work and recommendations to improve its outcomes in the short and long run. Also, suggestions for future research are also provided.

CHAPTER 2

Theoretical background

2.1 THERAPEUTIC ENZYMES: ORAL INHALATION OUTLOOK

European Medicines Agency (EMA) and European regulatory agencies define 'biological medicinal products' as "a protein or nucleic acid–based pharmaceutical substance used for therapeutic or *in vivo* diagnostic purposes, which is produced by means other than direct extraction from a native (nonengineered) biological source" [1].

US Food and Drug Administration (FDA) and US regulatory agencies, on the other hand, define 'biological products' or 'biologics' as "any virus, therapeutic serum, toxin, antitoxin or analogous product applicable to the prevention, treatment or cure of diseases or injuries of man" [2].

Despite discrepancies between regulatory definitions, there is a general consensus on describing a biopharmaceutical, biologic(al) medical product or biologic as any pharmaceutical drug product manufactured, extracted or semi synthesized from a biological source (human, animal, plant, fungal or microbial) [1, 2]. These usually comprise oligonucleotides (antisense oligonucleotides - ASO, RNA interference - RNAi, and aptamers), nucleic acids (RNA and DNA derivatives, genes), peptides, (recombinant-) proteins (interferons, interleukins, lung surfactant proteins, hormones, therapeutic enzymes, antibodies, others), lung surfactants, virus, living cells or even tissues.

Biopharmaceutical delivery can be achieved via different administration routes. Around 85% of the biologics being filed for approval are administered via the injectable route [3]. However, owing to the limited patient compliance, alternative delivery routes namely transdermal, oral and oral inhalation (among others) are being further developed through formulation or device-based approaches.

Transdermal delivery offers a painless alternative to injections being mainly used for low-molecular-mass hydrophobic drugs. Several methods have been developed to temporarily disrupt the skin structure, such as the coupling of different peptides (TD-1, SPACE, polyarginine), to deliver macromolecular drugs. Besides chemical-based formulation strategies to increase skin permeability, devices that are based on the use of ultrasound,

electric fields or microneedles have also been explored and proved to be effective, preventing the pain of administration. Despite the strategies previously described have enabled progress in the transdermal delivery of macromolecular drugs, challenges concerning its adoption given the complexity of the devices, including the size, and required expertise, can still be envisaged [4, 5].

Oral delivery, on the other hand, offers increased patient acceptance while not requiring a device, but the delivery of macromolecules is limited by enzymatic degradation in the gastrointestinal (GI) tract and reduced permeation across the intestinal epithelium. Additionally, the mucus layer on the epithelium provides a barrier for the diffusion of macromolecules, leading to poor drug absorption into systemic circulation and insignificant bioavailability of macromolecules. pH-sensitive hydrogels to protect the drug from low pH in the stomach, chitosans and chitosan derivatives to induce mucoadhesion and absorption enhancers are currently being studied to circumvent these limitations [4]–[6].

Oral inhalation or pulmonary delivery offers drug targeting, whether to the site of action in the lungs for topically acting drugs, or the site of absorption for systemically acting drugs. For topically acting drugs, the advantages of pulmonary delivery include the possibility to use a relatively low dose, a low incidence of systemic side effects and for some drugs a rapid onset of action [7]–[9]. For systemically acting drugs, oral inhalation replaces injection and tackles the reduced absorption in the gastrointestinal tract when the pulmonary epithelium displays an area >100 m^2 with an epithelial cell layer < 1 µm in thickness [10]. Nevertheless, delivering drugs by inhalation has its own hurdles. The respiratory tract has evolved defence mechanisms intended to keep inhaled materials out of the lungs, removing or inactivating them once they have been deposited [11]–[13]. Advanced formulation strategies are thus required. Additionally, it is necessary for a patient to use an inhaler device, and to use it correctly. These issues pose major challenges to the pharmaceutical industry and to the healthcare professionals. It is generally agreed that owing to the advantages described for the oral inhalation route, the challenges it poses are worth addressing allowing to fulfil unmet clinical needs [14].

Figure 2.1A showcases the current outlook of biopharmaceuticals in the oral inhalation pipeline that are present in ~13%, when compared to small and other molecules (Figure 2.1A). Of these, recombinant proteins take up 44% (Figure 2.1B) of which 25% (Figure 2.1C) are therapeutic enzymes.

The high specificity and catalytic efficiency of enzymes towards its own therapeutic targets, coupled with the advancement in recombinant DNA technology and the increase in large scale capacity of production renders them attractive and cost-effective when compared to other "class" of biopharmaceuticals.

Concerning the oral inhalation route, there are only three marketed products (Table 2.1), all corresponding to the same therapeutic enzyme – deoxyribonuclease I or Dornase alfa (DNAse I). DNAse I is a therapeutic enzyme that selectively cleaves/hydrolyzes the DNA present in the sputum/mucus of cystic fibrosis patients, reducing viscosity in the lungs and improving clearance of secretions. This ultimately reduces the risk of infection in these patients. Pulmozyme® was the first DNAse I solution to be marketed for the local treatment of cystic fibrosis, by Genentech in 1996 in the USA, New Zealand, Europe, Canada, Argentina, Japan and Australia. This was also filed for a new indication - treatment of infections of the respiratory tract - by the same company in the USA. More than 20 years later, a genetically engineered variant of DNAse I biogeneric/biosimilar solution - Tigerase® was marketed by the International Biotech Center (IBC) Generium, in 2019 in the Russian Federation. Other genetically or chemically engineered improved variants of DNAse I targeting not only cystic fibrosis but also COVID-19 associated morbidities are also under development or being tested across different clinical trials phases. Besides DNAse I, alteplase and superoxide dismutase also feature in the therapeutic enzymes' oral inhalation portfolio. Alteplase is a serine protease that assists fibrin, a non-globular protein involved in the clotting of blood, in the conversion of plasminogen to plasmin [15] that will degrade the blood clots. A liquid solution of alteplase has been filed as a new formulation by the University College London (UK) for the treatment of COVID-19 associated morbidities. Superoxide dismutase liquid solution for inhalation is also

under phase II and phase I clinical trials, with LT-1002/ PC-SOD by LTT Bio-Pharma, Co, Ltd (Japan) indicated for Idiopathic Pulmonary Fibrosis and COPD, respectively.

Regardless of the disease indication, type of filing, development stage or clinical phase (Figure 2.1D), all therapeutic enzymes present in the oral inhalation pipeline are liquid solutions to be administered via nebulization. However, most of the administered drug never reaches the lung through nebulization. This is either retained within the nebulizer or released into the environment during expiration. On average, only 10% of the dose placed in the nebulizer is deposited in the lungs [16]. In addition, liquid dosage forms are more prone to contamination not only during administration, requiring cleaning in between uses, but also in the long run, from a stability standpoint, thus demanding cold chain storage. Alternative delivery platforms such as dry powder inhalers (DPIs), that rely on solid dosage forms could be envisaged to address these shortcomings with delivery efficiencies between 40-90% and increased shelf-life. Nevertheless, there are still some challenges when working towards solid dosage forms for DPIs starting with the patient lung features, particle deposition underlying mechanisms and drug product development.

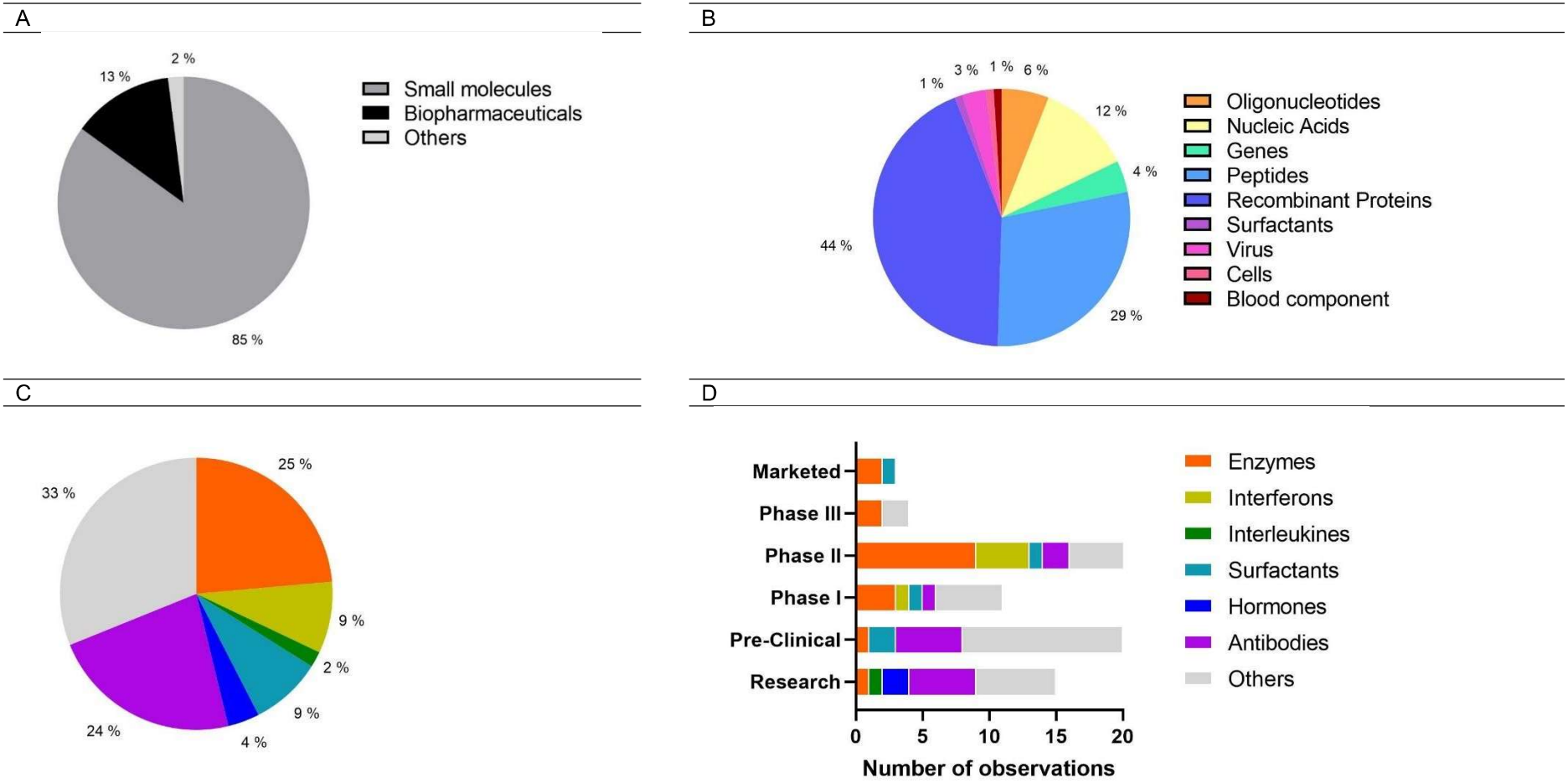

Figure 2.1 *– A. Inhalation products pipeline: small molecules still at the forefront of the inhalation products pipeline. B. Inhalable biopharmaceuticals distribution by categories; C. Inhalable recombinant proteins distribution by categories, D. development, pre- and clinical trials phases. The data was retrieved from PharmaCircle, August 2020* [3].

Table 2.1 *– Therapeutic enzymes present in the inhalation pipeline and respective owner company, disorder, therapeutic function, dosage form and general comments. Data retrieved from PharmaCircle, August 2020* [3].

Product name	Company	Disorder	Therapeutic function	Dosage form	Comment
MARKETED					
Tigeraze Inhalation Solution/Dornase alfa (2019)	International Biotech Center (IBC) Generium	Cystic fibrosis	Extracellular DNA cleavage in the airway to facilitate mucus clearance.	Liquid solution for liquid inhalers /nebulizers	Filed as biogeneric/biosimilar. Marketed in Russia.
Pulmozyme ®/ Dornase alfa	Genentech, Inc. (USA)	Infections respiratory tract			Marketed in the USA.
Pulmozyme ®/ Dornase alfa (1996)		Cystic fibrosis			Filed as new molecular entity (NME). Marketed in the USA, New Zealand, Europe, Canada, Argentina, Japan and Australia.
PHASE III					
Dornase Alfa Inhalation Solution	University of Missouri (USA)	COVID-19 associated morbidities	Extracellular DNA cleavage in the airway to facilitate mucus clearance in COVID19 patients [17].	Liquid solution for liquid inhalers /nebulizers	-
PHASE II					
Alteplase Inhalation Formulation	University College London (UK)		Fibrinolytic Agents Tissue-type Plasminogen Activators Antithrombotic Agents Thrombolytic Agents		
Dornase Alfa Inhalation Solution	Boston Children's Hospital (USA)	COVID-19 associated morbidities	Extracellular DNA cleavage in the airway to facilitate mucus clearance in COVID19 patients [17].	Liquid solution for liquid inhalers /nebulizers	Filed as new formulation.
	Acibadem University (Turkey)				
	University of South Alabama (USA)				

PRX-110/ Alidornase alfa	Protalix BioTherapeutics, Inc. (Israel)	Cystic Fibrosis	Extracellular DNA cleavage in the airway to facilitate mucus clearance.	Liquid solution for liquid inhalers /nebulizers	Filed as biobetter. Plant cell-expressed recombinant form of DNAse I. Chemically modified to render DNAse I resistant to inhibition induced by actin interaction. [18]
PulmoXEN	Pharmsynthez Inc.	Cystic Fibrosis	Human DNAse I replacement.	Undisclosed	Filed as new molecular entity in Russian federation. PulmoXen is a polysialic acid - conjugated form of rhDNase I that is being developed using Xenetic Biosciences, Inc. patented PolyXen® delivery technology that allows enhanced stability and pharmacodynamic profile of the enzyme in the mucus. Studies confirmed superiority of PulmoXen with respect to stability and enzymatic activity when digesting DNA in sputum from cystic fibrosis patients when compared to Pulmozyme [19].
LT-1002/ PC-SOD	LTT Bio-Pharma, Co, Ltd. (Japan)	Idiopathic Pulmonary Fibrosis	Superoxide dismutase mimetics.	Liquid solution for liquid inhalers /nebulizers	Filed as NME in South Korea.
PHASE I					
Pulmozyme ®/ Dornase alfa	Genentech, Inc. (USA)	Infections pandemic COVID19	Extracellular DNA cleavage in the airway to facilitate mucus clearance in COVID19 patients [17]	Liquid solution for liquid inhalers /nebulizers	Filed as new indication in the USA.
JHL1922/Dornase alfa	JHL Biotech (China)	Cystic Fibrosis	Extracellular DNA cleavage in the airway to facilitate mucus clearance		Filed as biogeneric/biosimilar.

LT-1002/ PC-SOD	LTT Bio-Pharma, Co, Ltd. (Japan)	COPD	Superoxide dismutase mimetics		Filed as new molecular entity (NME) in Japan.
PRE-CLINICAL					
Theradux Inhalation / OrPro	National Jewish Health Inc.	Cystic Fibrosis COVID-19 associated morbidities	Acts to thin mucus in the lungs by preventing excess molecular bonds from forming in mucus layers. Thinner mucus is more easily cleared from the airways of people with cystic fibrosis	Liquid solution for liquid inhalers /nebulizers.	Filed as NME.
RESEARCH					
Theradux Inhalation / OrPro	National Jewish Health Inc.	COPD Emphysema Bronchiectasis Asthma	Acts to thin mucus in the lungs by preventing excess molecular bonds from forming in mucus layers. Thinner mucus is more easily cleared from the airways of people with cystic fibrosis	Liquid solution for liquid inhalers /nebulizers.	Filed as NME.

2.2 TOWARDS DRY POWDER INHALER FORMULATIONS OF THERAPEUTIC ENZYMES

2.2.1 The Patient

2.2.1.1 Anatomy and Physiology of the Lungs

Prior knowledge on both the anatomy and physiology of the airways is essential to understand the dynamics of inhalable drug delivery systems within the lung while providing insight on how these should be formulated from a drug absorption standpoint.

The lung airways are usually grouped in two main regions [20, 21]: the conducting airway and the respiratory airway (Figure 2.2). Their structure and layout in the lung are widely described by the Weibel-A mathematical model [21]. This is a symmetric tree model that divides the lung into 24 stages (0-23), each corresponding to an airway generation (or level of bifurcation) that branch symmetrically into two similar smaller branches. Such stages allow for the prediction and profiling of aerosol deposition along the respiratory tract based on luminal diameter, length and angle of the bronchi [21].

The conducting region of the airways constitutes the upper portion (Figure 2.2), starting at the mouth/nose and following the trachea, bronchi, bronchioles, and terminal bronchioles, which correspond to the stages 0 (trachea) – 16 (terminal bronchioles). The surface area together with the presence of smooth muscle cells gradually increases along these stages conversely to air velocity. Within the conducting airway, no gas exchange takes place. Its main role is to transport the gas to the respiratory airway whilst ensuring that inspired gasses are filtered, humidified and heated to provide the alveoli with air identical to the preexisting environment conditions [21].

The respiratory region of the airways constitutes the lower portion (Figure 1), consisting of the respiratory bronchioles, alveolar ducts, and alveolar sacs, which corresponds to the stages 17 (respiratory bronchioles) – 23 (alveolar sacs).

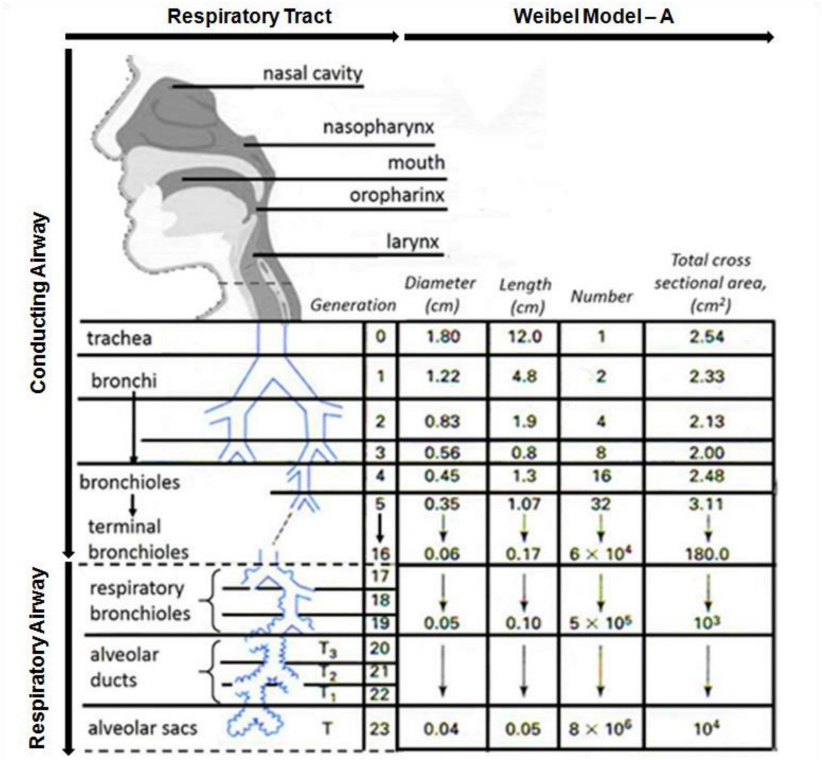

Figure 2.2 – *Conducting and Respiratory Airways of the respiratory tract according to the Weibel – A mathematical model. Adapted from* [20] *and* [21].

Its inherent physical characteristics are different when compared to the conducting airway given the distinct function of this region: gas exchange. The surface area is approximately 100 m^2, while the conducting airway is 2-3 m^2, allowing for much greater contact with the inspired gas or therapeutic aerosol. Herein, the thickness of the fluid and cell layers shifts from the mm to the nm in the conducting airway and from the mm to the μm range, in the respiratory airway [20, 21].

Both conducting and respiratory airways epithelium is covered by a mucus gel. However, the alveoli are lined with a pulmonary surfactant, a lipoprotein-based complex consisting of 90% lipid and 10% protein, which is synthesized, secreted, and recycled in these structures. This pulmonary surfactant plays a dual role of reducing surface tension at the air-liquid interface, preventing the alveoli from collapsing, while defending the host from inhaled pathogens and

particles, enabling their movement to the upper airways. Due to these peculiar properties, lung surfactant also plays an important role in drug delivery and absorption, enhancing, for instance, the solubility of steroidal drugs (glucocorticosteroids), by extending their residence time within the lung [20]. On the other hand, it was reported that some antibiotics and deposited nanoparticles may impact the biophysical surfactant function, metabolism and particle clearance, sometimes resulting in particle induced toxicity [13], [22, 23]. In the case of large molecules, such as biopharmaceuticals, the lung surfactant can cause them to aggregate, becoming insoluble, potentiating their elimination or immunogenic events.

2.2.1.2 Underlying Mechanisms of Particle Deposition, Absorption and Clearance in the Lungs

Besides lung's anatomy and physiology, particle deposition and clearance mechanisms are also relevant when designing a drug delivery system. The specific pattern of deposition determines the local doses in the lung and the subsequent redistribution and clearance of deposited particles [12].

The mechanisms involved in particle deposition are ruled by a combination of different factors such as particle size, shape, breathing rate, respiration volume and health condition of the individual. Table 2.2 presents the main mechanisms of particle deposition reported in the literature [20, 21]. Inertial Impaction and Gravitational Sedimentation are often regarded in the literature [20, 21], [12] as the most significant deposition mechanisms for drug delivery.

Table 2.2 – *Overview of the underlying mechanisms, aerodynamic particle size range and lung region incidence of different particle deposition in the lungs* [20, 21], [12].

	Underlying mechanism	Aerodynamic particle size range	Lung region incidence
Inertial Impaction	This mechanism takes place when the particle momentum is too large for it to change direction in an area where there is a rapid change in the direction of the bulk airflow. Impaction increases with air velocity, particle size and particle density.	≥5 µm	Conducting Airway
Gravitational Sedimentation	Governed by the (higher) gravitational force acting on the particles being more dominant	0.5–5 µm	Respiratory Airways

	than the (lower) dragging force imposed by the airflow. The rate of sedimentation deposition increases with particle size and density while decreasing with flow rate.		
Interception	Particles deposited by interception usually present noncircular shapes (fibers) and do not diverge from their air streamline. Due to their elongated shape, particles are deposited as soon as they contact the airway wall. Interception increases as the airway diameter becomes smaller.	-	Conducting/Respiratory Airways
Brownian Diffusion	Particles move randomly across the streamline due to collisions with gas molecules, depositing upon contact with the airway wall. Diffusion increases with decreasing particle size and airflow rate. However, most of these particles are exhaled by the expiratory airflow.	<0.5 μm	Respiratory Airway
Electrostatic Precipitation	Results from charged particles inducing image charges of opposite sign onto the surfaces of the airways that are electrically conducting while normally uncharged. Charged particles then become electrostatically attracted to the airway walls, and as a consequence, deposition takes place.	-	Conducting /Respiratory Airways

Following particle deposition, absorption, and *in vivo* mechanisms such as mucocilliary clearance, clearance by macrophages and proteolytic degradation may take place [24].

In mucocilliary clearance, ciliated cells drive the particles trapped in the mucus – through coordinated ciliary beat – from the lower airways to the pharynx, where they can be either swallowed and degraded in the gastrointestinal tract or ejected.

Macrophages migrate to the particles and phagocytize them via chemotaxis involving opsonization. Once particles are internalized in the macrophages, these are disintegrated, for instance, by enzymes in lysosomes.

Another clearance mechanism in the lungs is proteolysis carried out by enzymes, especially peptidases and proteases [11].

Strategies to circumvent mucocilliary and macrophage clearance include the use of encapsulating nano systems [25]. Concerning proteolysis carried out by enzymes, there is a

complex relationship between degradation and molecular weight. Natural peptides less than 3,000 Da are rapidly degraded in the lung, with the exception of peptides in “ring”-like structures (e.g. cyclosporine) or that have chemical modifications on their N or C termini which block peptidases action. Larger biomolecules, between 6,000 and 50,000 Da (e.g. insulin, vaccines antigens, cytokines, growth factors) are relatively resistant to most proteases and have good bioavailabilities, partly because their termini are often positioned inside the globular structure of the protein and not available for hydrolysis [5].

Pulmonary administration of recombinant proteins, including therapeutic enzymes, and peptides also entails safety issues. The use of absorption enhancers, which are frequently added to the formulation to obtain systemic absorption of large proteins can damage epithelial surfaces. On the other hand, the use of protease inhibitors might result in the increase of local concentration in the lung breaking the protease/anti-protease equilibrium. Another important concern in inhaled protein delivery is the possibility of immunological reactions because the body may recognize these molecules as antigens. However, pulmonary delivery of most therapeutic proteins and peptides has been regarded as safe. Finally, the excipients used to obtain an appropriate delivery media for pulmonary administration, such as polymeric micro- or nano-particles, may also have a detrimental effect [11], [26].

2.2.2 The Drug Product Development

To accommodate patient features, drug product development towards safe and effective DPI formulations of enzymes encompasses the challenge of balancing between biopharmaceutical nature of the API, formulation, particle engineering technology and device/delivery platforms supported by proper analytical testing. The combination of these factors should yield a DPI formulation in which, at least:

i. Enzyme structure must be maintained until deposition and absorption in the site of action, to avoid immunogenic response induced by physio-chemical degradation mechanisms.

ii. Enzyme activity should be preserved so the therapeutic target can be attained.

iii. The aerodynamic particle size distribution (aPSD) of the dry powder dosage form should fall between 1 and 5 μm, so it reaches the deep lung.

2.2.2.1 Biopharmaceutical nature of the API

Enzymes structural levels (from primary to quaternary structure) and biological activity can be affected during processing, storage and device actuation by physico-chemical instability mechanisms [11]. Thus, excipient, particle engineering process parameters, packaging selection and device design are pivotal to mitigate the impact of each one of the mentioned operation units. The physico-chemical instability mechanisms include denaturation and non-covalent aggregation (physical degradation), covalent aggregation, deamidation, oxidation, and/or glycation (chemical degradation). These may trigger immunogenic reactions or loss of enzyme activity.

Denaturation refers to the reversible or irreversible unfolding of the enzyme with subsequent exposure of its hydrophobic residues buried in the interior of the structure. Extremely high or low temperatures, organic solvents, air interfaces, shear stresses or high salt concentrations are some of the physical stresses that underpin this instability mechanism. Loss of biological activity of the denatured compound is only observed if a domain from the active site is affected. This mechanism is usually reversible for single domain proteins conversely to multi-domain proteins [27], [11].

Non-covalent aggregation results in the formation of soluble low-order aggregates (non-covalent), potentially becoming insoluble by growing over time. Biological activity is partially or completely lost, even for the forms that manage to stay soluble. This mechanism can be reversible or irreversible for low-order aggregates and irreversible for high-order aggregates [11].

Covalent aggregation occurs through intermolecular thiol-disulphide exchange, which may occur for proteins containing both free thiols (cysteine residues) and disulphide bonds. The thiol of one protein carries out a nucleophilic attack on a disulphide linkage of another protein molecule. The result is a new intermolecular disulfide bond with conservation of the free

thiolate ion. A further propagation of this process leads to high molecular weight aggregates, which are generally insoluble, resulting in the irreversible loss of biological activity and in immunogenic events [5].

Deamidation takes place through the hydrolysis of the side chain amide group on glutamine or asparagine residues to yield a carboxylic group (Glutamate or aspartate respectively) which is generally favored in neutral or alkaline conditions. Such can result in the formation of non-covalent and/or covalent aggregates. Thus, biological activity is frequently lost and irreversible [11].

Oxidation is more likely to occur in amino acids such as methionine, cysteine, histidine, tyrosine, and tryptophan with formation of oxide derivatives that are larger, more polar and less flexible. Such features might impact on enzyme stability by changing the secondary and the tertiary structure ultimately leading to the irreversible loss of biological activity [11], [5].

Finally, glycation, also known as the Maillard reaction, refers to the interaction between reducing sugars often used as enzyme stabilizers (fructose, maltose, lactose, glucose, and xylose) in both liquid and solid formulations, with proteins amino groups forming carbohydrate adducts, especially at extreme temperature and pH conditions. Frequently occurs on lysine side chains, although it can occasionally take place on arginine, asparagine, and glutamine side chains. Over time, the glycated products can yield a class of heterogeneous chemical compounds that can permanently alter the enzyme structure and function resulting in the irreversible loss of biological activity and immunogenic reactions [11], [26].

Strategies to overcome physico-chemical instability of proteins include protein engineering (e.g. replacement of cysteine residues in proteins to prevent covalent intermolecular bonding), protein drying since most of the degradation mechanisms are water-mediated, and addition of stabilizing excipients [28].

2.2.2.2 Formulation

When developing DPI formulations, two main strategies are usually considered [9], [29], [30]: the *carrier-based* strategy, in which the Active Pharmaceutical Ingredient (API) is blended with

an inert excipient, a coarse carrier, where upon aerosolization, the API detaches from the carrier surface, depositing in the deep lung while the coarse carrier is retained in the mouth or in the conducting airway by Stage 0 (Figure 2.2); and the *carrier-free or composite strategy* where the API is dissolved or suspended in a solvent or anti-solvent, respectively, along with the adequate excipients followed by solvent removal yielding particles within the inhalable size range. This latter can be further divided into two sub-groups, the *excipient-based* and *excipient-free* approaches for which several particle engineering technologies or combination of technologies can be employed as it will be described in the next section [8], [31, 32]. The excipient-based approach can yield microencapsulated nanoparticles, coated particles, encapsulated particles, and amorphous solid dispersions, amongst others. In the carrier-free-excipient-free particles, the API can be delivered alone or coated with a similar or distinct API [9].

Of the strategies described, the carrier-free based one is applicable to biomolecules and enables the production of formulations with enhanced aerodynamic performance, improving drug delivery to the target site of action, minimizing the amount of drug required in the formulation while delivering the same drug concentration to the target site. This minimizes the potential toxicity and adverse side effects for the patient [16–18]. Enzymes can be high potency APIs requiring lower doses (in the µg range) to achieve their therapeutic effect. As a result, excipients may be added not only as bulking agents not only to allow accurate metering but also to stabilize the enzyme and enhance bulk powder dispersibility [9]. As such, the carrier-free-excipient-based is the one explored in the present thesis. The challenge in developing these formulations is related to the limited array of excipients or inactive ingredients approved by the FDA for delivery to the lungs while stabilizing the biopharmaceutical-based API as well as the scarce information published regarding the excipients toxicity [16]. In table 2.3, an overview of excipients usually considered for dry powder inhaler formulation is presented, where their role is briefly elaborated, from a biopharmaceutical (BP) and oral inhalation (OI) standpoints.

Table 2.3 – *Categories and role of pharmaceutical excipients usually considered for dry powder inhaler formulation from a biopharmaceutical (BP) and oral inhalation (OI) standpoints* [9][33].

Categories	Representative examples	Role	
		BP standpoint	OI standpoint
Buffering agents	Citrate, acetate, histidine, glycine, phosphate, Tris.	• Physical and chemical stability: pH control • Buffer-ion specific interactions with protein.	• Mitigate disproportionation. • Control solid-state form in vivo. • Improve tolerability.
Amino acids	Alanine, leucine, trileucine, isoleucine, glycine.	• Specific interactions with protein. • Buffering and tonicifying agents. • Natural compounds that stabilize proteins and macromolecules against environmental stress (temperature, dehydration).	• Hydrophobic shell former to improve bulk powder dispersibility. • Stability: pH control agent. • Mitigate disproportionation.
Osmolytes	Sucrose, trehalose, sorbitol, glycine, proline, glutamate, glycerol, urea.	• Specific interactions with protein. • Antioxidant (His, Met). • Buffering and tonicifying agents. • Natural compounds that stabilize proteins and macromolecules against environmental stress (temperature, dehydration).	-
Non-reducing sugars and carbohydrates	Sucrose, trehalose, sorbitol, mannitol.	• Protein stabilizer in liquid and solid states. • Tonicifying agents.	• Carriers, filler, or bulking agent. • Taste masking. • Increase glass transition temperature and reduce long-range (diffusional) molecular mobility.
Salts	Calcium chloride.	• Tonicifying agents. • Stabilizing or destabilizing effects on proteins. • Control-specific reaction pathways (e.g., oxidation). • Protective effect against thermal unfolding	
Surfactants and phospholipids	Polysorbate 20, Polysorbate 80, DSPC, DPPC.	• Competitive inhibitor of protein adsorption. • Competitive inhibitor of protein surface denaturation.	• Force-control agents that decrease attractive forces between particles. • PK/PD: controlled-release agents Modify pharmacokinetics.

Note: Most of the excipients described are not FDA approved (like trehalose and leucine). DSPC – Distearoylphosphatidylcholine; DPPC – Dipalmitoylphosphatidylcholine; EDTA - Ethylenediamine tetraacetic acid; DTPA - Diethylenetriamine pentaacetate

Table 2.3 (cont.) – *Categories and role of pharmaceutical excipients usually considered for dry powder inhaler formulation from a biopharmaceutical (BP) and oral inhalation (OI) standpoints* [33, 34].

Categories	Representative examples	Role	
		BP standpoint	OI standpoint
Chelators and anti-oxidants	EDTA, DTPA, amino acids (Histidine, Methionine), ethanol.	• Bind metal ions. • Free radical scavengers.	• Control-specific reaction pathways (e.g., oxidation)
Specific ligands	Metals, ligands, amino acids, polyanions	• Bind protein and stabilizes native conformation against stress induced unfolding. • Bind may also affect protein's conformational flexibility.	

Note: EDTA - Ethylenediamine tetraacetic acid; DTPA - Diethylenetriamine pentaacetate.

2.2.2.3 Particle engineering technologies employed in carrier-free DPI formulation strategy

In the following sub-sections, some of the standard technologies currently available in the industry as well as innovative ones for the preparation of carrier-free powders are further explored.

Freeze drying

Freeze-drying is the most common technique to generate protein based dry powders. It has been used to generate a respirable insulin formulation for inhalation: Afrezza®. However, it is a time-consuming and costly particle engineering technology challenging to scale-up. In addition, freeze drying generally yields a dried cake and therefore might require an additional step to generate respirable particles for subsequent DPI formulation, usually by milling, which also involves exposure of the biopharmaceutical to heat and shear stresses. Alternatively, spray freeze-drying involves the atomization of a biopharmaceutical solution into a cryogenic liquid, usually nitrogen, followed by a lyophilization step, not requiring further processing [11].

Spray drying

Spray drying (SD) has emerged as a noteworthy approach for preparing DPI formulations due its relative simplicity, cost-effectiveness and scalability [35]. In SD, a liquid feed is atomized by a nozzle into a heat expansion chamber in which a stream of hot gas (e.g. air or nitrogen) flash dries the droplets, forming particles which are collected downstream. It is particularly applicable for processing labile molecules such as biopharmaceuticals, since the suspended or dissolved solids are subjected to evaporative cooling during particle formation and to short residence times. There are several parameters that can be adjusted in the SD process, allowing a superior level of control over the final particle attributes such as particle size distribution, density, surface roughness, morphology, and residual solvents/moisture levels so that adequate stability, flow and aerodynamic properties of the bulk powder are achieved. Moreover, a thorough understanding on the SD process thermodynamics, atomization conditions and fluid dynamics allows the scale-up of SD processes so that the particle properties are maintained across scales [36, 37].

Biopharmaceuticals, therapeutic enzymes included, processed by spray drying are at risk of degradation due to dehydration, exposure to heat stress as well as shear stress and air-water interfacial adsorption during atomization. However, thermal degradation is rarely observed for proteins during SD due to evaporative cooling and to the dynamic increase of the protein unfolding temperature as the water is removed. During the feed atomization, the protein is also exposed to high shear stress. This is due to spatial differences in fluid velocities within the nozzle between the feed and atomization gas. In general, this would not cause any major stability issue; nevertheless, in combination with tendency for protein adsorption to the gas-water interface, significant aggregation of sensitive proteins may be observed, being a dominant source of denaturation in the SD process. Careful selection of operating parameters and excipients can play a significant role in preventing these phenomena. [11], [26], [36].

Many studies have demonstrated the feasibility of spray-drying to produce inhaled biopharmaceutical formulations with the desired aerodynamic properties. Inhaled formulations

prepared by spray-drying have already been attempted with many proteins, peptides, and other biopharmaceuticals. In 2006, the inhaled insulin powder, Exubera® (Pfizer), became the first commercial spray-dried protein hormone (later withdrawn from the market). Spray-dried particles containing plasmid DNA (pDNA) have been produced with a particle size of 3–5 μm and 44–60% yield, and spray-drying did not compromise the transfection efficiency of the pDNA [32]. Spray dried small interfering RNA/poly(lactic-co-glycolic acid) (siRNA/PLGA) particles with different stabilizers (mannitol, trehalose, and lactose) produced particles with an MMAD between 2 and 5 μm, yields ranging from 20 to 60%, and preservation of siRNA biological activity [32]. Spray-dried recombinant human growth hormone (rhGH) particles with dimethyl-β-cyclodextrin (DMβCD) as a pulmonary absorption enhancer and stabilizer resulted in particles with a fine particle fraction (FPF) as high as 53% [38]. Spray-dried alternatives of PLGA microspheres for depot liquid crystal formulation of triptorelin pamoate and lanreotide acetate were approved in 2010 and 2013, respectively. An inhaled human parathyroid hormone (PTH) formulation displaying 4.5 μm particle diameter, MMAD 3.9–5.9 μm, 90% emitted dose, and 61% FPF, had 186% bioavailability relative to subcutaneous administration in rats and resulted in no acute lung inflammation after 48 h [36]. Spray-drying of liposomal DNA produced smooth, spherical, 4 μm particles with better gene transfer in cell culture than either fresh solution or lyophilized formulations [38].

Spray drying has also been extensively studied in the case of enzymes, being these mostly used as model biopharmaceuticals (lysozyme, trypsin, catalase, ß-galactosidase) given its easy access and functional analysis [38]. rhDNase was one of the few therapeutic enzymes administered to the lungs reported in the literature [39], whose spray dried dosage forms successfully displayed an aerodynamic particle size within the inhalable range with a FPF not higher than 50%.

Next generation particle engineering technologies

The application of supercritical fluids (SCF), namely supercritical carbon dioxide ($scCO_2$), to dry proteins is relatively new, when compared with freeze and spray drying, previously

described. SCFs are defined as compressed gases above their critical pressure and temperature. In this range, a SCF exists as a single phase with liquid-like density values that enable appreciable solvation power and gas-like viscosity that facilitate mass transfer. These properties can be fine-tuned by adjusting pressure and temperature. In pharmaceutical applications, $scCO_2$ is generally used due to the relatively low critical temperature (31.2 ºC) and pressure (74 bar). In addition, it is a non-flammable, non-toxic, chemically inert and inexpensive solvent [40]. Generally, the solubility of proteins in $scCO_2$ is rather limited; hence $scCO_2$ has been explored mostly as an anti-solvent or as an atomization adjuvant. In the gas anti-solvent technique, the drug solution and operating parameters must be designed so that the solvent is miscible with $scCO_2$. The drug solution is atomized into a pressurized vessel, in which the $scCO_2$ dissolves the atomized droplet, triggering precipitation of the drug. In other configurations, namely supercritical assisted atomization, $scCO_2$ is solubilized in the liquid solution up to near-saturation conditions, forming an expanded liquid phase; the solution is then sprayed into a precipitator at atmospheric pressure in warm nitrogen environment at a certain temperature. The solubilization of carbon dioxide may lead to a reduction in droplet pH, which should be addressed by the addition of a buffer [11], [40].

Adsorption Spray Drying is an emerging particle engineering technology based on a new equipment developed by Inhalation Sciences, Sweden – LaminarPace™ [41]. This technology driving force for drying liquid feeds is absorption instead of evaporation (as in Spray Drying), this way addressing the need of processing sensitive molecules such as biopharmaceuticals at room temperature. Moreover, the laminar flow inside the unit as well as the collection method enables very high yields for small batches, below 100 mg, being particularly suitable for pre- or early clinical as well as high added value substances.

2.2.2.4 Dry Powder Inhaler Delivery Platforms

Pulmonary delivery devices/platforms can be divided into three main categories: nebulizers, pressurized metered-dose inhalers (pMDIs) and dry powder inhalers (DPIs) – none of the

devices is clinically superior and device selection should be guided by factors such as formulation properties, target dose, convenience, cost, and patient preference [42].

Nebulizers

Nebulizers were the first developed devices for pulmonary drug delivery, and have been used for over a century, remaining a practical means of delivering inhaled medications to very young children and patients unable to use other devices. Compared with other types of devices, nebulizers offer a particularly effective and acceptable delivery system for infants and young children, because they enable inhalation during tidal breathing [42]. Nebulizers convert a liquid medication into an aerosol by applying compressed gas (jet nebulizers) or ultrasonic vibrations (ultrasonic nebulizers), or alternatively using vibrating mesh technology (mesh nebulizers) [20, 21], [43].

Jet nebulizers disperse liquid preparations into droplets by resorting to a compressed gas stream that is forced through a small orifice creating a pressure drop and velocity increase, ultimately leading to the aspiration of the liquid through a capillary from the reservoir (Bernoulli principle). The resulting aerosol impacts on the device baffles and is subsequently disintegrated into smaller droplets [42]. The larger droplets return into the device reservoir to undergo nebulization once again, whilst smaller particles are emitted from the nebulizer. Jet nebulizers generate a continuous flow of aerosol, which yields considerable losses during the expiratory phase of the patient and considerable release into the surrounding air. This limits the effectiveness of the aerosolized drug since low rates of lung deposition is observed [20]. Efficiency also depends on the patient's aspiratory flow, which in turn is dependent on the patient's age. In infants under 12 months, aspiratory flow rate is lower than that of nebulizer output, so although such patients inhale a dense cloud of aerosol, they are not able to inhale all of it.

The second class of nebulizers is the ultrasonic nebulizer. The underlying principle consists on the vibrations of a piezo-electric crystal (transducer) driven by an alternating electrical field [21]. These nebulizers present the advantage of nebulizing high volumes in a relatively short

time, although particle size is higher than that produced using other systems of nebulization. Moreover, they tend to be inefficient for the nebulization of suspensions, viscous solutions, or solutions with a high surface tension [20]. Due to the heating of the liquid phase during ultrasonic nebulization, a denaturation of drugs can occur, particularly if that drug is a peptide or a protein [11]. Usually, they are not used as a first line means of administration and there is a tendency to move from these to the vibrating mesh technology. The latest generation of nebulizers comprises the mesh nebulizers, which employ vibrating mesh technology. This principle uses a mesh or a plate with multiple apertures to produce an aerosol. This is obtained by using a piezoelectric element which either vibrates a transducer horn or which is annular and encircles the mesh causing it to vibrate. In both cases, the liquid is pumped through the perforated mesh generating homogeneous particles [21]. The aerosol particle size and flow are determined by the diameter of the aperture holes. The nebulization time is short (1–6 min), the aerosol velocity is low (1m s−1), and the residual volume is minimal (0.1–0.3 mL). Moreover, these nebulizers are portable, handheld, and function without noise [20, 21].

Pressured metered dose inhalers (pMDIs)

pMDIs comprise a canister containing the formulation, a metering valve, and a spray actuator. A pMDI formulation consists in a propellant based solution or suspension containing the drug and/or additives such as a surfactant or lubricant. The propellants currently used are hydrofluoroalkanes (HFAs) given the need to replace the chlorofluoroalkanes (CFCs), because of their known detrimental effect on the ozone layer [42].

However, due to the greenhouse effect, HFAs use in the formulation has also been gradually discouraged. Optimal lung delivery with pMDIs requires coordination between the actuation of the device and inhalation. For a correct device handling, the patient should fully expire before placing the mouthpiece of the device between the lips, and upon the start of a slow inhalation, the canister should be pressed downwards. Finally, the patient is advised to hold his or her breath for 10 s to promote the sedimentation of particles in the peripheral airways. Actuation before inspiration, actuation at the end of aspiration, actuation in the mouth but inhalation

through the nose, or inhalation stopped by the actuation constitute some of the frequent handling errors that take place when using pMDIs [20, 21], [42]. Such renders these devices quite unsuitable for the pediatric population as they require a good coordination between actuation and inhalation that these patients are not always able to achieve, especially if they are children below 6 years. Moreover, since the aerosol is emitted with high velocity, this causes a marked deposition of an important part of the dose (30–65%) in the upper respiratory part (mouth, oropharynx and larynx). Such impaction (which can be more pronounced in children than in adults due to the shorter distance between the device mouth piece and oropharynx) decreases the dose delivered deep into the lungs and contributes to increasing systemic absorption and side effects (local or general) [20]. Drugs delivered via a pMDI hardly achieve a dose greater than 20% to the alveoli while other devices, such as dry powder inhalers which will be presented next, can increase the dose well above this percentage [21].

Dry Powder Inhalers (DPIs)

DPIs have gained momentum in recent years because of their potential advantages over the previously described delivery systems: small portable devices with no need for propellants while requiring little to no coordination between actuation and inhalation, ultimately resulting in improved patient adherence [42]. DPIs ability to deliver the formulation to the patient mainly depends on inspiratory airflow generated by the patient and the turbulence induced inside the device, determined by the resistance against the inhalation flow required to produce a pressure drop of 4 kPa through the device, a value envisaged by Pharmacopoeias for the evaluation of emitted dose [43]. DPIs are classified as high, medium, and low-resistance devices. Through low-resistance DPIs, like Breezhaler® and Aerolizer®, the disaggregation and the micro dispersion of the dry powder formulation highly depends on the patient's inhalation airflow rate, because the role of the resistance-induced turbulence is negligible in these cases. The low resistance DPIs require a higher inspiratory airflow rate and effort, which frequently cannot be achieved by patients suffering from a disease-induced airflow limitation. As such, an increased variability on the delivered dose of these DPIs is often observed.

This flow rate dependency is minimized in the presence of a minimum regimen of turbulence as in the case of medium-resistance DPIs, showcased in Table 3. Both the disaggregation and the micro-dispersion of the dry powder are optimized in these circumstances even in the absence of a maximal inspiratory flow rate.

Table 2.4 *– Dry Powder Inhalers (DPIs) currently available in the market. Inspiratory resistance, flow rate and resistance level for each DPI. Values at 4 KPa pressure drop.*

Dry powder Inhaler	Inspiratory flow rate ($L.min^{-1}$)	Inspiratory DPI resistance ($kPa^{0.5}.L.min^{-1}$)	Resistance level
Rotahaler®	~160	0.013	Low
Spinhaler®	~120	0.016	Low
Breezhaler®	111	0.017	Low
Aerolizer®	102	0.019	Low
Dishaler®	~98	0.021	Low
Ellipta®	74	0.027	Medium
Novolizer®	72	0.027	Medium
Accuhaler/Diskus®	72	0.027	Medium
Genuair®	64	0.031	Medium
Nexthaler®	54	0.036	Medium
Twincaps®	Non disclosed	Non disclosed	Medium
TwinMax®	Non disclosed	Non disclosed	Medium
PowdAir®	Non disclosed	Non disclosed	Medium
Turbohaler®	54	0.039	High
Handihaler®	37	0.058	High
Pappilon®	Non disclosed	Non disclosed	Adjustable

High resistance DPIs, such as the Turbohaler® and the Handihaler®, on the other hand, even if allowing a lower inspiratory flow rate, proved to affect particle generation and dispersion of powdered drug substantially [44].

2.2.2.5 Analytical Characterization

Appropriate analytical characterization is pivotal to account for safety and effectiveness across all stages of drug product development. When producing dry powder inhaler formulations featuring therapeutic enzymes or any other biopharmaceutical as API, the same two angles previously elaborated, have to be considered: inhalation and biopharmaceutical standpoints.

To assess if a dry powder based formulation is suitable from an inhalation standpoint, powder morphology (shape, size), physicochemical and aerodynamic properties should be tested as listed in Table 2.5. When generating a therapeutic enzyme or biopharmaceutical dry powder based formulation, physicochemical degradation may occur, depending on the process conditions used. Table 2.6 lists some of the techniques that could be used for this purpose.

Table 2.5 – *Overview of the available analytical techniques for powder characterization from an inhalation standpoint.*

	Analytical Method	**Particle Attribute**
Morphology properties	Laser Diffraction (LD)	Size distribution
	Scanning Electron Microscopy (SEM)	Shape
	Pycnometry	Density
	Brunauer-Emmet-Teller	Specific surface area
	Mercury Intrusion Porosimetry	Porosity
		Apparent density
Physicochemical properties	Differential Scanning Colorimetry (DSC)	Glass Transition Temperature (T_g)
		Crystallization Temperature (T_c)
		Melting Temperature (T_m)
	X-Ray Powder Diffraction (XRPD)	Diffraction pattern
	Karl-Fisher (KF) titration method	Water content
	Thermogravimetric Analysis (TGA)	Water content
	Gas Chromatography (GC)	Solvent content
	Dynamic Vapour Sorption (DVS)	Higroscopicity
	High Performance Liquid Chromatography (HPLC)	Drug concentration; Purity
Aerodynamic Performance	Andersen Cascade Impaction	Fine Particle Fraction (FPF)
		Mass Median Aerodynamic Diameter (MMAD)

Table 2.6 - *Overview of the available analytical techniques for the biopharmaceutical characterization.*

	Analytical Method	**Biopharmaceutical Attribute**
Physicochemical & Structural properties	Biological analysis	Activity (enzymes)
	Differential scanning fluorimetry	Melting Temperature (T_m)
	Circular Dichroism	Structure

	Size-exclusion chromatography (SEC) SDS-PAGE Dynamic light scattering Mass spectroscopy	Purity, Molecular weight (or size), oligomerization or aggregation (Protein)
	Isoelectric focusing: Zeta potential Ion exchange chromatography Affinity chromatography	Charge / Deamidation (Protein)
	Reversed phase HPLC Peptide analysis	Oxidation (Protein)

REFERENCES

[1] "European Medicines Agency," [Online]. Available: https://www.ema.europa.eu/en, accessed March 2021.

[2] "U.S. Food and Drug Administration," [Online]. Available: https://www.fda.gov/vaccines-blood-biologics, accessed March 2021.

[3] "PharmaCircle." https://www.pharmacircle.com/info/, accessed August 2020.

[4] S. Mitragotri, P. A. Burke, and R. Langer, "Overcoming the challenges in administering biopharmaceuticals: Formulation and delivery strategies," *Nature Reviews Drug Discovery*, vol. 13, no. 9. Nature Publishing Group, pp. 655–672, Sep. 01, 2014, doi: 10.1038/nrd4363.

[5] S. A. Shoyele and A. Slowey, "Prospects of formulating proteins/peptides as aerosols for pulmonary drug delivery," *Int. J. Pharm.*, vol. 314, no. 1, pp. 1–8, 2006, doi: 10.1016/j.ijpharm.2006.02.014.

[6] K. A. Johnson, "Preparation of peptide and protein powders for inhalation," *Adv. Drug Deliv. Rev.*, vol. 26, no. 1, pp. 3–15, 1997, doi: 10.1016/S0169-409X(97)00506-1.

[7] C. Ehrhardt, "Inhalation Biopharmaceutics: Progress Towards Comprehending the Fate of Inhaled Medicines," *Pharm. Res.*, vol. 34, no. 12, pp. 2451–2453, 2017, doi: 10.1007/s11095-017-2304-2.

[8] M. Hoppentocht, P. Hagedoorn, H. W. Frijlink, and A. H. de Boer, "Technological and practical challenges of dry powder inhalers and formulations," *Adv. Drug Deliv. Rev.*, vol. 75, pp. 18–31, 2014, doi: 10.1016/j.addr.2014.04.004.

[9] J. G. Weers and D. P. Miller, "Formulation Design of Dry Powders for Inhalation," *Journal of Pharmaceutical Sciences*, vol. 104, no. 10. John Wiley and Sons Inc., pp. 3259–3288, Oct. 01, 2015, doi: 10.1002/jps.24574.

[10] S. Di Gioia *et al.*, "Nanocomplexes for gene therapy of respiratory diseases: Targeting and overcoming the mucus barrier," *Pulm. Pharmacol. Ther.*, vol. 34, pp. 8–24, 2015, doi: 10.1016/j.pupt.2015.07.003.

[11] F. Depreter, G. Pilcer, and K. Amighi, "Inhaled proteins: Challenges and perspectives," *Int. J. Pharm.*, vol. 447, no. 1–2, pp. 251–280, Apr. 2013, doi: 10.1016/j.ijpharm.2013.02.031.

[12] C. Darquenne, "Particle deposition in the lung," *Encycl. Respir. Med.*, pp. 300–304, 2006.

[13] J. G. Weers *et al.*, "Pulmonary formulations: what remains to be done?," *J Aerosol Med Pulm Drug Deliv*, vol. 23 Suppl 2, pp. S5-23, 2010, doi: 10.1089/jamp.2010.0838.

[14] S. P. Newman, "Drug delivery to the lungs: Challenges and opportunities," *Therapeutic Delivery*, vol. 8, no. 8. Future Medicine Ltd., pp. 647–661, Jul. 01, 2017, doi:

10.4155/tde-2017-0037.

[15] T. H. Nguyen and C. Ward, “Stability characterization and formulation development of alteplase, a recombinant tissue plasminogen activator.,” *Pharm. Biotechnol.*, vol. 5, pp. 91–134, 1993, doi: 10.1007/978-1-4899-1236-7_3.

[16] N. R. Labiris and M. B. Dolovich, “Pulmonary drug delivery. Part II: The role of inhalant delivery devices and drug formulations in therapeutic effectiveness of aerosolized medications,” *Br. J. Clin. Pharmacol.*, vol. 56, no. 6, pp. 600–612, 2003, doi: 10.1046/j.1365-2125.2003.01893.x.

[17] A. P. Earhart, Z. M. Holliday, H. V. Hofmann, and A. G. Schrum, “Consideration of dornase alfa for the treatment of severe COVID-19 acute respiratory distress syndrome,” *New Microbes and New Infections*, vol. 35. Elsevier Ltd, May 01, 2020, doi: 10.1016/j.nmni.2020.100689.

[18] “Protalix Biotherapeutics”, http://protalix.com/products/prx-110-alidornase-alfa/, accessed July 2021.

[19] “Xenetic Biosciences”, https://www.xeneticbio.com/news-media/press-releases/detail/94/xenetic-biosciences-inc-announces-collaboration-with, accessed July 2021.

[20] H.D.C. Smyth and A.J. Hickey, Ed., Controlled Pulmonary Drug Delivery, Advances in Delivery Science and Technology, © Controlled Release Society 2011, doi: 10.1007/978-1-4419-9745-6_2.

[21] G. P. Nokhodchi, Ali; Martin, Ed., Pulmonary Drug Delivery Advances and Challenges, 2015, ISBN: 978-1-118-79954-3.

[22] L. Zhang, D. Pornpattananangkul, C.-M. Hu, and C.-M. Huang, “Development of Nanoparticles for Antimicrobial Drug Delivery,” *Curr. Med. Chem.*, vol. 17, no. 6, pp. 585–594, Feb. 2010, doi: 10.2174/092986710790416290.

[23] H. Yu, J. Teo, J. W. Chew, and K. Hadinoto, “Dry powder inhaler formulation of high-payload antibiotic nanoparticle complex intended for bronchiectasis therapy: Spray drying versus spray freeze drying preparation,” *Int. J. Pharm.*, vol. 499, no. 1–2, pp. 38–46, 2016, doi: 10.1016/j.ijpharm.2015.12.072.

[24] M. Geiser, “Update on Macrophage Clearance of Inhaled Micro-and Nanoparticles.”, *J Aerosol Med Pulm Drug Deliv.*, 23(4):207-17, 2010, doi: 10.1089/jamp.2009.0797.

[25] D. Cipolla, I. Gonda, and H.-K. Chan, “Liposomal formulations for inhalation.,” *Ther. Deliv.*, vol. 4, no. 8, pp. 1047–72, 2013, doi: 10.4155/tde.13.71.

[26] S. Ohtake, Y. Kita, and T. Arakawa, “Interactions of formulation excipients with proteins in solution and in the dried state,” *Advanced Drug Delivery Reviews*. 2011, doi: 10.1016/j.addr.2011.06.011.

[27] A. . Fallis, “No Title No Title,” *J. Chem. Inf. Model.*, vol. 53, no. 9, pp. 1689–1699, 2013,

doi: 10.1017/CBO9781107415324.004.

[28] M. C. McElroy, C. Kirton, D. Gliddon, and R. K. Wolff, “Inhaled biopharmaceutical drug development: nonclinical considerations and case studies.,” *Inhal. Toxicol.*, vol. 25, no. 4, pp. 219–32, 2013, doi: 10.3109/08958378.2013.769037.

[29] M. J. Telko and A. J. Hickey, “Dry Powder Inhaler Formulation,” *Resp. Care*, vol. 50, pp. 1209–1227, 2005, doi: 10.2165/00128413-200615470-00016.

[30] A. M. Healy, M. I. Amaro, K. J. Paluch, and L. Tajber, “Dry powders for oral inhalation free of lactose carrier particles,” *Adv. Drug Deliv. Rev.*, vol. 75, pp. 32–52, 2014, doi: 10.1016/j.addr.2014.04.005.

[31] S. A. Shoyele and S. Cawthorne, “Particle engineering techniques for inhaled biopharmaceuticals,” *Adv. Drug Deliv. Rev.*, vol. 58, no. 9–10, pp. 1009–1029, 2006, doi: 10.1016/j.addr.2006.07.010.

[32] A. Langford, B. Bhatnagar, R. Walters, S. Tchessalov, and S. Ohtake, “Drying technologies for biopharmaceutical applications: Recent developments and future direction,” *Dry. Technol.*, vol. 36, no. 6, pp. 677–684, 2018, doi: 10.1080/07373937.2017.1355318.

[33] M. A. H. Capelle, R. Gurny, and T. Arvinte, “High throughput screening of protein formulation stability: Practical considerations,” *Eur. J. Pharm. Biopharm.*, vol. 65, no. 2, pp. 131–148, 2007, doi: 10.1016/j.ejpb.2006.09.009.

[34] J. G. Weers and D. P. Miller, “Formulation Design of Dry Powders for Inhalation,” *Journal of Pharmaceutical Sciences*, vol. 104, no. 10. John Wiley and Sons Inc., pp. 3259–3288, Oct. 01, 2015, doi: 10.1002/jps.24574.

[35] R. Vehring, “Pharmaceutical particle engineering via spray drying,” *Pharm. Res.*, vol. 25, no. 5, pp. 999–1022, 2008, doi: 10.1007/s11095-007-9475-1.

[36] M. Ameri and Y. F. Maa, “Spray drying of biopharmaceuticals: Stability and process considerations,” *Dry. Technol.*, vol. 24, no. 6, pp. 763–768, 2006, doi: 10.1080/03602550600685275.

[37] L. Chen, T. Okuda, X.-Y. Lu, and H.-K. Chan, “Amorphous powders for inhalation drug delivery,” *Adv. Drug Deliv. Rev.*, 2016, doi: http://dx.doi.org/10.1016/j.addr.2016.01.002.

[38] J. T. Pinto *et al.*, “Progress in spray-drying of protein pharmaceuticals: Literature analysis of trends in formulation and process attributes,” *Dry. Technol.*, 2021, doi: 10.1080/07373937.2021.1903032.

[39] Y. F. Maa *et al.*, “Effect of spray drying and subsequent processing conditions on residual moisture content and physical/biochemical stability of protein inhalation powders,” *Pharm. Res.*, vol. 15, no. 5, pp. 768–775, 1998, doi: 10.1023/A:1011983322594.

[40] P. W. Labuschagne, R. Adami, S. Liparoti, S. Naidoo, H. Swai, and E. Reverchon, “Preparation of rifampicin/poly(D,L-lactice) nanoparticles for sustained release by supercritical assisted atomization technique,” *J. Supercrit. Fluids*, vol. 95, pp. 106–117, 2014, doi: 10.1016/j.supflu.2014.08.004.

[41] S. Soltani, P. Gerde, F. Acevedo, and A. Rasmuson, “Counter-current spray drying with stream separation: Computational modeling of a novel dryer design,” *Chem. Eng. Res. Des.*, vol. 93, no. June, pp. 163–173, 2015, doi: 10.1016/j.cherd.2014.05.023.

[42] K. Berkenfeld, A. Lamprecht, and J. T. McConville, “Devices for dry powder drug delivery to the lung.,” *AAPS PharmSciTech*, vol. 16, no. 3, pp. 479–90, 2015, doi: 10.1208/s12249-015-0317-x.

[43] N. Islam and E. Gladki, “Dry powder inhalers (DPIs)-A review of device reliability and innovation,” *Int. J. Pharm.*, vol. 360, no. 1–2, pp. 1–11, 2008, doi: 10.1016/j.ijpharm.2008.04.044.

[44] R. W. Dal Negro, “Dry powder inhalers and the right things to remember: A concept review,” *Multidisciplinary Respiratory Medicine*, vol. 10, no. 1. BioMed Central Ltd., 2015, doi: 10.1186/s40248-015-0012-5.

CHAPTER 3

Dry powder inhaler formulation of Cu,Zn-superoxide dismutase by spray drying: a proof-of-concept

Running heads:

- *Is it possible to spray dry a model therapeutic enzyme of a biologic while keeping its conformation and functional activity?*

This chapter has been published as:

Fernandes D A, Leandro P, Costa E, Corvo ML: *Dry powder inhaler formulation of Cu,Zn-superoxide dismutase by spray drying: a proof-of-concept.* Powder Technology 389 (2021) pp. 131-137.

Fernandes D A, Barros R, Moura C, Costa E, Corvo M L: *Impact of Spray Drying on Superoxide Dismutase Activity in Composite Systems with Optimal Aerodynamic Performance for Dry Powder Inhalers.* Journal of Aerosol Medicine and Pulmonary Drug Delivery, Vol 30, Issue 4, Drug Delivery to the Lungs 27, December 2016, Edinburgh, Scotland.

Fernandes D A, Leandro P, Corvo M L, Costa E: *Spray Drying of Biopharmaceuticals: A Successful Case-Study for Pulmonary Drug Delivery.* Bioprocessing Summit Europe 2018, Lisboa, Portugal.

3.1 OVERVIEW

Despite the advantages of targeting the pulmonary route through dry powder inhalers (DPI), the efficient delivery of biologics to the lungs still presents a considerable challenge: the generation of a powder with adequate aerodynamic properties while preserving the integrity of the biologic. Hence, the particle engineering technology employed to meet this balance plays a pivotal role.

Goal: The present work describes a proof-of-concept study to investigate the effect of spray drying (SD) outlet temperature (T_{out}), atomization flow rate (Rot_{atom}) and feed flow rate (F_{feed}) on powder properties such as particle morphology and aerodynamic performance but also on the enzyme activity and protein conformational stability of a trehalose:leucine spray-dried powder featuring Cu,Zn-superoxide dismutase (Cu,Zn-SOD) as a model Active Pharmaceutical Ingredient (API).

Results: Morphology and aerodynamic performance of the SD powders were determined by scanning electron microscopy (SEM), focused ion beam – SEM, laser diffraction and Andersen Cascade Impaction. For each SD run, enzyme activity retention (EAR) was measured by spectrophotometry and the protein melting temperature by differential scanning fluorimetry. To further understand the interaction between input and output variables, a statistical analysis was performed using SIMCA v13.0.3.0 software.

Conclusions: Cu,Zn-SOD:trehalose:leucine spray dried powders were successfully generated upon different processing conditions, displaying fine particle fractions of ≈60 % and EAR ranging 50-80 % with no loss of protein conformational stability. This technology thus proved to be suitable to prepare Cu,Zn-SOD based DPI powders within the considered working ranges.

3.2 INTRODUCTION

Significant advances on recombinant DNA technology and the repurpose of chemical synthesis, coupled with the rising capacity of large-scale production of therapeutic biologics, are paving the way towards the cumulative increase of macromolecules in the pharmaceutical industry pipeline [1-3]. In particular, inhaled formulations are increasingly attractive not only to treat respiratory diseases but also systemic diseases due to the large surface area available for drug absorption and the avoidance of first-pass metabolism. This ultimately translates into a rapid onset of the drug action, reducing the required drug load and minimizing adverse side effects, whilst improving patient compliance over injectables [3].

Pulmonary delivery can be performed using three main platforms: nebulizers, pressurized metered-dose inhalers (pMDIs) and dry powder inhalers (DPIs) [4]. Biologics, such as Dornase alfa (Pulmozyme®, Tigerase®) for the treatment of Cystic Fibrosis and other respiratory infections, have already been successfully formulated in nebulizers [5, 6]. However, its liquid state nature may result in the early stability loss for some biological molecules upon storage when compared to solid state formulations [8-10]. Moreover, nebulization requires long periods of dosing due to inefficient drug deposition, leading to drug wastage and require device sterilization between uses [9]. On the other hand, pMDIs use for biologics administration is relatively scarce [11-13] given the exposure of the drug to shear stress during device actuation along with the complexity of generating stable formulations in the commonly used propellants [10]. Finally, DPIs address these shortcomings, taking advantage of more stable solid based formulations and without any need for propellants.

Despite the advantages of targeting the pulmonary route through DPIs, the efficient delivery of biologics to the lungs still presents a significant challenge: the generation of an aerosol with adequate aerodynamic properties while preserving the integrity of the biologic. Hence, the particle engineering technology employed to meet this balance plays a pivotal role.

Spray Drying (SD) emerges as a viable technology given its relative simplicity (one-step process), cost effectiveness and scalability with increased control over key aerosol features

that impact its aerodynamic performance such as particle size, shape, internal structure, surface, among others, by fine-tuning formulation composition and process parameters [11][15]. This has been widely employed to prepare inhalable dry powder dosage forms as already described in [16]-[19]. This technology is also regarded as suitable for biologics due to the mild temperature exposure through evaporative cooling and short residence times. In addition, the wide range of SD scales commercially available, including miniaturized set-ups with low volume requirements, render it a promising alternative when working with these rather expensive molecules.

Spray dried powder dosage forms for DPIs may comprise Active Pharmaceutical Ingredients (APIs) alone or combined with excipients. Enzymes can be high potency APIs requiring lower doses (in the µg range) to achieve their therapeutic effect. As a result, excipients may be added as bulking agents only to enable accurate metering [20]. Non reducing sugars and amino acids are the standard, most safe and simple excipients used to formulate spray dried powder dosage forms for DPIs featuring an enzyme or any other biopharmaceutical as API. Non-reducing sugars exert their stabilizing effect by replacing hydrogen bonds that otherwise would be formed between water molecules and the enzyme in the dry solid state. Non-reducing sugars also allow to circumvent the Maillard reaction. In this reaction, induced by temperature, reducing sugars react with the amino groups from the enzymes forming a carbohydrate adduct. Besides occurring a protein modification (glycation), one of the byproducts of the Maillard reaction is water which can trigger enzyme aggregation mechanisms. The water replacement theory, previously elaborated for non-reducing sugars, was also proposed to explain the stabilization induced by the amino acids. In particular, hydrophobic amino acids (amino acids that have hydrophobic groups in their side chains) can orient their hydrophobic groups towards the air at the air/liquid interface during the drying process, avoiding adsorption and denaturation of the enzyme. Moreover, the hydrophobic surface they provide to the spray dried particles helps improve the aerodynamic performance [20].

Herein, the impact induced by SD on the aerodynamic performance, enzyme activity retention (EAR) and conformational stability of Cu,Zn-Superoxide Dismutase (Cu,Zn-SOD), embedded in a trehalose:leucine powders for DPIs, is assessed by screening three process variables - Outlet temperature (T_{out}), Feed and Atomization flow rates (F_{feed} and Rot_{atom}). Cu,Zn-SOD was used as a model enzyme since it is a protein often implicated as potential drug in a broad spectrum of oxidative stress related diseases, from Cystic Fibrosis to Rheumatoid Arthritis, catalyzing the dismutation of superoxide radicals and so providing the first line of defense against reactive oxygen species [21].

3.3 MATERIALS AND METHODS

3.1.1 Materials

Bovine erythrocytes Cu,Zn-SOD (S7571, 32 g/mol) was purchased from Sigma (St. Louis, MO, USA). D-trehalose dihydrate and L-leucine were purchased from EMD Millipore Corp. (Billerica, MA USA). Ultra-pure type II Millipore water from a Milli-Q water purification system was used in all studies.

3.1.2 Methods

3.3.2.1 Spray Drying

The feed solutions for SD comprised trehalose:leucine (4:1) (composition previously optimized [21]) at 2 % (w/w) of solids content in double distilled deionized water (ddH_2O) at pH 6-7. Cu,Zn-SOD, was added at 0.1 % (w/w) concentration. Spray drying was performed at a lab-scale (Mini Spray Drier BUCHI, model B-290 (Büchi Labortechnik AG, Flawil, Switzerland) equipped with a two-fluid-nozzle (orifice 0.7 mm, core/cap 1.5 mm) refrigerated by external water bath re-circulation. T_{out}, F_{feed} and Rot_{atom} were the factors selected to study SD induced stress on Cu,Zn-SOD. For each variable two levels (low and high) were set. T_{out} range was defined based on a minimum suitable temperature for evaporating ddH_2O and on Cu,Zn-SOD melting temperature (T_m). For the high level of T_{out}, a temperature value exceeding Cu,Zn-SOD melting Temperature was chosen to assess its actual impact on enzyme activity retention and conformational stability. The feed and atomization flow rates low and high values were defined so it would fall in the range tested for the previously optimized excipient matrix of trehalose:leucine in [21], intended for inhalation. The atomization flow rate is expressed in mm unit of the spray dryer rotameter that controls this process parameter.

Overall, T_{out}, F_{feed} and Rot_{atom} ranges were adjusted in agreement with a full factorial experimental design 2^3, plus an additional center point, resulting in a total of nine different

tests (Table 3.1). Nitrogen was used as drying gas flow rate (F_{drying}) and together with SD feed solutions composition was kept constant across trials.

Table 3.1 – *Spray Drying conditions tested, according to the defined design of experiments (DoE).*

Test	T_{out} (°C)	Rot_{atom} (mm)	F_{feed} (g.min^{-1})	F_{drying} (kg.h^{-1})	Schematic representation of the defined DoE
1	65	40	3	35	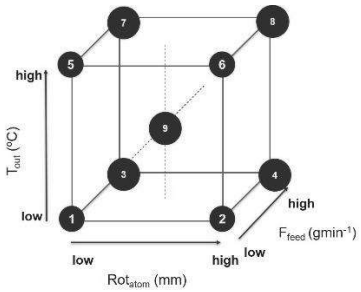
2		60	3		
3		40	9		
4		60	9		
5	95	40	3		
6		60	3		
7		40	9		
8		60	9		
9	80	50	6		

Note: T_{out} – Outlet temperature; Rot_{atom} – Atomization flow rate expressed in mm unit of the spray dryer rotameter that controls this process parameter (40 mm ~ 0.86 kgh^{-1} ; 60 mm ~ 2.1 kgh^{-1}); F_{feed} – Feed flow rate; F_{drying} – Drying flow rate.

3.3.2.2 Powder and Protein Characterization

3.3.2.2.1 Scanning Electron Microscopy and Focused Ion Beam Scanning Electron Microscopy

The shape, surface of the dry powders was assessed by Scanning Electron Microscopy (SEM) and the inner morphology by Focused Ion Beam (FIB)–SEM. SD powder samples were attached to adhesive carbon tapes (Ted Pella, Inc., CA, USA) and the excess removed by a jet of pressurized air. The samples were exposed to vacuum for 2 hours and coated with a 15 nm gold layer (South Bay Technologies, former Polaron, model E5100, San Clement, CA). A scanning electron microscope (JEOL JSM-7001/Oxford INCA Energy 250/HKL, Japan) in high vacuum mode was used with a typical accelerating voltage between 5 and 20 kV. FIB–SEM was performed to observe the inner cross-section of individual particles, Ga^+ ions were accelerated to 30 kV at 2 pA and the etching depth was kept around 300 nm. A thin layer of ~30 nm of carbon was deposited on the material surface to minimize Ga contamination.

3.3.2.2.2 Laser Diffraction

Particle size distribution was determined by Laser Diffraction (LD) using the particle size analyzer Sympatec HELOS in combination with RODOS and the ASPIROS modules (Sympatec GmbH, Clausthal-Zellerfel, Germany). The optical bench of the HELOS module (H3330) was equipped with R1 and R4 Fourier lenses that cover particle sizes between 0.18-35 µm and 1.8-350 µm, respectively. The sample vials were prepared in a glove box and filled with powder until one third of the vial was complete. The vials were then inserted into ASPIROS module and powders dispersed at 3.0 bar pressure with compressed air and a feed rate velocity of 18 $mm.s^{-1}$, while targeting an optical concentration (C_{opt}) above 1 %. Particle size (Dv10, Dv50 and Dv90) was computed using WINDOX5.0 software (Sympatec GmbH, Clausthal-Zellerfel, Germany) and span values determined as (Dv90-Dv10)/Dv50.

3.3.2.2.3 Andersen cascade impaction

Powders aerodynamic performance was assessed *in vitro* using an eight-stage gravimetric Andersen cascade impactor (Copley 88 Scientific Ltd., Nottingham, UK). All powders were hand-filled inside a glovebox with controlled relative humidity below 10%, in HPMC size 3 capsules (Capsugel, Basel, Switzerland) with 20 ± 0.4 mg of each formulation, in triplicate, and were actuated for 4 s, using a Plastiape device HR model 7 at 60 $L.min^{-1}$, targeting a pressure drop of 4 kPa. The filter from each stage was weighted before and after each actuation. The fine particle fraction (FPF) was determined as the percentage of the powder mass emitted from the capsule displaying an aerodynamic diameter below 5 µm. The Mass Median Aerodynamic Diameter (MMAD) and the Geometric Standard Deviation (GSD) were retrieved from CITDAS software (Copley 88 Scientific Ltd., Nottingham, UK).

3.3.2.2.4 Cu,Zn-SOD recovery yield and Enzyme Activity Retention

For each SD run, total protein was quantified using a modified Lowry method [21]. Aiming to avoid excipients interference in the assay, trehalose and leucine were previously removed by

enzyme precipitation with trichloroacetic acid at 10%. Cu,Zn-SOD enzymatic activity measurements were performed in triplicate using the SOD Assay Kit – WST (Sigma, St. Louis, MO, USA) and a UV/Vis spectrophotometer Shimadzu UV 160A spectrophotometer (Shimadzu Corporation, Kyoto, Japan). Herein, the water-soluble tetrazolium salt WST-1 (2-(4-Iodophenyl)-3-(4-nitrophenyl)-5-(2,4-disulfophenyl)-2H-tetrazolium, monosodium salt) is reduced by superoxide radical anions, generated by the xanthine/xanthine oxidase system, to a water-soluble formazan (WST-1 formazan) dye that absorbs at 440 nm. In the presence of Cu,Zn-SOD, the produced superoxide radical anions are oxidized to O_2 or reduced to H_2O_2, instead of reducing WST-1 thus decreasing WST-1 formazan dye formation and color development ($\lambda_{440\ nm}$). EAR was determined considering the Cu,Zn-SOD enzymatic activity before SD as 100%.

3.3.2.2.5 Differential Scanning Fluorimetry

Differential Scanning Fluorimetry (DSF) was performed in triplicate using a thermal cycler (CFX96 Touch™ Real-Time PCR Detection system; BIO-RAD) set to equilibrate samples at 20 °C for 10 minutes followed by an increase up to 97 °C at a rate of 1 °C.min^{-1}, with fluorescence acquisition every 0.2 °C. The thermal denaturation assays were performed on 96-well plates, using a final volume of 50 µL containing 10 µg of Cu,Zn-SOD before (Before SD; Cu,Zn-SOD in optimized excipient matrix mimicking the feed solution) and after SD (After SD) and 0.05 µL of SYPRO® Orange (Invitrogen) stock solution diluted 2000x. The temperature scan curves were fitted to a sigmoidal dose-response function, and the T_m values were obtained. The T_m values after SD ($T_{m\ After\ SD}$) were compared to those obtained before SD ($T_{m\ Before\ SD}$) to obtain the ΔT_m ($T_{m\ After\ SD}$- $T_{m\ Before\ SD}$). An increase in protein stability was considered when $\Delta T_m \geq +2$ °C [22].

3.3.2.3 Statistical Analysis

To further understand the interaction between the studied factors (T_{out}, Rot_{atom} and F_{feed}) on the morphology, aerodynamic performance, protein yield, EAR and ΔT_m of Cu,Zn-SOD

powders, a multivariate statistical analysis based on partial least squares (PLS) regression model was performed using SIMCA v13.0.3.0 software (Umetrics).

3.4 RESULTS AND DISCUSSION

Outlet temperature (T_{out}), feed (F_{feed}) and atomization (Rot_{atom}) flow rates were the factors selected to study spray drying induced stress on Cu,Zn-SOD:trehalose:leucine powders based on a risk assessment and previous knowledge around the potential impact of these process parameters on the studied outputs.

Morphology and aerodynamic performance of the spray dried powders were determined to evaluate their suitability from an inhalation standpoint. To assess the impact of the tested process variables on Cu,Zn-SOD, the total protein was quantified, enzyme activity retention (EAR) and conformational stability (through T_m shift) were measured for each SD run. To further understand the interaction between the input (T_{out}, Rot_{atom} and F_{feed}) and output variables (morphology, aerodynamic performance, protein yield and, EAR and $T_{m\ After\ SD}$) of Cu,Zn-SOD:trehalose:leucine powders, a multivariate statistical analysis based on partial least squares (PLS) regression model was also performed.

3.4.1 Impact of process variables on Morphology and Aerodynamic Performance of Cu,Zn-SOD SD Powders

The shape and surface of the dry powders was assessed by Scanning Electron Microscopy (SEM) and the inner morphology by Focused Ion Beam (FIB)–SEM. The SEM micrographs of the nine SD powders were very similar among each other, regardless of the test condition, presenting a spherical and slightly shriveled outer particle morphology (Figure 3.1A). On the other hand, FIB-SEM micrographs showed two different inner particle morphologies (when comparing particles of the same size): solid particles for lower T_{out}, (Figure 3.1B; Test 1) and hollow particles (Figure 3.1B; Test 5 and Test 9) for higher T_{out}. As previously reported by Vehring et al [23], for glycoprotein particles, the higher the drying gas temperature (considering the remaining process parameters constant), the lower the particle density, ultimately translating in the increase of the void in the particle's core. However, herein, protein concentration is 0.1% against 99.9% of excipients (trehalose and leucine), hence, particles

lower density as a function of T_{out} is more likely to be driven by these rather than by Cu,Zn-SOD drying kinetics.

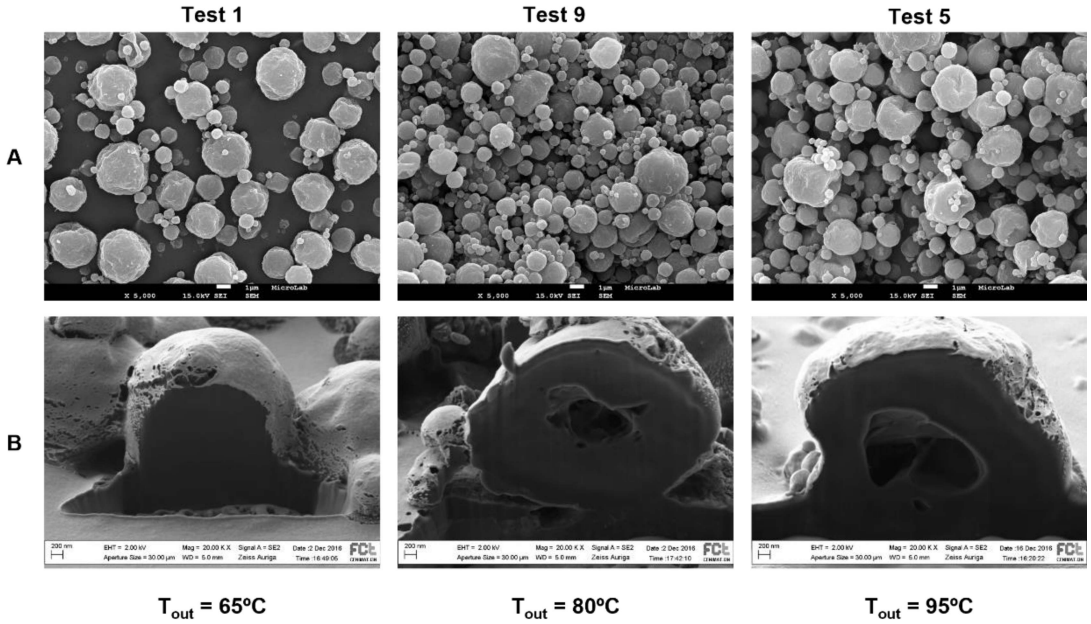

Figure 3.1 *- Scanning electron microscopy (SEM) (A) and focused ion beam (FIB)-SEM (B) micrographs of obtained Spray Drying (SD) powders as a function of outlet temperature (T_{out}) for Tests 1 and 5 sharing the same atomization (Rot_{atom}) and feed flow (F_{feed}) rates and for Test 9, the center point. The outer particle morphology was very similar among each other (A), presenting spherical and slightly shriveled particles, with a particle size within the inhalable size range but with. two different inner particle morphologies (B)* Scale bars: 1 μm (A) and 200 nm (B).

According to the same study [23], spray dried trehalose particles displayed the same density and solid inner core, regardless of the T_{out} employed. Spray dried leucine, on the other hand, behaves differently. Leucine is expected to crystallize during drying due its low solubility, enriching the receding droplet surface because of its low mobility [24], resulting in an outer shell/skin. The higher the $T_{out,}$ the faster the drying kinetics and the larger is the leucine surface enrichment of the shell/skin [24], through which the remaining water is diffused or evaporates yielding lower density particles. These observations are in line with the results obtained in this study, as to the solid inner core particles corresponds the lowest T_{out} and to the hollow inner core particles corresponds the highest T_{out}. In addition, the increase in size of the void in the particle's core seems to follow the increase in T_{out}, when comparing Tests 5 and 9 (Figure 3.1B). Moreover, the apparent particle size observed in the SEM (~0.5 - 3 μm) and FIB-SEM

(~1.5 µm) micrographs is also in agreement with the particle size distribution (Dv50 and span) quantitatively determined by LD (Table 3.2).

***Table* 3.2 –** *Particle size distribution (Dv50, span) determined by laser diffraction, aerodynamic particle size distribution (MMAD and GSD) and fine particle fraction based on Emitted Dose (FPF_{ED}.) determined by Anderson Cascade Impaction, for the tested conditions.*

	Particle Size Distribution		Aerodynamic Particle Size Distribution		Fine Particle Fraction	
Test	**Dv50 (µm)**	**span**	**MMAD (µm)**	**GSD**	**FPF_{ED} (%)**	**±sd**
1	2.3	1.9	3.7	1.7	48.2	2.17
2	1.6	1.9	2.7	1.8	59.8	0.69
3	2.1	2.1	3.5	1.8	47.4	4.47
4	1.7	1.8	2.8	1.8	57.8	2.91
5	2.1	1.9	3.3	1.7	52.8	6.23
6	1.5	1.9	2.8	1.6	60.6	5.24
7	2.3	2.0	3.8	1.7	45.3	2.01
8	1.5	1.9	2.6	1.7	61.4	2.76
9	1.9	1.9	3.0	1.7	57.1	2.63

Note: Each test corresponds to a Spray drying outlet temperature (T_{out}), atomization (Rot_{atom}) and feed (F_{feed}) flow rate conditions according to Table 3.1. Dv50 – Mean particle size span – (Dv90-Dv10)/Dv50. MMAD – mass median aerodynamic diameter; GSD – geometric standard diameter; sd – standard deviation.

Particle size is independent of T_{out} and F_{feed} as similar ranges of Dv50 and span can be observed both for low (Dv50 = 1.6-2.3 µm, span = 1.8-2.1 at T_{out} = 65 ºC; F_{feed} = 3 $g.min^{-1}$) and high (Dv50 = 1.5-2.3 µm, span = 1.9-2.0 at T_{out} = 95 ºC; F_{feed} = 9 $g.min^{-1}$) levels of these process variables. Rot_{atom} is thus the predominant factor responsible for the different particle size between tests with distinct values for this parameter: the higher the value of Rot_{atom} the lower the Dv50 values, as a consequence of a lower droplet size, as reported in previous studies [21][25].

The ACI tests performed to assess the powders aerodynamic performance resulted in FPF based on Emitted Dose (FPF_{ED}) ranging from 45.3 ± 2.01 to 61.4 ± 2.76% with a capsule Emitted Dose higher than 98%. The obtained FPF_{ED} and MMAD (Table 3.2) followed the same trend observed for particle size distribution being mainly dependent once again on Rot_{atom} regardless of T_{out} and F_{feed} values. In fact, the highest range of FPF (57.8 ± 2.91 to 61.4± 2.76%) and the lowest range of MMAD (2.6 to 2.8 µm) obtained match the test conditions performed for the high level of Rot_{atom} (60 mm).

3.3.3 Impact of process variables on Cu,Zn-SOD Enzyme Activity Retention and Conformational Stability

The Cu,Zn-SOD recovery yield, enzyme activity retention (EAR) and conformational stability were determined for all nine tests. Protein yield values were higher than 60% with EAR values ranging from 55 ± 5% to 80 ± 5% (Table 3.3).

***Table* 3.3 –** *Protein yield and enzyme activity retention (EAR) for all test conditions.*

Test	Protein yield (%)	Enzyme activity retention (%)
1	>95	50-60
2	90-95	65-75
3	90-95	65-75
4	80-85	70-80
5	>95	50-60
6	90	65-75
7	60-65	70-80
8	80-85	75-85
9	75-80	70-80

Note: Each test corresponds to a spray drying outlet temperature (T_{out}), atomization flow rate (Rot_{atom}) and feed flow rate (F_{feed}) condition, according to Table 3.1.

The protein yield observed for tests 1 and 5 sharing the same low-level values of Rot_{atom} and F_{feed} (40 mm, 3 $gmin^{-1}$) exceeded 95%. The lowest EAR values (55 ± 5%) were also obtained for tests 1 and 5 powders. The lower F_{feed} employed in these tests entails an increase of the residence time of the solution exposed to the shear stress induced by the interaction between the liquid feed and gas stream [26]. Additionally, the lower Rot_{atom} results in larger droplet sizes yielding particles with higher residual water content (for the same drying flow rate) [20][23] that, given the greater mobility, may trigger agglomeration events, rendering the protein´s active site less accessible for reaction.

T_{out} had a negligible impact, as EAR values were similar both at 65ºC and 95ºC for the same Rot_{atom} and F_{feed} conditions.

The conformational stability of a protein is often associated with its melting temperature (T_m), defined as the temperature at which half of the protein is in an unfolded state [22]. The higher the T_m, the more stable is the protein conformation. Cu,Zn-SOD conformational stability was assessed by monitoring its T_m before and after SD. An increase and decrease in protein

stability was considered when $\Delta T_m \geq +2$ ºC and $\Delta T_m \leq -2$ ºC, respectively [22]. In Figure 3.2A, a slight stabilizing effect induced by the presence of trehalose:leucine excipient system could be observed on Cu,Zn-SOD, before spray drying, as its T_m value increased from 75.6 ± 0.3 to 77.2 ± 1.0 ºC. As shown in Figure 3.2C, a statistically relevant shift on T_m (p-value ≤ 0.05) was only obtained for Tests 1, 5, 6 and 7 after spray drying.

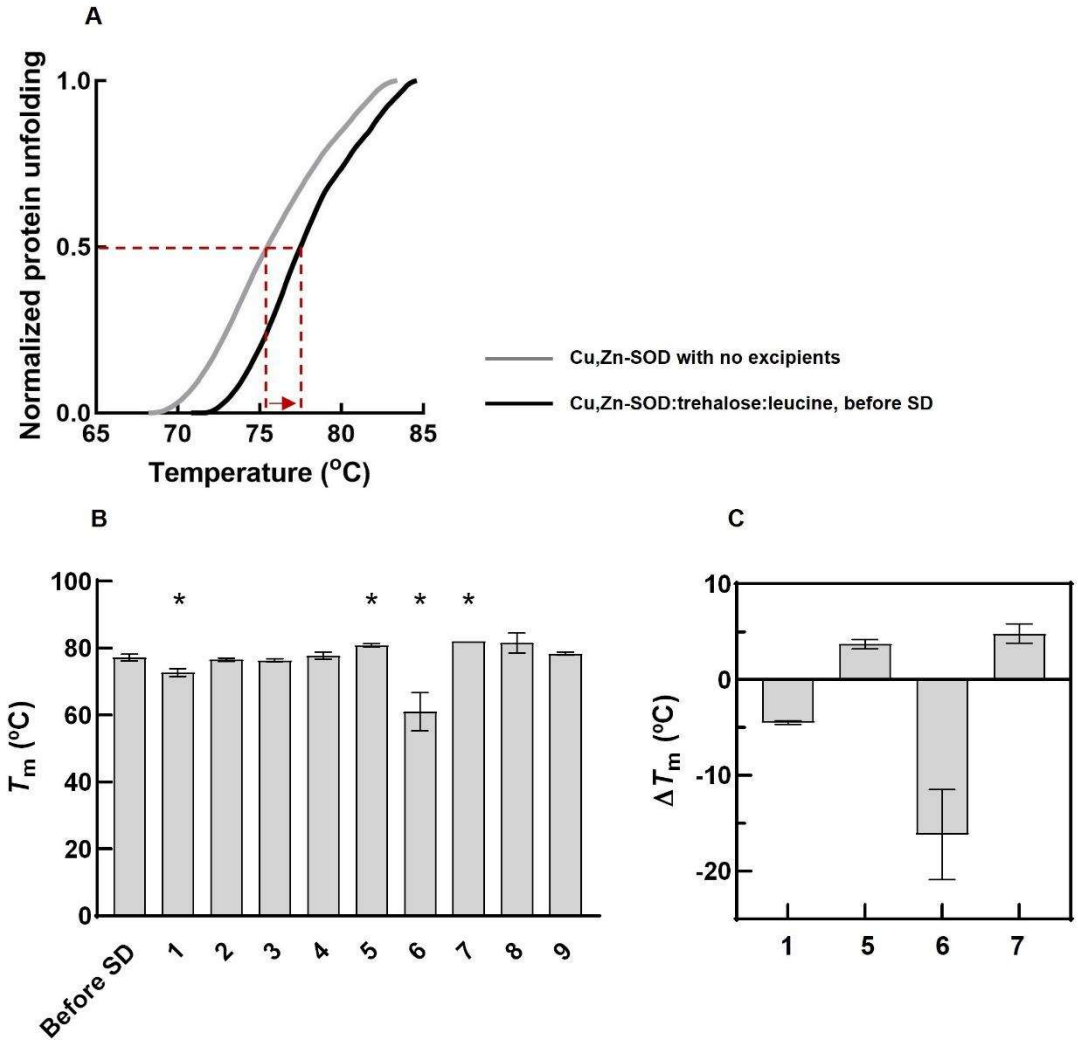

Figure 3.2 - Analysis of Cu,Zn-SOD thermal denaturation, before and after spray drying (SD), monitored by differential scanning fluorimetry (DSF) A. Cu,Zn-SOD denaturation profile before SD in the absence and presence of trehalose:leucine excipient; the determined melting temperatures (T_m) *are shown for the enzyme in the absence (75.6 ± 0.3 ºC) and presence of excipients (77.2 ± 1.0 ºC), corresponding to a* ΔT_m *= 1.6 °C ± 0.7 ºC.* **B.** T_m determined by DSF before SD (Before SD) and after SD, for all test conditions (1-9) and representing the mean ± standard deviation (n=3); statistically significant difference between after SD test conditions and Before SD: *p ≤ 0.05. **C.** Tm shifts (ΔT_m) calculated for the test conditions where a statistically significant difference (p ≤ 0.05) of T_m

was observed (B). $\Delta T_m \geq +2$ ºC was obtained when SD trials were performed at a higher T_{out} (95 °C) namely, test 5 (ΔT_m = 3.7 ± 0.5 ºC) and 7 (ΔT_m = 4.8 ± 1.0 ºC).

A $\Delta T_m \geq +2$ ºC was obtained when SD trials were performed at a higher T_{out} (95 °C) namely, test 5 (ΔT_m = 3.7 ± 0.5 ºC) and 7 (ΔT_m = 4.8 ± 1.0 ºC). This could be possibly attributed to the lower residual water content of the spray dried powders at higher temperatures, ultimately reducing Cu,Zn-SOD interaction with the excipient matrix and stabilizing the protein conformation. Negative ΔT_m (≤ -2 ºC) were only observed for trials 1 (ΔT_m = -4.5 ± 0.2 ºC) and 6 (ΔT_m = -16.1 ± 4.7 ºC) both performed at the lowest F_{feed}. For trial 1, a decrease in both T_m and EAR was observed. However, SD using condition 6 resulted in a protein with lower conformational stability but with an EAR of 70%. It must be emphasized that loss of protein conformational stability is not necessarily linked to a lower enzyme activity as a change in protein conformation leading to structural instability may result in a favorable electrostatic potential in the catalytic pocket for substrate binding [28].

3.4 Input and Output Variables Interaction assessed by Statistical Analysis

In order to fine-tune the process aiming to maximize powder performance and protein stability, a multivariate statistical analysis was carried out to further understand the interaction between T_{out}, Rot_{atom} and F_{feed} – inputs – on powder morphology (Dv50), aerodynamic performance (MMAD, FPF), Cu,Zn-SOD EAR and $T_{m\ after\ SD}$ – outputs – as shown on Table 3.4.

Table 3.4 – *Direct, (+), or inverse, (-) relationship (in grey) between input (T_{out}, Rot_{atom}, F_{feed}) and output (Dv50, MMAD, FPF, EAR, $T_{m\ after\ SD}$) variables that allowed for the best PLS regression model fit (R^2>0.7) and prediction (Q^2>0.5; R^2- Q^2<0.2-0.3) retrieved by SIMCA.*

	T_{out}	Rot_{atom}	F_{feed}	R^2	Q^2	R^2-Q^2
Dv50	-	(-)	-	0.92	0.89	0.03
MMAD	-	(-)	-	0.88	0.84	0.04
FPF_{ED}	-	(+)	-	0.89	0.87	0.02
EAR	-	(+)	(+)	0.82	0.72	0.10
$T_{m\ After\ SD}$	(+)	-	-	0.78	0.72	0.06

Note: Dv50 – Mean particle size; MMAD – Mass Median Aerodynamic Diameter; FPF_{ED} – Fine Particle Fraction based on Emitted Dose; EAR – Enzymatic Activity Retention; $T_{m\ After\ SD}$ – Melting Temperature after Spray Drying.

This showcases which input variables allowed for the best fit (R^2>0.7 [29]) and prediction (Q^2>0.5; R^2- Q^2<0.2-0.3 [29]) of the derived PLS regression models describing each one of the output variables.

PLS regression models obtained for Dv50, MMAD and FPF displayed the best fit and prediction only when considering Rot_{atom} as input parameter.

No PLS regression models could be obtained for protein yield as a function of the tested input variables. Concerning EAR, the PLS regression model obtained exhibited the best fit and prediction when this was simultaneously predicted by Rot_{atom} and F_{feed}. The higher the Rot_{atom} and F_{feed} the higher the EAR as previously elaborated.

PLS regression models obtained for $T_{m\ After\ SD}$ displayed the best fit and prediction when this was described as a function of T_{out}. F_{feed} and Rot_{atom}, on the other hand, had a negligible impact within the explored ranges, suggesting that the shear stress induced by these parameters does not impair the protein conformational stability.

When assessing if any PLS regression model could be derived displaying good fit and prediction among output variables (Table 3.5), this was only possible for Dv50, MMAD and FPF_{ED}. The lower the Dv50, the lower the MMAD and the higher the FPF_{ED}. Despite showcasing a correlation coefficient (R^2) of 0.0749<<0.7 (threshold above which a model is considered to present a good fit [29]), EAR seemed to be inversely correlated with protein yield (Table 3.3).

Table 3.5 – *Direct, (+), or inverse, (-) relationship (in grey) between output (Dv50, MMAD, FPF, EAR, $T_{m\ after\ SD}$) variables that allowed for the best PLS regression model fit (R^2>0.7) and prediction (Q^2>0.5; R^2- Q^2<0.2-0.3) retrieved by SIMCA.*

	Dv50	**MMAD**	**FPF_{ED}**	**EAR**	**$T_{m\ After\ SD}$**	**R^2**	**Q^2**	**R^2-Q^2**
Dv50	-	(+)	(-)	-	-	0.91	0.89	0.02
MMAD	(+)	-	(-)	-	-	0.97	0.96	0.01
FPF_{ED}	(-)	(-)	-	-	-	0.90	0.88	0.02
EAR	-	-	-	-	-	-	-	
$T_{m\ After\ SD}$	-	-	-	-	-	-	-	

Note: Dv50 – Mean particle size; MMAD – Mass Median Aerodynamic Diameter; FPF_{ED} – Fine Particle Fraction based on Emitted Dose; EAR – Enzymatic Activity Retention; $T_{m\ After\ SD}$ – Melting Temperature after Spray Drying.

This may be due to excipients co-precipitation with the enzyme, when adding the trichloroacetic acid, or to the inefficient removal of the supernatant. The presence of these excipients in the protein solution, could have contributed to an overestimation of protein concentration, ultimately resulting in lower EAR values as enzyme activity was calculated as a function of protein used in the assay (specific enzyme activity). No PLS regression models could be obtained when correlating EAR and $T_{m\ After\ SD}$.

3.5 CONCLUSIONS

In the present work, spray dried Cu,Zn-SOD:trehalose:leucine powders for DPIs were successfully generated while preserving enzymatic activity and protein conformational stability. In addition, the impact induced by SD on powder and enzyme properties was accessed by screening three process variables - T_{out}, Rot_{atom} and F_{feed}. Particle size and aerodynamic performance of the SD powders was mainly affected by Rot_{atom} while enzyme activity was mainly influenced by Rot_{atom} and F_{feed} and conformational stability by T_{out}. T_{out} also seemed to have impacted powders inner particle morphology.

Among output variables, it was only possible to establish a correlation between Dv50, MMAD and FPF_{ED} - the lower the Dv50, the lower the MMAD and the higher the FPF_{ED}. However, no correlation could be found between EAR and $T_{m\ After\ SD}$ shift with the remaining output variables. The obtained data also suggests that higher values of T_{out}, $Rot_{atom,\ and}$ F_{feed} can be employed to successfully spray dry Cu,Zn-SOD embedded in trehalose:leucine inhalable powders.

REFERENCES

[1] B. S. Sekhon, “Biopharmaceuticals: An overview,” *Thai J. Pharm. Sci.*, vol. 34, no. 1, pp. 1–19, 2010, doi: 10.1007/978-94-017-0926-2_1.

[2] D. J. A. Crommelin, G. Storm, R. Verrijk, L. De Leede, W. Jiskoot, and W. E. Hennink, “Shifting paradigms: Biopharmaceuticals versus low molecular weight drugs,” *Int. J. Pharm.*, vol. 266, no. 1–2, pp. 3–16, 2003, doi: 10.1016/S0378-5173(03)00376-4.

[3] E. Bodier-Montagutelli, A. Mayor, L. Vecellio, R. Respaud, and N. Heuzé-Vourc’h, “Designing inhaled protein therapeutics for topical lung delivery: what are the next steps?,” *Expert Opin. Drug Deliv.*, vol. 15, no. 8, pp. 729–736, 2018, doi: 10.1080/17425247.2018.1503251.

[4] D. A. Fernandes, R. Barros, C. Moura, E. Costa, and M. L. Corvo, “Impact of Spray Drying on Superoxide Dismutase Activity in Composite Systems with Optimal Aerodynamic Performance for Dry Powder Inhalers.”, Journal of Aerosol Medicine and Pulmonary Drug Delivery, Volume 30, Issue 4, 2017, doi: 10.1089/jamp.2017.ab02.abstracts.

[5] J. S. Wagener and O. Kupfer, “Dornase alfa (Pulmozyme),” *Curr. Opin. Pulm. Med.*, vol. 18, no. 6, pp. 609–614, 2012, doi: 10.1097/MCP.0b013e328358d51f.

[6] R. P. Saha *et al.*, “Repurposing Drugs, Ongoing Vaccine, and New Therapeutic Development Initiatives Against COVID-19,” *Front. Pharmacol.*, vol. 11, no. August, pp. 1–33, 2020, doi: 10.3389/fphar.2020.01258.

[7] Y. Guo, E. Shalaev, and S. Smith, “Physical stability of pharmaceutical formulations: Solid-state characterization of amorphous dispersions,” *TrAC - Trends Anal. Chem.*, vol. 49, pp. 137–144, 2013, doi: 10.1016/j.trac.2013.06.002.

[8] U. Angkawinitwong, G. Sharma, P. T. Khaw, S. Brocchini, and G. R. Williams, “Solid-state protein formulations,” *Ther. Deliv.*, vol. 6, no. 1, pp. 59–82, 2015, doi: 10.4155/tde.14.98.

[9] R. Dalby and J. Suman, “Inhalation therapy: Technological milestones in asthma treatment,” *Adv. Drug Deliv. Rev.*, vol. 55, no. 7, pp. 779–791, 2003, doi: 10.1016/S0169-409X(03)00077-2.

[10] K. Berkenfeld, A. Lamprecht, and J. T. McConville, “Devices for dry powder drug delivery to the lung.,” *AAPS PharmSciTech*, vol. 16, no. 3, pp. 479–90, 2015, doi: 10.1208/s12249-015-0317-x.

[11] É. Quinn, R. Forbes, A. Williams, M. Oliver, L. McKenzie, T. Purewal, “Protein conformational stability in the hydrofluoralkane propellants tetrafluoroethane and heptafluoropane analysed by Fourir transform Raman spectroscopy”, International Journal of Pharmaceutics, 186, pp. 31-41, 1999, doi: 10.1016/s0378-5173(99)00135-

0.

[12] H. Li, P. Seville “Novel pMDI formulations for pulmonary delivery of proteins”, International Journal of Pharmaceutics, 385, pp. 73-78, 2010, doi:10.1016/j.ijpharm.2009.10.032.

[13] Y. Tan, Z. Yang, X. Peng, F. Xin, Y. Xu, M. Feng, C. Zhao, H. Hu, C. Wu, “A novel bottom-up process to produce nanoparticles containing protein and peptide for suspension in hydrofluoroalkane propellants”, International Journal of Pharmaceutics, 413, pp. 167-173, 2011, doi: 10.1016/j.ijpharm.2011.03.069.

[14] S. A. Shoyele and S. Cawthorne, “Particle engineering techniques for inhaled biopharmaceuticals,” *Adv. Drug Deliv. Rev.*, vol. 58, no. 9–10, pp. 1009–1029, 2006, doi: 10.1016/j.addr.2006.07.010.

[15] M. Ameri and Y. F. Maa, “Spray drying of biopharmaceuticals: Stability and process considerations,” *Dry. Technol.*, vol. 24, no. 6, pp. 763–768, 2006, doi: 10.1080/03602550600685275.

[16] C. Moura, "Improved Particle Engineering and DPI Formulation for Optimal Pulmonary Delivery" (Doctoral Dissertation, Nova School of Science and Technology, Portugal), 2016.

[17] J. G. Weers *et al.*, “Pulmonary formulations: what remains to be done?,” *J Aerosol Med Pulm Drug Deliv*, vol. 23 Suppl 2, pp. S5–23, 2010, doi: 10.1089/jamp.2010.0838.

[18] N Shetty, D. Cipolla, H. Park, Q. Zhou, “Physical stability of dry powder inhaler ”, *Expert Opinion on Drug Delivery*, vol. 17, 2019, doi: 10.1080/17425247.2020.1702643.

[19] P. Mah *et a*l., “The use of hydrofobic amino acids in protecting spray dried trehalose formulations against moisture-induced changes”, European Journal of Pharmaceutics and Biopharmaceutics 144, 2019, doi: 10.1016/j.ejpb.2019.09.014.

[20] J. G. Weers and D. P. Miller, “Formulation Design of Dry Powders for Inhalation,” *Journal of Pharmaceutical Sciences*, vol. 104, no. 10. John Wiley and Sons Inc., pp. 3259–3288, Oct. 01, 2015, doi: 10.1002/jps.24574.

[21] P. Marcelino *et al.*, “Therapeutic activity of superoxide dismutase-containing enzymosomes on rat liver ischaemia-reperfusion injury followed by magnetic resonance microscopy,” *Eur. J. Pharm. Sci.*, vol. 109, no. July, pp. 464–471, 2017, doi: 10.1016/j.ejps.2017.09.008.

[22] G. A. Senisterra and P. J. Finerty, “High throughput methods of assessing protein stability and aggregation,” *Mol. Biosyst.*, vol. 5, no. 3, pp. 217–223, 2009, doi: 10.1039/b814377c.

[23] R. Vehring, W. R. Foss, and D. Lechuga-Ballesteros, “Particle formation in spray drying,” *J. Aerosol Sci.*, vol. 38, no. 7, pp. 728–746, 2007, doi:

10.1016/j.jaerosci.2007.04.005.

[24] A. L. Feng, M. A. Boraey, M. A. Gwin, P. R. Finlay, P. J. Kuehl, and R. Vehring, “Mechanistic models facilitate efficient development of leucine containing microparticles for pulmonary drug delivery,” *Int. J. Pharm.*, vol. 409, no. 1–2, pp. 156–163, 2011, doi: 10.1016/j.ijpharm.2011.02.049.

[25] S. Focaroli *et al.*, “A Design of Experiment (DoE) approach to optimise spray drying process conditions for the production of trehalose/leucine formulations with application in pulmonary delivery,” *Int. J. Pharm.*, vol. 562, no. November 2018, pp. 228–240, 2019, doi: 10.1016/j.ijpharm.2019.03.004.

[26] S. Vonhoff, "The influence of atomization conditions on protein secondary and tertiary structure during microparticle formation by spray-freeze-drying", (Doctoral dissertation, Friedrich-Alexander-Universität Erlangen-Nürnberg, Germany), 2010.

[27] D. Psimadas, P. Georgoulias, V. Valotassiou, and G. Loudos, “Molecular Nanomedicine Towards Cancer :,” *J. Pharm. Sci.*, vol. 101, no. 7, pp. 2271–2280, 2012, doi: 10.1002/jps.

[28] H. X. Zhou and X. Pang, “Electrostatic Interactions in Protein Structure, Folding, Binding, and Condensation,” *Chem. Rev.*, vol. 118, no. 4, pp. 1691–1741, 2018, doi: 10.1021/acs.chemrev.7b00305.

[29] L. Eriksson, E. Johansson, N. K.- Wold, C. Wikstrom, and S. Wold, “Design of Experiments, Principles and Applications,” *Umetrics AB, Ümea Learnways AB, Stocholm, 2000,* ISBN 91-973730-0-1.

CHAPTER 4

Spray drying process fine-tuning to produce biopharmaceutical dry powder inhaler formulations

Running heads:

- *Two-fluid versus Ultrasonic nozzles: Which one is the most suitable to produce biopharmaceutical dry powder inhaler formulations in a spray drying process?*
- *Is it possible to increase recovery yields via spray drying set-up improvement?*

This chapter has been published as:

Fernandes DA, Barros R, Moura C, Pereira J, Corvo ML, Costa E: *Ultrasonic versus Two-Fluid Nozzle in a Spray Drying Process: A Comparative Study for the Production of Dry Powder Inhaler Formulations for Biopharmaceutical Delivery.* Drug Delivery to the Lungs 2017, The Aerosol Society 2017; Vol 31, Issue 2, pp 135-138.

Fernandes DA, Silva M F, Barros R, Moura C, Pereira J, Corvo ML, Costa E: *Spray Drying of Inhalable Biopharmaceuticals: Comparing Atomizing Systems,* 10th iMED.Ulisboa Postgraduate Students & 3rd i3DU Meeting 2018.

4.1 OVERVIEW

In this chapter, the work developed to render the spray drying process milder and more efficient to produce biopharmaceutical dry powder inhaler (DPI) formulations is presented. Nozzle type, length and surface area of the drying chamber and implementation of a mesh as gas distributor were studied as potential sources of improvement in reducing the shear stress to which the biopharmaceutical may be exposed during atomization on the spray drying process, as well as limiting the loss of powder to the drying chamber walls. Hence, chapter 4 is organized in two sections:

- ***Two-fluid (2F) versus Ultrasonic (US) nozzle***
- **Less is more – Miniaturizing spray drying trials via other setup improvements**

Goals:

- ***Two-fluid versus Ultrasonic nozzle –*** to assess the use of a 180 kHz US nozzle as an alternative atomizing system over the conventional 2F nozzle to produce spray dried DPI formulations (placebo) intended for biopharmaceutical delivery.
- **Less is more – Miniaturizing spray drying trials via other setup improvements –** to assess if it is possible to spray dry powders (placebo) in the mg range with yield > 50% using a drying chamber with reduced length and surface area and a gas distributor mesh. This would allow the increase of the biopharmaceutical fraction within the formulation without further need of increasing its nominal mass.

Results:

- ***Two-fluid versus Ultrasonic nozzle –*** Inhalable powders were successfully generated by the Two-fluid nozzle conversely to Ultrasonic generated powders which were outside the orally inhalable size range displaying Fine Particle Fractions (FPF) below 17%. Nevertheless, Ultrasonic generated powders exhibited a narrower particle size distribution span and its use did not affect powder solid state properties. Although

not suitable for oral inhalation, the features of the powder produced show its potential to process biopharmaceuticals for delivery through routes other than oral inhalation.

- **Less is more – Miniaturizing spray drying trials via other setup improvements –** It was possible, for the tested excipient system, to reduce the minimum batch size of a conventional lab-scale spray dryer from ~5 g to 100 mg (50-fold) with yield > 50%. Also, an increase in yield by 10-fold could be observed. As such, an increase of the relative fraction of the biologic within the formulation from 0.1% to 5% (50-fold) also becomes possible, while maintaining its nominal mass and within an acceptable yield, This allows more representative results of the process to be obtained in an economically viable way.

Conclusions:

Based on the outcomes of the present chapter the spray drying setup most suitable to produce low scale biopharmaceutical DPI formulations, in a milder and efficient manner, features the 2F nozzle, the mesh gas distributor and the drying chamber with reduced length and surface area.

4.2 INTRODUCTION

When developing a dry powder inhaler (DPI) formulation featuring a biologic as API, powder aerodynamic performance and conformational stability are key. Hence, the particle engineering technology employed to meet this balance plays a pivotal role.

As mentioned in previous chapters, spray drying (SD, Figure 4.1 A) could be a viable fit, usually comprising three operation steps: atomization, drying and powder collection [1].

Figure 4.1 – *A. Lab scale Mini Spray Dryer Buchi; B. Two-fluid Nozzle* [2]*; C. Ultrasonic Nozzle* [3].

However, the atomization step might constitute a stress source from a biopharmaceutical integrity standpoint. Conventional lab scale spray drying units are often equipped with two-fluid (2F) nozzles (Figure 4.1 B). These produce a spray by causing the interaction between a high velocity compressed gas stream with a liquid feed [4]. However, 2F nozzle underlying mechanism may result in the biologic degradation due to the potential of its migration towards the air-liquid interface [5]–[7]. One possible way to circumvent these shortcomings is the use of Ultrasonic (US) nozzles (Figure 4.1 C). The spray generated by the US nozzle results from the breakup of unstable capillary waves developed in the liquid feed introduced onto the rapidly vibrating atomizing surface on the nozzle. This confers the spray a low-velocity profile

when compared to the 2F nozzle, thus rendering the US nozzle, potentially, more bio-friendly [8]–[10].

Herein, the use of the US nozzle is assessed as an alternative atomizing system in the production of composite based DPI formulations intended for biopharmaceutical delivery in a SD process.

Besides exploring new ways of rendering the SD process milder through a different atomizing system, other options were considered to render it also more efficient, yield-wise, ultimately allowing one to reduce the batch size from g to mg range and as such, working with lower biopharmaceutical mass requirements. Thus, a metallic mesh (Figure 4.2 B) was installed between the drying gas outlet and the drying chamber so the turbulence of the drying gas could be attenuated [11, 12], and less powder lost to the walls. In addition, a drying chamber with reduced length and surface area (Figure 4.2), when compared to a conventional one (Figure 4.1 A) was employed to meet the same purpose.

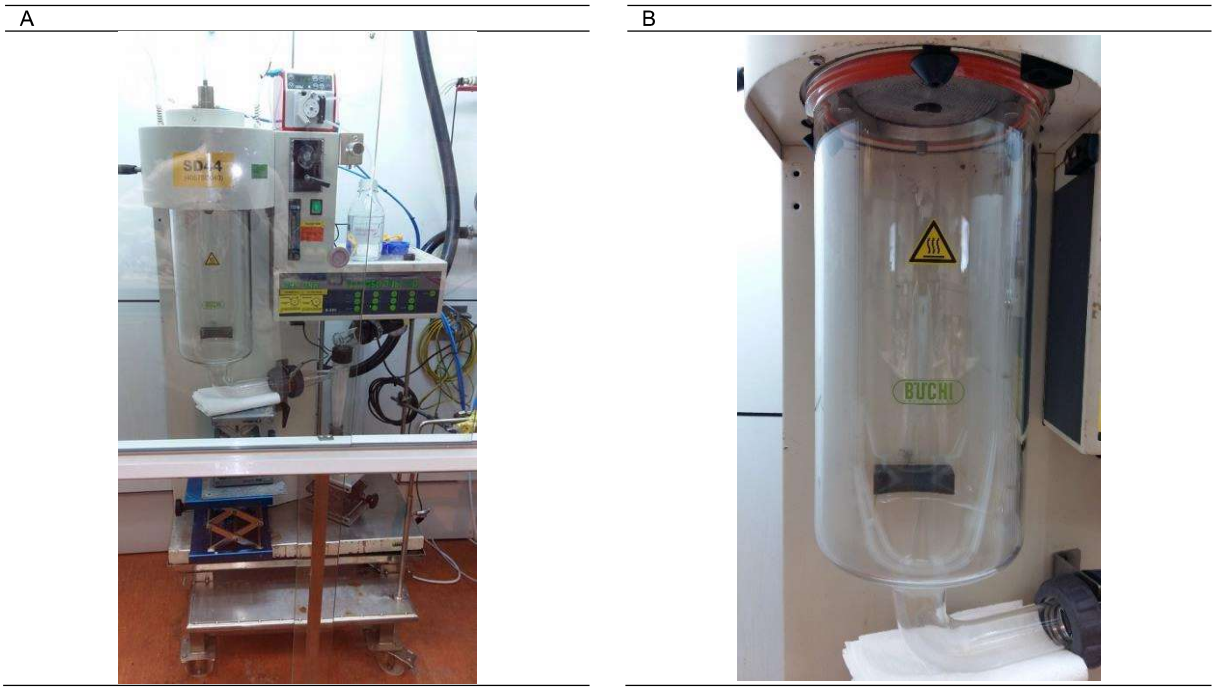

Figure 4.2 – *A. Spray drying setup featuring the drying chamber with reduced length and surface area; B. Zoom-in of the mesh installed.*

4.3 MATERIALS AND METHODS

4.3.1 Materials

D-trehalose dihydrate and L-leucine were purchased from EMD Millipore Corp. (Billerica, MA USA). Ultra-pure type II Millipore water from a Milli-Q water purification system was used in all studies.

4.3.2 Methods

4.3.2.1 Spray Drying

Two-fluid versus Ultrasonic nozzle

The feed solutions for SD comprised trehalose:leucine (4:1) (composition previously optimized [13]) at 2 % (w/w) of solids content in water at pH 6-7. Spray drying was performed at a lab-scale Mini Spray Drier BUCHI, model B-290 (Büchi Labortechnik AG, Flawil, Switzerland) equipped with a 180 kHz US nozzle (Büchi Labortechnik AG, Flawil, Switzerland) refrigerated by a nitrogen gas recirculation stream at room temperature and a 2F nozzle (orifice 0.7 mm, core/cap 1.5 mm, Büchi Labortechnik AG) refrigerated by external water bath re-circulation. A stepwise approach involving three stages (1-3) was used to assess the suitability of the US nozzle as an atomization system over the 2F nozzle to produce spray dried DPI formulations intended for biopharmaceutical delivery (Table 4.1).

1. **Ultrasonic nozzle fine-tuning in a SD process (US_X) –** Solids concentration (C_{solids}) and outlet temperature (T_{out}) were the selected parameters to study the resulting powder properties obtained by SD using the US nozzle while fixing drying (F_{drying}) and feed (F_{feed}) flowrates at fine-tuned values that allowed a homogeneous spray pattern. For each process variable (C_{solids}, T_{out}), two levels (low and high) were set (Table 4.1). C_{solids} and T_{out} ranges were defined based on previous work performed with the 2F nozzle to produce inhalable trehalose:leucine composite powders featuring a model biopharmaceutical (Cu,Zn-Superoxide Dismutase) [14]; Such resulted in a full factorial experiment 2^2, as depicted in

Table 4.1 (tests US_1 - US_4), plus an additional center point (test US_5) making a total of five experiments, for this stage.

2. **Benchmark of Ultrasonic with Two-fluid nozzle at the same SD conditions (2F_X) –** The SD tests performed at stage 1 were then reproduced using the 2F nozzle (tests 2F_1 - 2F_5, Table 4.1) while adjusting the atomization flow rate (R_{atom}), so that the same theoretical droplet size, estimated by the Kelvin-Helmholtz and Rayleigh-Taylor models [15], when using the US nozzle could be attained.
3. **Benchmark of Ultrasonic with Two-fluid nozzle at their respective optimized SD conditions from an inhalation standpoint ($2F_{op}$_X) –** The SD tests performed at stage 2 (tests $2F_{op}$_1 - $2F_{op}$_5) were then reproduced using the 2F nozzle but at previously [14]F_{drying} and R_{atom} optimized conditions that allowed for increased values of fine particle fraction (FPF) of trehalose:leucine based composite systems.

Table 4.1 – *Set of test conditions defined according to the described experimental design for each stage.*

180 kHz Ultrasonic (US)						
Stage	**Test**	**C_{solids} (%)**	**T_{out} (°C)**	**F_{feed} (g.min^{-1})**	**F_{drying} (kg.h^{-1})**	
1	**US_1**	1	65	3.5	20	-
	US_2	1	95			
	US_3	3.5	65			
	US_4	3.5	95			
	US_5	2.3	80			
Two-Fluid (2F)						
Stage	**Test**	**C_{solids} (%)**	**T_{out} (°C)**	**F_{feed} (g.min^{-1})**	**F_{drying} (kg.h^{-1})**	**R_{atom} (mm)**
2	**2F_1**	1	65	3.5	20	45
	2F_2	1	95			
	2F_3	3.5	65			
	2F_4	3.5	95			
	2F_5	2.3	80			
3	**2Fop_1**	1	65		35	60
	2Fop_2	1	95			
	2Fop_3	3.5	65			
	2Fop_4	3.5	95			
	2Fop_5	2.3	80			

Note: C_{solids} – solids concentration; T_{out} – solids concentration; F_{feed} – feed flow rate; F_{drying} – drying flow rate; R_{atom} – atomization flow rate.

The feed solutions for SD comprised trehalose:leucine (4:1) (composition previously optimized [13]) at 2% (w/w) of solids content in water at pH 6-7. Spray drying was performed at a lab-scale Mini Spray Drier BUCHI, model B-290 (Büchi Labortechnik AG, Flawil, Switzerland) equipped with a 2F nozzle (orifice 0.7 mm, core/cap 1.5 mm, Büchi Labortechnik AG) refrigerated by external water bath re-circulation. To test the alternative spray drying set-up (Alt_SD), two spray drying conditions - a worst and best-case scenarios - that could impact process yield, were selected from a previously executed DoE [14]. The worst-case scenario would correspond to a lower process yield, consisting on lower T_{out}, lower F_{atom} (larger droplet size) and higher F_{feed} (Test 3, Table 4.2) while the best-case scenario would cover the opposite (Test 6, Table 4.2). F_{drying} was kept constant. Assuming that the typical minimum batch size for a conventional lab-scale spray dryer is ~5 g, four batch sizes ranging from 100 mg – 1 g of trehalose:leucine (4:1) spray dried powders were considered for each scenario. The spray drying runs were executed from lower-higher batch sizes to spot the minimum amount that was possible to produce with a process yield > 50%.

Table 4.2 – *Set of test conditions defined according to the described experimental design.*

Test	T_{out} (°C)	R_{atom} (mm)	F_{feed} (g.min^{-1})	F_{drying} (kg.h^{-1})
3_0.1	65	40	9	35
3_0.25				
3_0.5				
3_1				
6_0.1	95	60	3	
6_0.25				
6_0.5				
6_1				

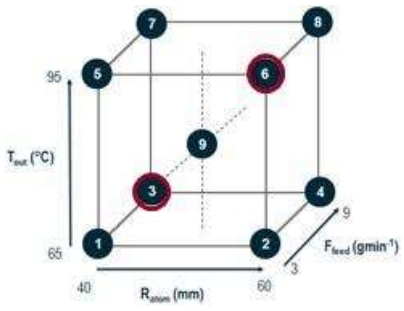

Note: T_{out} – solids concentration; R_{atom} – atomization flow rate; F_{feed} – feed flow rate; F_{drying} – drying flow rate.

4.3.2.2 Powder Characterization

4.3.2.2.1 Scanning Electron Microscopy

The shape and surface of the dry powders was assessed by Scanning Electron Microscopy (SEM). SD powder samples were attached to adhesive carbon tapes (Ted Pella, Inc., CA,

USA) and the excess removed by a jet of pressurized air. The samples were exposed to vacuum for 2 hours and coated with a 15 nm gold layer (South Bay Technologies, former Polaron, model E5100, San Clement, CA). A scanning electron microscope (JEOL JSM-7001/Oxford INCA Energy 250/HKL, Japan) in high vacuum mode was used with a typical accelerating voltage between 5 and 20 kV.

4.3.2.2.2 Laser Diffraction

Particle size distribution was determined by Laser Diffraction (LD) using the particle size analyzer Sympatec HELOS in combination with RODOS and the ASPIROS modules (Sympatec GmbH, Clausthal-Zellerfel, Germany). The optical bench of the HELOS module (H3330) was equipped with R1 and R4 Fourier lenses that cover particle sizes between 0.18-35 µm and 1.8-350 µm, respectively. The sample vials were prepared in a glove box and filled with powder until one third of the vial was complete. The vials were then inserted into ASPIROS module and powders dispersed at 3.0 bar pressure with compressed air and a feed rate velocity of 18 $mm.s^{-1}$, while targeting an optical concentration (C_{opt}) above 1 %. Particle size (Dv10, Dv50 and Dv90) was computed using WINDOX5.0 software (Sympatec GmbH, Clausthal-Zellerfel, Germany) and span values determined as (Dv90-Dv10)/Dv50.

4.3.2.2.3 X-Ray Powder Diffraction

The crystallinity of the powders was assessed by X-ray powder diffraction (XRPD) (X'Pert PRO X-ray diffraction system, PANalytical). The measurements were performed using a Bragg-Brentano configuration featuring a detector 1D X'Celerator. The samples were measured over a 2θ interval from 5 to 40 º with a step size of 0.0167 º.

4.3.2.2.4 Differential Scanning Calorimetry

The thermograms of the spray dried powders were obtained using a differential scanning calorimeter (DSC) (Model Q200 from TA Instruments; Focus Scientific, Ireland) equipped with a Refrigerated Cooling System (RCS). The equipment is daily calibrated with indium.

Approximately 2 - 7 mg of sample were weighted into a pinhole aluminium pan. During the analysis, the sample and the reference were under a continuous dry nitrogen purge (50 $mL.min^{-1}$). The powder samples were analysed at +/- 0.8 ºC every 60 seconds with a heating ramp of 5.00 $ºC.min^{-1}$ from -20 ºC to 300 ºC. The data was retrieved by TA Universal Analysis software.

4.3.2.2.5 Karl-Fisher oven titration

The water content of the spray-dried samples was determined using Karl-Fischer (KF) oven titration. For the analysis, 50 mg of each sample were weighted into a weighing boat and then deposited into a 774 oven sample processor (Metrohm Ltd., Antwerp, Belgium) operating with dried Nitrogen gas at 40 $ml.min^{-1}$.

4.3.2.2.6 Andersen Cascade Impaction

Powders aerodynamic performance was assessed using an eight-stage gravimetric Andersen Cascade Impactor (ACI, Copley 88 Scientific Ltd., Nottingham, UK), as previously described [14]. All powders were hand-filled inside a glovebox at controlled relative humidity below 10%, in HPMC size 3 capsules (Capsugel, Basel, Switzerland) with 20 ± 0.4 mg of each formulation, in triplicate. These were actuated for 4 seconds, using a Plastiape device HR model 7 at 60 $L.min^{-1}$, (pressure drop of 4 kPa). The filter from each stage was weighed before and after each actuation. The FPF was determined as the percentage of the powder mass emitted from the capsule displaying an aerodynamic diameter below 5 µm. The mass median aerodynamic diameter (MMAD) and the geometric standard deviation (GSD) were retrieved from CITDAS software (Copley 88 Scientific Ltd., Nottingham, UK).

4.3.2.2.7 Statistical Analysis

To further understand the interaction between the studied factors (T_{out}, Rot_{atom} and F_{feed}) on the morphology and aerodynamic performance of the powders, a multivariate statistical

analysis based on partial least squares (PLS) regression model was performed using SIMCA v13.0.3.0 software (Umetrics).

4.4 RESULTS AND DISCUSSION

Two-fluid versus Ultrasonic nozzle

Spray dried powders were successfully generated when employing the US nozzle. However, at the highest C_{solids} (3.5%(w/w)) and T_{out} (95 ºC) combination (test US_4), the US nozzle was not able to continuously sustain a homogeneous spray. This might be explained by nozzle overheating under high temperatures, since only gas is used as cooling fluid, enabling a less efficient heat transfer than the liquid-based cooling system of the 2F nozzle. As a result, the premature precipitation of the feed solution solids could take place within the nozzle, ultimately affecting the atomization. For this reason, US_2 test at 95 ºC was not performed and tests 2F_2, 2F_4, $2F_{op}$_2 and $2F_{op}$_4, were thus excluded for benchmarking purposes.

4.5.1 2F and US powder characterization

According to the SEM micrographs, all the US generated powders are mainly composed by spherical and then irregular, collapsed shaped particles which is depicted in Figure 4.3 A&B for test US_1. All US powders are outside the inhalable size range (Dv50 > 5 µm, Table 4.3), regardless of the tested conditions. Conversely, SEM micrographs of all the 2F generated powders only presented spherical and slightly shriveled particles with a particle size (PS) within the inhalable size range for all tested conditions (Table 4.3), as showcased in Figure 4.3 C&D for tests 2F and $2F_{op}$, respectively.

The apparent PS observed in the SEM micrographs is also in agreement with the PSD quantitatively determined by laser diffraction for both US and 2F powders. PS seems to increase with C_{solids} regardless of the atomization system used when comparing between tests US_1 & US_3, 2F_1 & 2F_3 and $2F_{op}$_1 & $2F_{op}$_3 tests (Table 4.3). This in agreement with previous reports in the literature [13], [15]. In the particular case of 2F nozzle, PS decreased when using higher values of R_{atom} and F_{drying} ($2F_{op}$_1, $2F_{op}$_3 and $2F_{op}$_5) as already observed in previous studies [13, 14], [16]. Regarding PSD span, this is indeed narrower for the US

nozzle, evidencing one of the main expected advantages of using this nozzle over the 2F (Table 4.3).

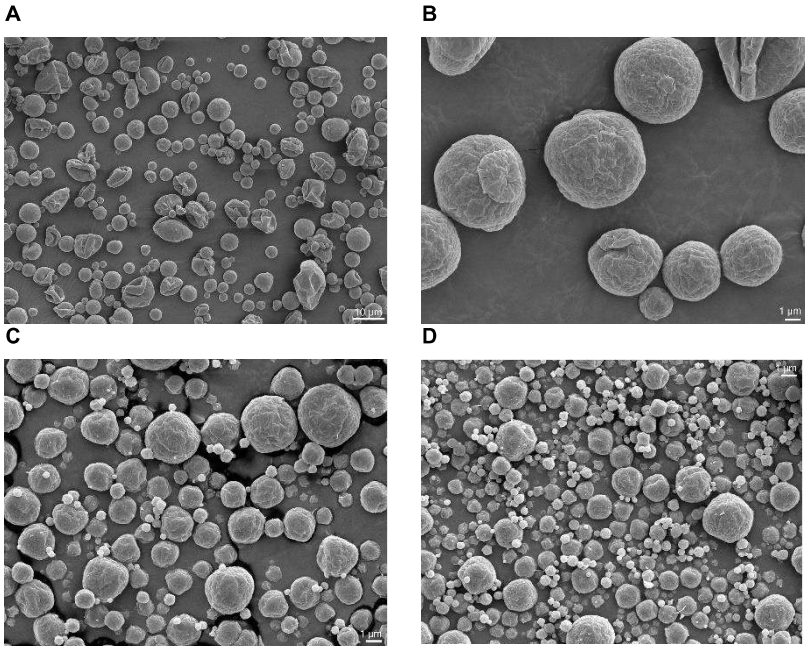

Figure 4.3 – *SEM micrographs for both US and 2F generated powders for test 1. A – Test US_1 (x1000); B – Test US_1 (x5000); C – Test 2F_1 (5000x); D – Test 2F$_{op}$_1 (x5000).*

Concerning powders solid state properties these seem to be the same irrespective of the atomizing system used. XRPD patterns (Figure 4.4) reveal an amorphous halo, which is attributed to the amorphous trehalose while the diffraction peaks correspond to leucine in its crystalline form.

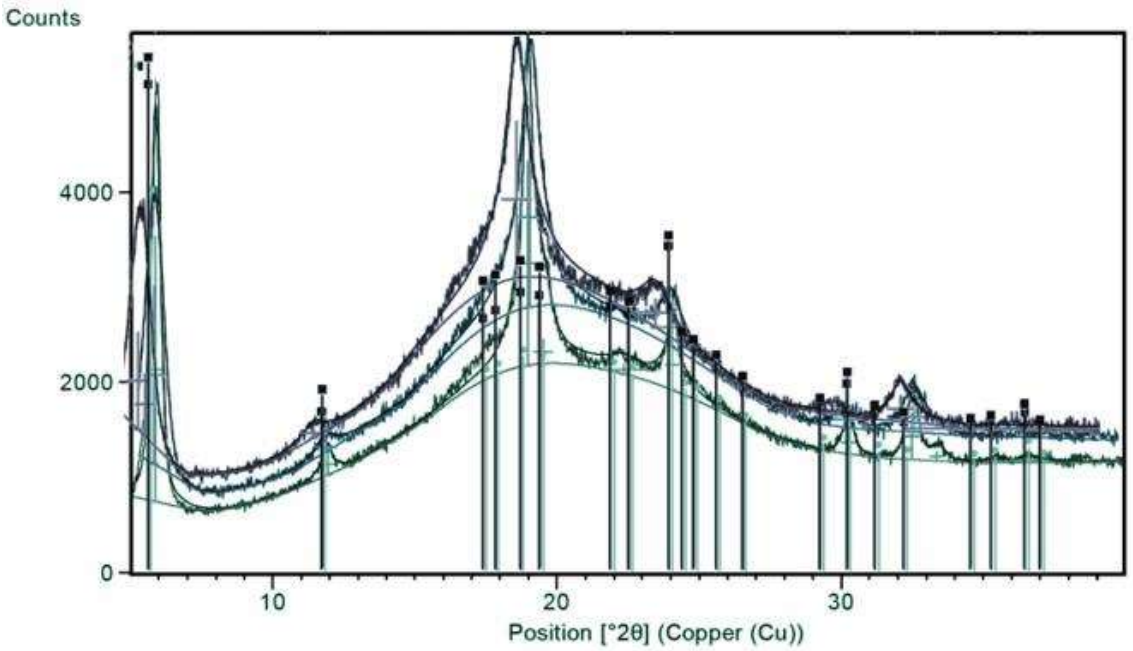

Figure 4.4 – XRPD patterns obtained for tests US_1 (green line), 2F_1 (light blue) and $2F_{op}$_1 (dark blue).

It is worthwhile mentioning, however, that the diffraction peaks of tests US_3 and US_5 were more intense when compared with the other tests. Inoue et al. [17] observed that different XRD peak intensities of $CaSO_4.2H_2O$ crystals could be associated with their different morphologies and so a similar conclusion could be withdrawn herein, i.e, leucine crystals of US_3 and US_5 might display a different morphology from the crystals of the remaining tests because of drying and recrystallization kinetics at those particular conditions. These assumptions are consistent with the trend perceived in the reversible DSC thermograms (Figure 4.5) as a glass transition (T_g) of ~120 ºC can be observed for all SD powders, evidencing the amorphous state of trehalose. In addition, the total DSC thermograms exhibit the melting temperature (T_m) of leucine also suggesting that this is present in its crystalline form.

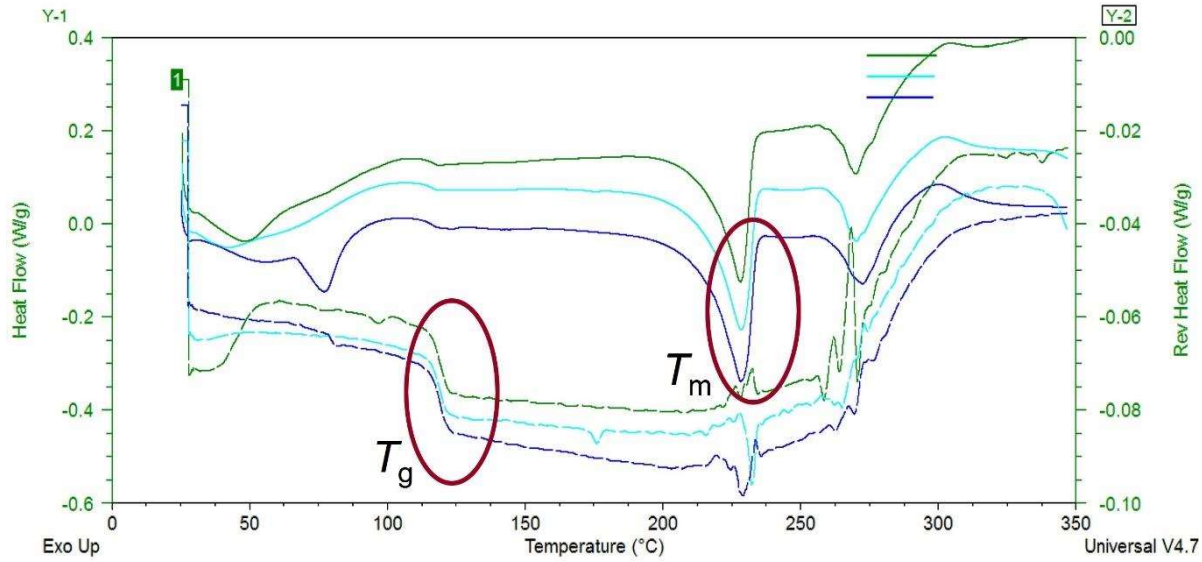

Figure 4.5 – DSC thermograms obtained for tests US_1 (green line), 2F_1 (light blue) and $2F_{op}$_1 (dark blue).

Regarding water content (KF) this ranged from 2.4-3.9% for the US nozzle and for the 2F, from 1.6 to 3.2% (Table 4.3). When comparing the water content of the powders generated at the same temperature (65 ºC) with the US nozzle versus 2F nozzle, it could be observed that this would be lower for 2F nozzle powders. As previously mentioned, the refrigeration system of the US nozzle is gas-based, meaning that heat transfer is not so efficient causing overheating. Therefore, atomization would sometimes stop briefly, wetting the camera. This may have resulted in the increase of the relative saturation at the outlet of the drying chamber leading to the difference in water content between powders generated using each of the nozzles. For both atomizing systems, water content seems to decrease with solids concentration, as expected [18].

Despite the PS of US powders was outside the inhalable size range, ACI tests were still performed to assess whether there would be a potential for nasal applications (where target aerodynamic Dv50 > 10 µm). FPF ranging from 4-17% with a capsule emitted dose (ED) higher than 94% were obtained for the US nozzle while for the 2F nozzle, FPF ranged from 58-90% with a capsule ED higher than 91% (Table 4.3). For both atomizing systems, FPF seems to decrease with C_{solids}, when comparing US_1 & US_3, 2F_1 & 2F_3, $2F_{op}$_1 & $2F_{op}$_3 (Table 4.3). FPF along with mass median aerodynamic diameter (MMAD) results followed the

same trend observed for PSD. The smaller the PS, the higher the FPF and the smaller the MMAD, when comparing between US_1, 2F_1 & $2F_{op}$_1; US_3, 2F_3 & $2F_{op}$_3; US_5, 2F_5 & $2F_{op}$_5.

4.5.2 Input and output variables interaction by statistical analysis

To strengthen the previous qualitative observations, a multivariate statistical analysis was carried out to further understand the interaction between C_{solids}, T_{out} (both US and 2F nozzles), F_{drying} and R_{atom} (only 2F nozzle) – inputs – on the particle size (Dv50), water content (KF) and aerodynamic performance (MMAD, FPF) – outputs – of US and 2F generated powders. No models could be derived for the US data since no trend was observed amongst the results obtained, regardless of the studied output variables. This is not surprising considering the limited number of tests performed (only four, with operational challenges observed in US_4). For the 2F nozzle, Table 4.4 showcases which input variables allowed for the best fit (R^2>0.7 [19]) and prediction (Q^2>0.5; R^2- Q^2<0.2-0.3 [19]) of the derived PLS regression models describing its influence on each one of the output variables. PLS regression models obtained for Dv50, MMAD and FPF displayed the best fit and prediction when considering C_{solids}, F_{drying}, R_{atom} as input parameter. No good PLS model could be derived for KF, with a R^2 value<0.7 and Q^2 value<0.5, which might be due to the relatively small range of KF observed. Finally, T_{out} had a negligible impact on all the studied output variables. Thus, most of the qualitative conclusions previously withdrawn could be corroborated by the multivariate statistical analysis concerning the 2F generated powders (Table 4.4).

Table 4.3 *– Overview of the morphology (Dv50, span), solid state properties and aerodynamic performance (MMAD, GSD) for the tested conditions.*

	US_1	2F_1	$2F_{op}$_1	US_3	2F_3	$2F_{op}$_3	US_5	2F_5	$2F_{op}$_5
Dv50 (µm)	5.5	1.7	1.2	6.7	2.3	1.7	6.3	2.0	1.5
Span	1.6	1.8	2.0	1.4	2.0	2.1	1.5	2.1	2.0
XRPD	Crystalline Leucine								
DSC	Crystalline Leucine; Amorphous Trehalose								
KF (%)	3.9	3.2	2.5	3.8	2.8	1.6	2.4	2.5	2.0
FPF (%)	17	75	89	5	58	68	4	62	68

MMAD (µm)	6.5	2.8	2.3	N.A	3.3	3.1	7.8	3.4	2.8
GSD	2.3	1.7	1.8	N.A	1.8	1.7	1.7	1.8	1.7

Table 4.4 *– Input variables that allowed for the best PLS regression model fit (R^2>0.7) and prediction (Q^2>0.5; R^2-Q^2<0.2-0.3) (in grey) for each one of the output variables and respective dependence concerning the results obtained using the 2F nozzle. (+) stands for positive and (-) negative effect of X input on Y output variable. Ex: Dv50 increases with C_{solids} and decreases with F_{drying} and R_{atom}.*

Test	C_{solids}	T_{out}	F_{drying}	R_{atom}	R^2	Q^2
Dv50	(+)		(-)	(-)	0.99	0.96
MMAD	(+)		(-)	(-)	0.87	0.75
FPF	(-)		(+)	(+)	0.94	0.89

Less is more – Miniaturizing spray drying trials via setup improvements

To assess if it was possible to spray dry powders in the mg range with yield > 50%, a drying chamber with reduced length, surface area, direct discharge and a gas distributor mesh was used. Considering the experimental design from Table 4.2, the smaller batches of 100 mg were the first ones to be spray dried (Tests 3_0.1 and 6_0.1). Since yield came higher than 50% (defined success criteria) for both tests, the following batch sizes corresponding to higher amounts (Tests 3_0.25;0.5;1 and 6_0.25;0.5;1) were not performed.

No powder was visible in the drying chamber being the remaining mostly retained in the cyclone walls. One possible way to circumvent this while possibly increasing the yield, would be to introduce a vortex breaker in the cyclone.

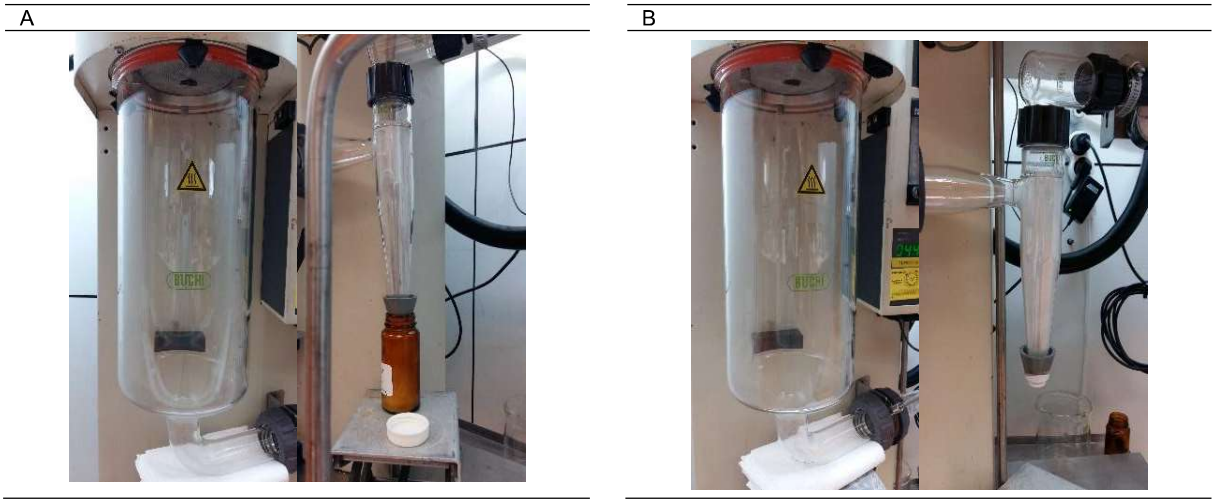

Figure 4.6 – *Drying chamber with reduced length and surface area and cyclone after performing A. test 3_0.1 and B: test 6_0.1.*

4.5 CONCLUSIONS

Herein, 180 kHz US nozzle was assessed as a possible alternative over the 2F nozzle to produce spray dried DPI formulations intended for biopharmaceutical delivery in a milder way. On the other hand, an alternative spray drying set-up featuring a mesh gas distributor, a drying chamber with reduced length and surface area and direct powder discharge was tested as way to render the spray drying process more efficient, allowing to increase the relative amount of biopharmaceutical within the formulation with an acceptable yield.

The US nozzle failed to generate powders within the orally inhalable size range with FPF below 17%, rendering it a poor candidate from an orally inhalation standpoint for biopharmaceutical delivery, when using the tested composite system. In addition, the cooling system of the US nozzle as is, causes overheating at higher SD temperatures which could potentially impair the biopharmaceutical integrity. On the contrary and as expected, 2F nozzle displayed a PS below 5 μm and FPF values ranging from 68-89%, which are 4-5 fold higher than the values achieved with the US nozzle, whether working at its respective optimized conditions or not. To strengthen and validate the outcomes of the present study, future work should include US testing with other excipient systems since C_{solids}/viscosity may impact US performance [8]. It is important to point out, though, that there were also some positive features to the US nozzle, such as a narrower PS span and maintenance of solid-state properties, that showcased its potential to maybe target biopharmaceutical delivery through other alternative routes such as nasal where PS should be outside the inhalable size range to prevent product deposition in the lungs. Thus, 2F nozzle was the atomizing system selected to conduct the alternative spray drying set-up study and further work that followed.

By implementing a metallic mesh gas distributor and a drying chamber with reduced length and surface area, it was possible to reduce the minimum batch size of a conventional lab-scale spray dryer from ~5 g to 100 mg (50-fold) for the tested excipient system with yield > 50%. As such, an increase of the relative fraction of the biologic within the formulation from 0.1% to 5% (50-fold) becomes possible, while maintaining its nominal mass and within an

acceptable yield. Ultimately, this allows more representative results of the process to be obtained in an economically viable way.

REFERENCES

[1] A. Langford, B. Bhatnagar, R. Walters, S. Tchessalov, and S. Ohtake, “Drying technologies for biopharmaceutical applications: Recent developments and future direction,” *Dry. Technol.*, vol. 36, no. 6, pp. 677–684, Apr. 2018, doi: 10.1080/07373937.2017.1355318.

[2] https://www.buchi.com/en/products/spray-drying-and-encapsulation/mini-spray-dryer-b-290, accessed December 2015.

[3] https://www.sono-tek.com/, accessed April 2016.

[4] Issenschaftlichen and D. N. Universit, Friedrich-alexanderFakult, “the Influence of Atomization Conditions on Protein Secondary and Tertiary Structure During Microparticle Formation By.”

[5] H. Okamoto, H. Todo, K. Iida, and K. Danjo, “Dry powders for pulmonary delivery of peptides and proteins,” *KONA Powder Part. J.*, vol. 20, no. March, pp. 71–83, 2002, doi: 10.14356/kona.2002010.

[6] S. A. Shoyele and S. Cawthorne, “Particle engineering techniques for inhaled biopharmaceuticals,” *Adv. Drug Deliv. Rev.*, vol. 58, no. 9–10, pp. 1009–1029, 2006, doi: 10.1016/j.addr.2006.07.010.

[7] G. A. Ledet, R. A. Graves, L. A. Bostanian, and T. K. Mandal, “Spray-Drying of Biopharmaceuticals,” in *Lyophilized Biologics and Vaccines*, Springer New York, 2015, pp. 273–297.

[8] J. J. O’Sullivan, E. A. Norwood, J. A. O’Mahony, and A. L. Kelly, “Atomisation technologies used in spray drying in the dairy industry: A review,” *Journal of Food Engineering*, vol. 243. Elsevier Ltd, pp. 57–69, Feb. 01, 2019, doi: 10.1016/j.jfoodeng.2018.08.027.

[9] F. Tatar Turan, A. Cengiz, and T. Kahyaoglu, “Evaluation of ultrasonic nozzle with spray-drying as a novel method for the microencapsulation of blueberry’s bioactive compounds,” *Innov. Food Sci. Emerg. Technol.*, vol. 32, pp. 136–145, Dec. 2015, doi: 10.1016/j.ifset.2015.09.011.

[10] F. Tatar Turan, A. Cengiz, D. Sandıkçı, M. Dervisoglu, and T. Kahyaoglu, “Influence of an ultrasonic nozzle in spray-drying and storage on the properties of blueberry powder and microcapsules,” *J. Sci. Food Agric.*, vol. 96, no. 12, pp. 4062–4076, Sep. 2016, doi: 10.1002/jsfa.7605.

[11] N. N. Menshutina, E. A. Lebedev, and M. G. Gordienko, “CFD analysis of the dispersed phase behavior for micropowders production via spray drying and ultrasonic

atomization," *Dry. Technol.*, vol. 37, no. 15, pp. 1891–1900, Nov. 2019, doi: 10.1080/07373937.2018.1541903.

[12] P. W. Longest, D. Farkas, A. Hassan, and M. Hindle, "Computational Fluid Dynamics (CFD) Simulations of Spray Drying: Linking Drying Parameters with Experimental Aerosolization Performance," *Pharm. Res.*, vol. 37, no. 6, Jun. 2020, doi: 10.1007/s11095-020-02806-y.

[13] E. Costa, F. Neves, and C. Moura, "Design of composite particles via spray drying for DPI formulations," *ONdrugDelivery*, no. 53, pp. 16–23, 2014.

[14] D. A. Fernandes, P. Leandro, E. Costa, and M. L. Corvo, "Dry powder inhaler formulation of Cu,Zn-superoxide dismutase by spray drying: A proof-of-concept," *Powder Technol.*, vol. 389, pp. 131–137, 2021, doi: 10.1016/j.powtec.2021.05.008.

[15] J. Vicente, J. Pinto, J. Menezes, and F. Gaspar, "Fundamental analysis of particle formation in spray drying," *Powder Technol.*, vol. 247, pp. 1–7, 2013, doi: 10.1016/j.powtec.2013.06.038.

[16] S. Focaroli *et al.*, "A Design of Experiment (DoE) approach to optimise spray drying process conditions for the production of trehalose/leucine formulations with application in pulmonary delivery," *Int. J. Pharm.*, vol. 562, no. November 2018, pp. 228–240, 2019, doi: 10.1016/j.ijpharm.2019.03.004.

[17] M. Inoue and I. Hirasawa, "The relationship between crystal morphology and XRD peak intensity on $CaSO4{\cdot}2H_2O$," *J. Cryst. Growth*, vol. 380, pp. 169–175, 2013, doi: 10.1016/j.jcrysgro.2013.06.017.

[18] A. Ziaee, A. B. Albadarin, L. Padrela, T. Femmer, E. O'Reilly, and G. Walker, "Spray drying of pharmaceuticals and biopharmaceuticals: Critical parameters and experimental process optimization approaches," *European Journal of Pharmaceutical Sciences*, vol. 127. Elsevier B.V., pp. 300–318, Jan. 15, 2019, doi: 10.1016/j.ejps.2018.10.026.

[19] S. . Eriksson, L.; Johansson, E.; Kettaneh-Wold, N.; Wikström, C.; Wold, "Design of experiments : principles and applications." Umeå : Umetrics, 2008.

CHAPTER 5

On the use of high- throughput differential scanning fluorimetry as a biopharmaceutical formulation screening platform

Running heads:

- *Is it possible to use high-throughput screening platforms to expedite biopharmaceutical formulation prior to spray drying?*

5.1 OVERVIEW

In this chapter, Differential Scanning Fluorimetry (DSF) is presented and explored as a high-throughput (HT) screening tool to downsize the formulation conditions leading to an increased biopharmaceutical stabilization prior to Spray Drying.

Goals: To examine the stability of the conformational structure of three model enzymes – Cu,Zn Superoxide Dismutase (SOD), Glucose Oxidase (GOx) and Catalase (Cat) – under a range of different conditions comprising pH, NaCl concentration, single and combo excipients (non-reducing sugars, hydrophobic and hydrophilic aminoacids), using HT-DSF.

Results: DSF protocol fine-tuning, pH and NaCl concentration optimum values could be determined. SOD, GOx and Cat remained stable in the tested excipient ratios except for Lysine that was discarded.

Conclusions: Although HT-DSF as a function of temperature allowed determining pH and NaCl concentration optimum values and discarding lysine, further narrow down of the tested excipients in the observed ratios is still required. HT-DSF as a function of time is thus hypothesized as path forward.

5.2 INTRODUCTION

Protein conformation, namely its unique three-dimensional (3D) organization or higher order structure is pivotal when developing stable, safe, and effective formulations, including dry powder inhalers (DPI). The inadequate folding of proteins may result in aggregation both in vitro (during the formulation process) and in vivo, being frequently a target for various degradation pathways both inside and outside the cell, ultimately repercussing in immunogenic events. As such, monitoring and characterizing protein conformation is a key element upon formulation [1] - [4].

The expected increase in the number of protein drugs highlights the need for improved methods to optimize the development of protein formulations. Excipients are usually employed during formulation to preserve protein structure. Their selection is a difficult and time-consuming process, mainly due to the complexity of protein structure and the specific physical and chemical properties involved. Practical experience has shown that there are no general approaches for protein stabilization and that for each protein a customized formulation needs to be developed. At present, protein formulation in the pharmaceutical industry is generally a slow process and could benefit from a fast formulation screening strategy. In this sense, the optimal combination of excipients can be found employing a high throughput (HT) formulation screening platform [5, 6]. Several HT techniques already exist to characterize the stability and activity of protein formulations as those described for transforming growth factor β3 - β3 TGF- in aqueous solutions [7].

The stability of a protein 3D structure is often associated with its melting temperature (T_m), defined as the temperature at which 50% of the protein is in an unfolded state [5], [8]. The higher the T_m, the more stable the protein conformation. Differential scanning calorimetry (DSC) and differential light scattering (DLS) are two analytical methods that can be used to determine protein T_m shifts upon different processing conditions [6],[8]–[13]. Nevertheless, both require relatively large sample volumes and protein concentrations, which is limiting especially with expensive molecules like biopharmaceuticals, along with low throughput.

Differential scanning fluorimetry (DSF), a technique with a high potential to be used as a HT formulation screening platform, addresses these shortcomings as it allows for the simultaneous testing of several conditions at lower protein concentrations. DSF monitors the thermal unfolding of proteins in the presence of a fluorescent dye with affinity for the hydrophobic residues of the protein, which become more exposed as this unfolds. The obtained melting curves are then used to determine the protein T_m. In this chapter, DSF is used to examine the stability of the 3D structure of three model enzymes, namely Cu, Zn superoxide dismutase (SOD), glucose oxidase (GOx) and catalase (Cat), under a range of different conditions comprising pH, NaCl concentration, single and combined (combo) excipients to expedite formulation selection prior to spray drying.

5.3 MATERIALS AND METHODS

Materials

The enzymes SOD from bovine erythrocytes (S7571-300KU), GOx from *Aspergillus niger* (G2133-250KU) and Cat from bovine liver (C40-500MG) were purchased from Sigma (St. Louis, MO, USA). Citrate acid, sodium chloride, acetate trihydrate, glacial acetic acid, sodium hydroxide, monopotassium phosphate, dipotassium hydrogen phosphate, sucrose, L-alanine, L-arginine and L-lysine were from MERCK (Darmstadt, Germany). D-trehalose dihydrate and L-leucine were purchased from EMD Millipore Corp. (Billerica, MA USA), Mannitol from SPI Pharma (Wilmington, USA) and Raffinose from AMRESCO (Solon, Ohio, USA). Ultra-pure type II Millipore water from a Milli-Q water purification system was used in all assays. Sypro® Orange 5000x stock solution was purchased from Sigma (St. Louis, MO, USA).

Methods

Differential scanning fluorimetry was performed on Real-Time PCR Detection system (CFX96 Touch™; BIO-RAD), using SYPRO® Orange as the fluorophore and 10 μg of each enzyme in a final volume of 50 μL. To fine-tune the DSF signal response in the presence of each enzyme, SYPRO® Orange 5000x was first tested at 2.5x, 5x and 10x final working solution (2000x, 1000x and 500x dilution, respectively). Two different temperature rates were tested (T1:20 to 90 ºC, 0.2 ºC/min; T2: 20 to 97 ºC, 1 ºC/min) with fluorescence acquisition using the FRET channel. Each enzyme was reconstituted in the buffer recommended by the supplier for GOx (50 mM sodium acetate, pH 5.1) and Cat (50 mM potassium phosphate, pH 7.0). For SOD, a 10 mM citrate buffer, 145 mM NaCl, pH 6 was used as described in [15]. For the HTF screening DSF assays were performed on a 96-well plate format and several variables were tested including pH, NaCl concentration and the presence of excipients (trehalose, mannitol, raffinose, sucrose, L-leucine, L-alanine, L-arginine, L-lysine.)

Assays were always performed in triplicate. The T_m was obtained by computing the first derivative of the melting curves and retrieving the temperature at the minimum(s) of the first derivative curve

5.4 RESULTS AND DISCUSSION

Differential scanning fluorimetry was used to explore and narrow formulation conditions for each enzyme, aiming to reduce the number of the spray dried prototypes. As such, T_m was monitored in the presence of different pH values, NaCl concentrations, single and combo excipients. Using as the basal value the computed T_m in the presence of the enzymes reconstitution buffer, the ΔT_m could be obtained.

The DSF signal response was firstly fine-tuned in the presence of each enzyme reconstituted in the respective buffer, for different SYPRO® Orange concentrations (2.5x, 5x and 10x) and at two different temperature rates (T1 and T2).

As depicted n Figure 5.1 regardless of the SYPRO® Orange concentration and temperature rate, the DSF profile was the same for all enzymes in their reconstitution buffers, displaying the same number and values of T_m. SOD presented two T_ms at 39 ± 2 ºC (T_{m1SOD}) and at 85 ± 2 ºC (T_{m2SOD}), GOx showcased one T_m (T_{mGOx}) at 66 ± 2 ºC and Cat also exhibited two T_ms (T_{m1Cat}) at 44 ± 2 ºC and 57 ± 2 ºC (T_{m2Cat}). Therefore, as a compromise between SYPRO® Orange concentration and run time, the 5x final fluorophore concentration and the T2 temperature rate were used for the following experiments.

5.4.1 Impact of pH and NaCl

Having fine-tuned the DSF signal response for each enzyme, the impact of pH and NaCl concentration on their T_m was assessed according to the conditions described on Table I. The pH range was set considering as reference value the pH of each enzyme's reconstitution buffer. These experiments were performed in the absence of NaCl, apart from SOD, containing 145 mM NaCl in its reconstitution buffer. Following the pH screening, three NaCl concentrations (Table 1) were tested at optimum pH for each enzyme (SOD: 0, 145 and 725 mM NaCl; GOx: 0, 100 and 680 mM NaCl; Cat: 0, 100 and 680 mM NaCl).

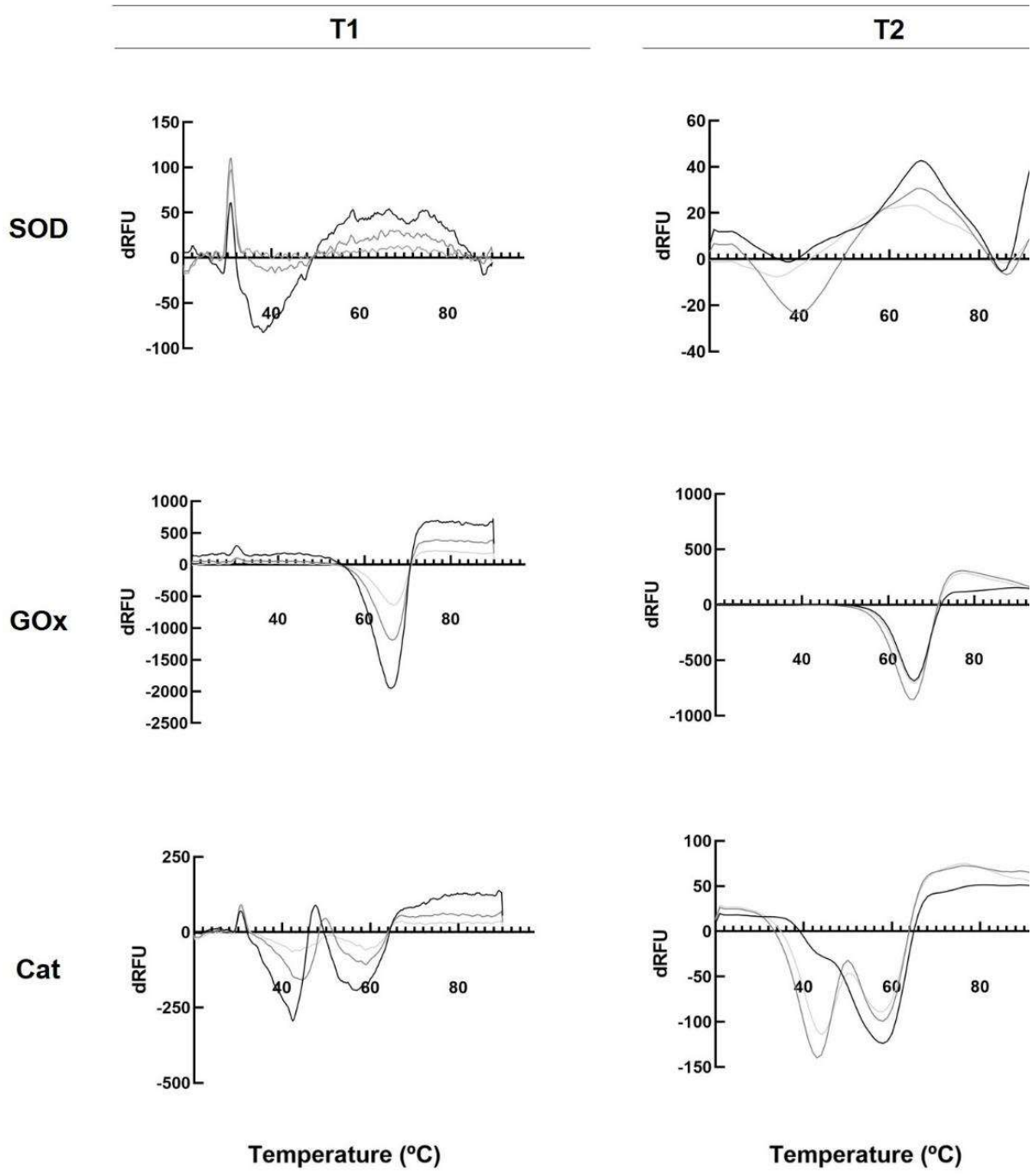

Figure 5.1 – *Cu,Zn superoxide dismutase (SOD), glucose oxidase (GOx) and catalase (Cat) using differential scanning fluorimetry (DSF). SYPRO® Orange was used at a final concentration of 2.5x (light grey), 5x (dark grey) and 10x (black). (T1) Temperature rates 20 to 90 ºC, 0.2 ºC/min; (T2) Temperature rates 20 to 97 ºC, 1 ºC/min). Melting curves represent the mean average of the three assays.*

When tested in the enzyme reconstitution buffer (10 mM citrate/145 mM NaCl) SOD displays just one T_m for pH < 6 namely 41 ± 2.1 ºC (pH 3) and 40 ± 0.0 ºC (pH 4) (Figure 5.2, Table II). This is in line with previous observations of SOD structural changes at pH < 5, resulting from

a potential loss of metals due to changes in the ionization status of the histidine and aspartate residues necessary for Cu and Zn binding [11].

Table 5.1 – pH and NaCl concentration (mM) conditions tested for Cu,Zn superoxide dismutase (SOD), glucose oxidase (GOx) and catalase (Cat).

	pH (buffer)	NaCl (mM) (buffer)
SOD	3, 4, 6 (10 mM citrate/145 mM NaCl)	0, 145, 725 (10 mM citrate/pH 6)
GOx	3, 4, 5 (50 mM sodium acetate)	0, 100, 680 (50 mM sodium acetate, pH 5)
Cat	6, 7, 8 (50 mM potassium phosphate)	0, 100, 680 (50 mM potassium phosphate, pH 7)

This data suggests that part of the enzyme is now more prone to denaturation (the same value for T_{m1SOD} *and* T_{m2SOD}) [14][15]. Several authors reported, in fact, that for pH below 5.6 and at room temperature, SOD enzymatic activity decreases [14]–[17].

For GOx, as the pH decreases, the computed T_m also decreased from 66 ± 2 ºC (pH 8) to 59 ± 1.9 ºC (pH 3) (Figure 5.2, Table 5.2). As previously reported, the tested pH range may lead to the dissociation of GOx subunits [18], ultimately resulting in an unstable environment that triggers an earlier unfolding.

The enzyme Cat maintained both T_ms (Figure 5.2, Table II) but showcased different profiles depending on the pH, namely the ratio between the fluorescence intensity of the transition states (Figure 5.2). T_{m1Cat} peak was less intense than T_{m2Cat} peak for pH < 7, suggesting that the domain/part of the protein corresponding to T_{m1Cat} could become more stable with less hydrophobic residues exposed at this pH condition. Conversely, for pH above 7, the opposite was observed. T_{m2Cat} peak was less intense than T_{m1Cat} peak, now suggesting that the domain of the protein corresponding to T_{m2Cat} could become more stable at this pH condition than the other domain. At pH 7, the ratio between peaks fluorescence intensity became balanced.

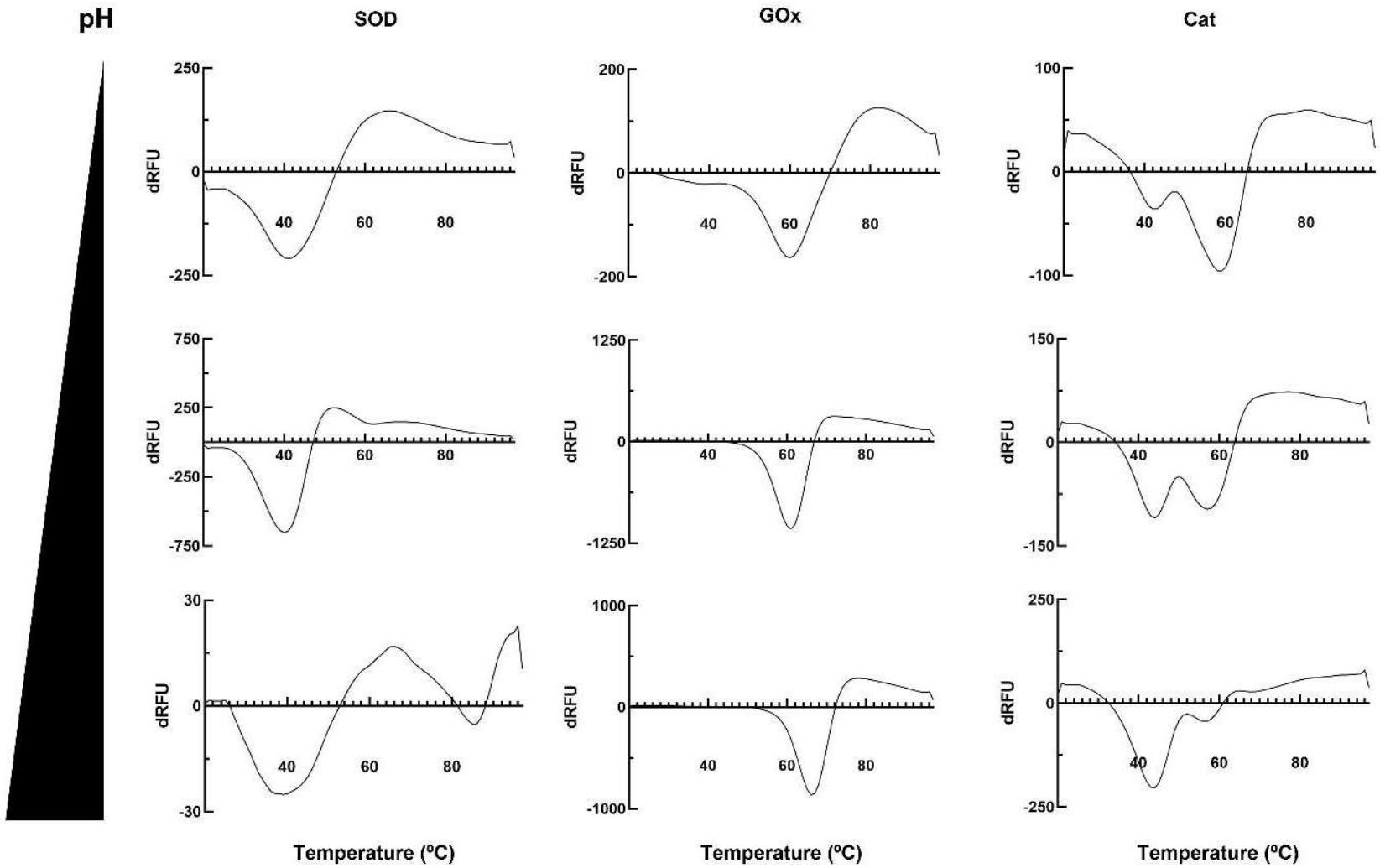

Figure 5.2 – *First derivatives of the melting curves obtained for Cu,Zn superoxide dismutase (SOD), glucose oxidase (GOx) and catalase (Cat), using differential scanning fluorimetry (DSF), as a function of pH. (SOD) pH 3, 4 and 6; (GOx) pH 3,4 and 5; (Cat) pH 6,7,and 8. Melting curves represent the mean of three assays. See text for details in buffers composition.*

Based on these results, the pH values of the reconstitution buffers for each enzyme selected to proceed with the screening analysis were pH = 6 (SOD), pH = 5 (GOx) and pH = 7 (Cat). Using these conditions, three NaCl concentrations were tested for each enzyme: 0, 100 and 145 mM (SOD) and 0, 680 and 750 mM (GOx and Cat).

Table 5.2 – *T_m values determined for* Cu,Zn superoxide dismutase (SOD), glucose oxidase (GOx) and catalase (Cat) *at the tested pH and NaCl concentration conditions using differential scanning fluorimetry (DSF).*

		SOD		GOx	Cat	
		T_{m1} (ºC)	T_{m2} (ºC)	T_m (ºC)	T_{m1} (ºC)	T_{m2} (ºC)
pH[a]	3	41 ± 2.1	-	59 ± 1.9	n.d.	n.d.
	4	40 ± 0.0	-	61 ± 0.0	n.d.	n.d.
	5	n.d.	n.d.	66 ± 2.0	n.d.	n.d.
	6	40 ± 1.3	85 ± 2.0	n.d.	42 ± 0.6	59 ± 1.2
	7	n.d.	n.d.	n.d.	44 ± 2.0	57 ± 0.0
	8	n.d.	n.d.	n.d.	44 ± 0.6	56 ± 0.6
NaCl (mM)[b]	0	43 ± 0.6	82 ± 0.6	64 ± 0.0	44± 2.0	58 ± 0.0
	100	n.d.	n.d.	67 ± 0.6	-	58 ± 0.0
	145	41 ± 0.6	83 ± 0.6	n.d.	n.d.	n.d.
	680	n.d.	n.d.	70 ± 0.0	-	-
	725	-	85 ± 0.6	n.d.	n.d.	n.d.

*Note: [a]Assays were performed in 10 mM citrate/145 mM NaCl buffer (SOD), 50 mM sodium acetate buffer (*GOx) and 50 mM potassium phosphate buffer *(*Cat*). [b]*Assays were performed in 10 mM citrate buffer, pH 6 *(*SOD), 50 mM sodium acetate buffer*, pH 5 (*GOx) and 50 mM potassium phosphate buffer*, pH 7 (*Cat*); (n.d.) not determined. Assays were performed in triplicate and data is represented as mean ± standard deviation.*

As shown in Figure 5.3 and Table 5.2, the presence of NaCl seemed to have particularly impacted GOx thermostability. For this enzyme, the higher the NaCl concentration, the highest the T_m (64 ± 0.0 ºC, 67± 0.6 ºC and 70 ± 0.0 ºC, for 0, 100 and 680 mM NaCl, respectively), resulting in an increased conformational stability. In the case of SOD, the absence of NaCl seemed to have stabilized T_{m1SOD} and slightly destabilized $T_{m2\ SOD}$. On the other hand, for the highest NaCl concentration (725 mM), SOD loses its $T_{m1,}$ suggesting that the enzyme becomes more stabilized now only displaying T_{m2} (85 ± 0.6 ºC). Concerning Cat, for a concentration of NaCl 100 mM, the enzyme only displays T_{m2} (58 ± 0.0 ºC for both concentrations). For 780 mM NaCl, no T_m could be retrieved.

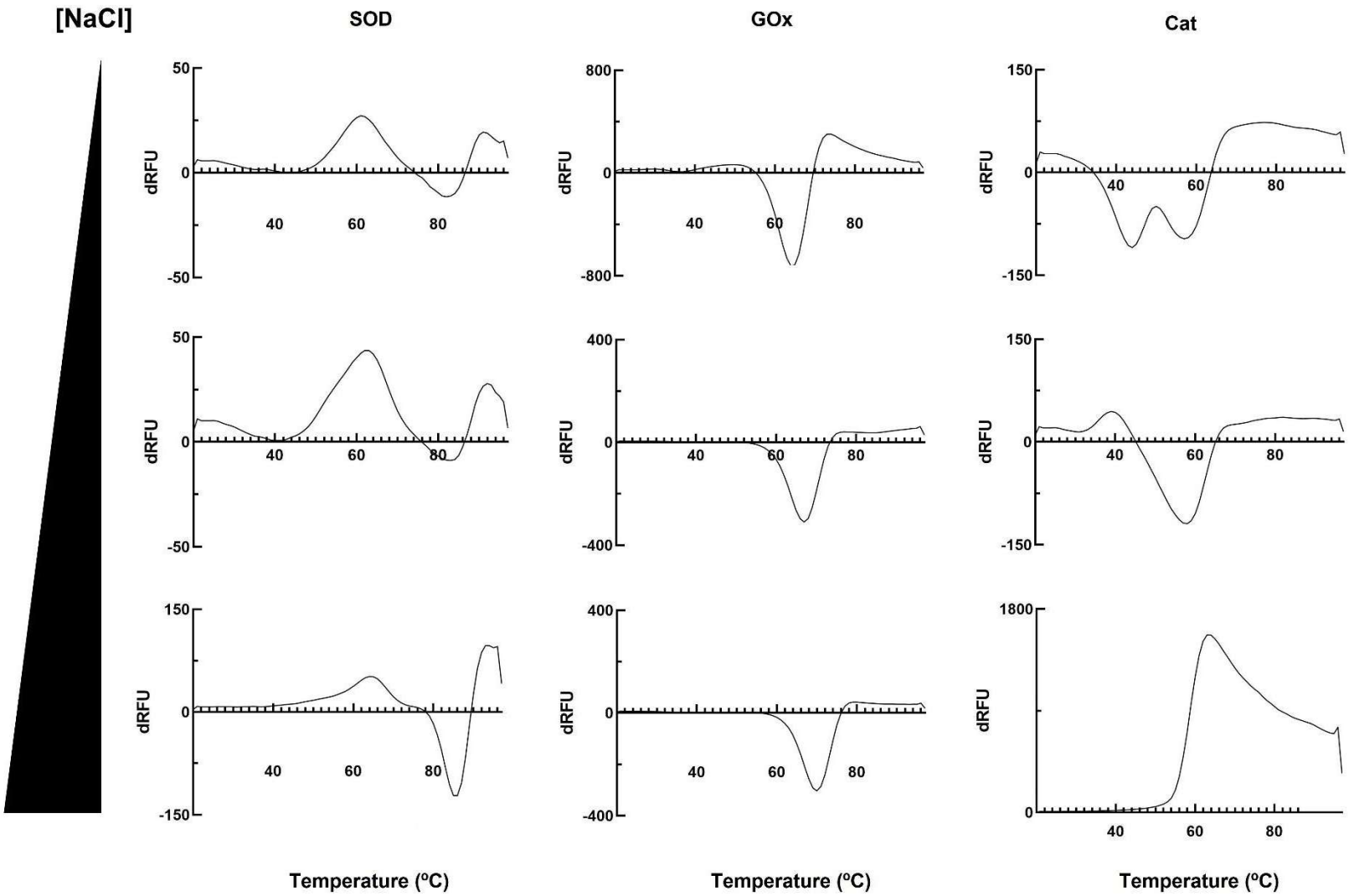

Figure 5.3 – *First derivatives of the melting curves obtained for Cu,Zn superoxide dismutase (SOD), glucose oxidase (GOx) and catalase (Cat), using differential scanning fluorimetry, as a function of increasing NaCl concentration. (SOD) 0, 145 and 780 mM NaCl; (GOx) 0, 100 and 680 mM NaCl; (Cat) 0, 100 and 680 mM NaCl. Melting curves represent the mean of three assays. See text for details in buffers composition.*

According to the obtained data, NaCl concentration of 145 mM (SOD) and 100 mM (GOx and Cat) were selected to proceed for the excipient screenings. Despite a higher NaCL concentration (680 mM) seemed to be beneficial for GOx, a lower concentration was selected to move forward, considering that from an inhalation standpoint, NaCl showcases physical stability issues in the long run.

5.4.2 Impact of single and combo excipients

After determining at which pH and NaCl concentration a more stable profile would be obtained, each enzyme was additionally combined with single excipients and then with excipient combos at different ratios (20:80, 50:50, 80:20). The ratios were defined based on previous studies on spray dried formulations intended for inhalation [19]–[21]. Eight excipients were chosen to be tested, namely four non-reducing sugars (trehalose, mannitol, raffinose and sucrose), two hydrophobic amino acids (L-leucine and L-alanine), and two hydrophilic amino acids (L-arginine and L-lysine). Excipient selection was, based on their potential for enzyme stabilization (positive and negative enzyme melting Temperature shifts), inhalation precedence and spray drying process development (High glass transition Temperatures) [20], [21], [30], [22]–[29].

In a first approach the DSF assays for excipients screening were performed in the absence and presence of the selected NaCl concentrations. As shown in Table 5.3, when combining SOD with the tested excipients, no effect induced by the used NaCl concentration could be detected. The same was also observed for GOx and Cat that maintained the number and values of their T_{ms}, regardless of the excipient tested.

For SOD, GOx and Cat, no significant stabilization ($\Delta T_m \leq \pm 2$ºC) and denaturation profile alteration was observed when each one was combined with the tested non-reducing sugars and the amino acids as showcased in Figures 5.4 where representative first derivatives of the melting curves obtained in the presence of trehalose, L-leucine and L-lysine are shown.

Table 5.3 – *T_m values determined for* Cu,Zn superoxide dismutase (SOD), glucose oxidase (GOx) and catalase (Cat) *in the absence of excipients (buffer) and presence of single excipient with and without (-) NaCl, using differential scanning fluorimetry (DSF).*

	SOD				GOx		Cat			
	NaCl (-)		NaCl 145 mM		NaCl (-)	NaCl 100 mM	NaCl (-)		NaCl 100 mM	
	T_{m1} (ºC)	T_{m2} (ºC)	T_{m1} (ºC)	T_{m2} (ºC)	T_m (ºC)		T_{m1} (ºC)	T_{m2} (ºC)	T_{m1} (ºC)	T_{m2} (ºC)
Buffer	39 ± 2.0	85 ± 2.0	41 ± 0.6	83 ± 0.6	66 ± 2.0	67 ± 0.6	44 ± 2.0	57 ± 2.0	-	58 ± 0.0
Tre	41 ± 1.7	85 ± 0.0	40 ± 0.0	86 ± 0.6	65 ± 0.0	65 ± 0.0	44 ± 0.0	55 ± 0.0	43 ± 0.0	54 ± 1.0
Man	39 ± 1.0	85 ± 0.0	40 ± 0.6	85 ± 0.6	66 ± 0.0	66 ± 0.6	42 ± 0.0	55 ± 0.6	43 ± 0.0	53 ± 0.6
Raf	40 ± 0.6	84 ± 0.6	41 ± 0.6	85 ± 0.0	65 ± 0.0	65 ± 0.0	41 ± 0.0	57 ± 0.0	43 ± 0.6	55 ± 0.0
Suc	39 ± 2.3	85 ± 0.6	41 ± 1.0	85 ± 0.0	65 ± 0.0	65 ± 0.0	-	55 ± 0.0	42 ± 0.0	42 ± 0.0
Ala	40 ± 0.6	85 ± 0.0	40 ± 2.1	85 ± 0.6	66 ± 0.6	65 ± 0.0	40 ± 0.6	57 ± 0.0	42 ± 0.0	55 ± 0.0
Arg	40 ± 1.2	86 ± 0.0	38 ± 0.0	88 ± 0.6	66 ± 0.6	65 ± 0.0	44 ± 0.0	57 ± 0.6	45 ± 0.6	54 ± 0.6
Leu	40 ± 1.2	85 ± 0.6	42 ± 1.2	85 ± 1.2	66 ± 0.6	65 ± 0.6	43 ± 0.0	57 ± 0.0	44 ± 0.6	54 ± 0.6
Lys	72 ± 0.6	-	71 ± 0.6	-	60 ± 0.6	60 ± 0.0	43 ± 1.0	-	43 ± 0.6	-

Note: (*Tre*) *Trehalose;* (*Man*) *Mannitol;* (*Raf*) *Raffinose;* (*Suc*) *Sucrose;* (*Ala*) L-*alanine;* (*Arg*) L-*arginine;* (*Leu*) L-l*eucine;* (*Lys*) *L-lysine. Assays were performed in triplicate and data represents mean ± standard deviation.*

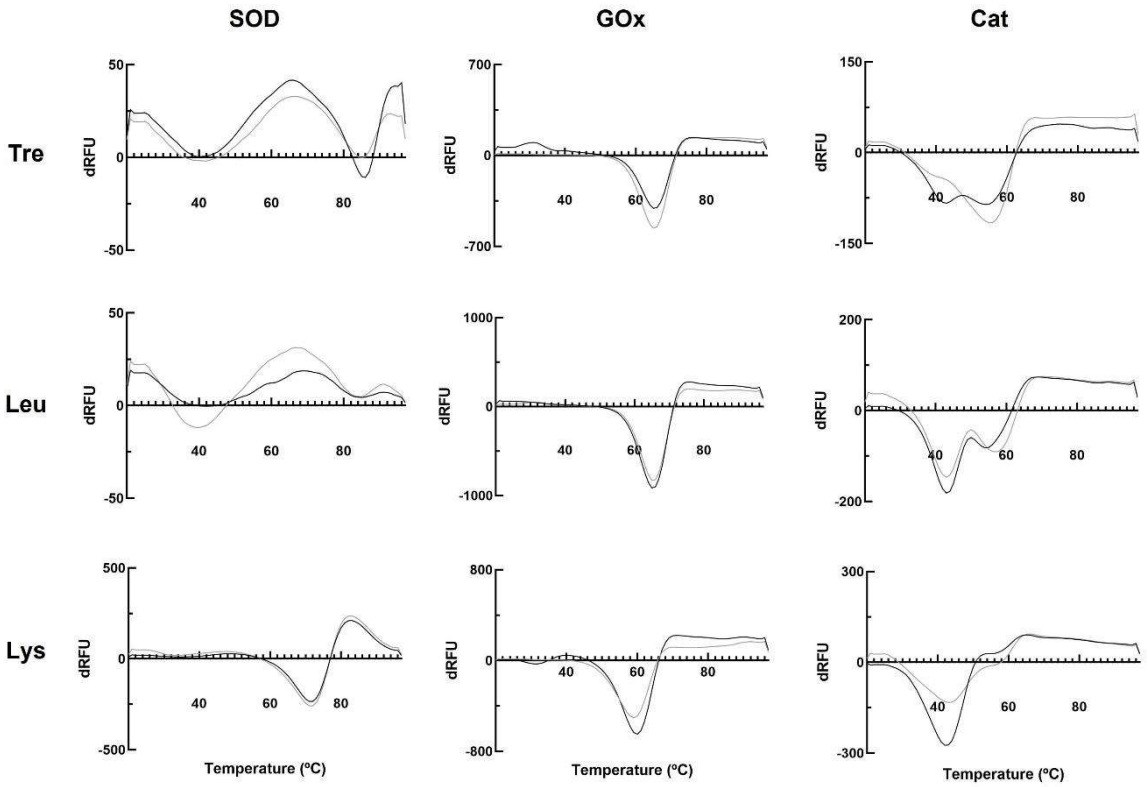

Figure 5.4 - *First derivatives of the melting curves for Cu.Zn superoxide dismutase (SOD), glucose oxidase (GOx) and catalase (Cat), using differential scanning fluorimetry (DSF), when combined with trehalose (Tre), L-leucine (Leu) and L-lysine (Lys). Assays were performed in the absence (grey line) and presence (black line) of 100 mM NaCl (GOx and Cat) or 145 mM NaCl for SOD). Melting curves represent the mean of three assays.*

The number of T_ms remained the same, yet, when Cat was combined with trehalose, raffinose and sucrose, the ratio between peaks fluorescence intensity altered. The hydrophilic (and positively charged) amino acid L-lysine significantly affected all three enzymes denaturation profile (Figure 5.4): SOD displayed only one T_m either in the absence (72 ± 0.6 ºC) and presence of 145 mM NaCl (71 ± 0.6 ºC); GOx T_m in the absence of NaCl decreased from 66 ± 2.0 ºC to 60 ± 0.6 ºC and from 67 ± 0.6 ºC to 60 ± 0.0 ºC ($\Delta T_m \geq -2$ºC) in the presence of 100 mM NaCl; and Cat lost its T_{m2} exhibiting a single T_m either in the absence (43 ± 1.0 ºC) and presence of 100 mM NaCl (43 ± 0.6 ºC). Following single excipient analysis, each sugar/amino acid (SUG:AA) were combined at three different ratios (20:80, 50:50, 80:20) in the absence of NaCl and at the previously inferred optimum pH for each enzyme, and the melting curves of SOD, GOx and Cat determined by DSF. As shown in Tables 5.4, 5.5 and 5.6 the results obtained with the different combination of excipients corroborated the previous observations on single excipients.

Table 5.4 – *T_m values determined for* Cu,Zn superoxide dismutase (SOD), *in the absence of excipients (buffer) and combined with sugar:amino acid (SUG:AA) combos at 20:80, 50:50 and 80:20, using differential scanning fluorimetry (DSF).*

	Sug:AA (20:80)		Sug:AA (50:50)		Sug:AA (80:20)	
	T_{m1} (ºC)	T_{m2} (ºC)	T_{m1} (ºC)	T_{m2} (ºC)	T_{m1} (ºC)	T_{m2} (ºC)
Tre:Ala	*	*	*	*	44 ± 0.0	87 ± 0.6
Tre:Arg	34 ± 0.0	85 ± 0.6	35 ± 0.6	86 ± 0.0	36 ± 0.0	86 ± 0.6
Tre:Leu	32 ± 4.9	87 ± 0.6	35 ± 1.0	78 ± 9.2	38 ± 0.6	85 ± 0.6
Tre:Lys	35 ± 1.0	73 ± 0.6	31 ± 0.6	76 ± 0.6	38 ± 0.0	87 ± 0.0
Man:Ala	37 ± 1.7	86 ± 0.6	37 ± 0.6	85 ± 0.6	35 ± 0.6	86 ± 0.6
Man:Arg	36 ± 0.6	84 ± 0.6	35 ± 2.1	84 ± 0.6	37 ± 0.6	85 ± 0.6
Man:Leu	38 ± 0.6	85 ± 0.0	36 ± 0.6	86 ± 0.0	38 ± 0.6	85 ± 0.0
Man:Lys	74 ± 0.0	-	76 ± 0.6	-	83 ± 0.6	-
Raf:Ala	38 ± 0.0	84 ± 1.7	38 ± 0.6	85 ± 0.0	37 ± 0.6	86 ± 0.6
Raf:Arg	35 ± 3.5	80 ± 6.4	36 ± 1.0	86 ± 1.0	36 ± 0.6	85 ± 0.6
Raf:Leu	37 ± 0.0	85 ± 0.0	38 ± 0.0	85 ± 0.0	*	*
Raf:Lys	74± 0.0		76± 0.0		*	*
Suc:Ala	35 ± 1.0	86 ± 0.6	36 ± 0.6	85 ± 1.5	36 ± 0.6	87 ± 0.0
Suc:Arg	36 ± 1.5	81 ± 5.1	37 ± 1.0	86 ± 1.0	38 ± 0.0	86 ± 0.0
Suc:Leu	37 ± 1.5	87 ± 1.2	36 ± 1.5	87 ± 1.0	36 ± 0.6	86 ± 0.6
Suc:Lys	74 ± 0.0	-	76 ± 0.0	-	83 ± 0.6	-
			Absence of excipients			
			T_{m1} (ºC)	T_{m2} (ºC)		
Buffer			39 ± 2.0	85 ± 2.0		

Note: (*Tre*) *Trehalose;* (*Man*) *Mannitol;* (*Raf*) *Raffinose;* (*Suc*) *Sucrose;* (*Ala*) L-*alanine;* (*Arg*) L-*arginine;* (*Leu*) L-l*eucine;* (*Lys*) *L-*l*ysine. *Melting curves did not allow to calculate the T_m. Assays were performed in triplicate and data represents mean ± standard deviation.*

For SOD, in the presence of L-lysine and the sugars mannitol and sucrose, irrespective of the SUG:AA ratios used, only one T_m was retrieved. In the presence of raffinose and the amino acids L-leucine and L-lysine the obtained melting curves did not allow determination of the T_m as well as for the trehalose:alanine combos at 20:80 and 50:50. Although for the majority of the remaining combos ΔT_{m1} and ΔT_{m2} were consistently < -2 ºC (indicating a destabilizing effect) when SOD was tested in the presence of Trehalose:Alanine at 80:20 the obtained ΔT_{m1} and ΔT_{m2} were of 5 and 2 ºC respectively. Interestingly for SOD the SUG:AA ratio of 80:20 did not present a negative impact for T_{m2}.As shown in Table 5.5 GOx seems to be less susceptible to the presence of L-lysine, as only in the presence of raffinose the melting curve did not render a Tm value. From the tested combos the SUG:AA ratios of 20:80 and 50:50 had a higher negative impact on the enzyme Tm, with ΔT_m reaching -2 ºC for trehalose:L-lysine, mannose;L-lysine and sucrose:L-Lysine (at 80:20 ratio).

Table 5.5 – *T_m values determined for glucose oxidase (GOx), in the absence of excipients (buffer) and combined with sugar:amino acid (SUG:AA) combos at 20:80, 50:50 and 80:20, using differential scanning fluorimetry (DSF).*

	Sug:AA (20:80)	Sug:AA (50:50)	Sug:AA (80:20)
	T_m (ºC)	T_m (ºC)	T_m (ºC)
Tre:Ala	65±0.0	66±0.0	66±0.0
Tre:Arg	66±0.0	66±0.0	66±0.0
Tre:Leu	65±0.0	65±0.0	65±0.0
Tre:Lys	64±0.0	65±0.6	65±0.0
Man:Ala	66±0.0	65±0.0	66±0.0
Man:Arg	66±0.0	66±0.0	66±0.0
Man:Leu	66±0.0	66±0.6	66±0.0
Man:Lys	64±0.0	66±0.0	66±0.0
Raf:Ala	65±0.6	65±0.0	66±0.6
Raf:Arg	66±0.0	66±0.0	66±0.0
Raf:Leu	66±0.0	66±0.0	65±0.0
Raf:Lys	64±0.0	65±0.0	66±0.0
Suc:Ala	66±0.0	66±0.6	66±0.6
Suc:Arg	66±0.0	66±0.0	66±0.0
Suc:Leu	66±0.0	65±0.0	65±0.0
Suc:Lys	64±0.0	66±0.0	66±0.0
		Absence of excipients	
		T_m (ºC)	
Buffer		66 ± 2.0	

*Note: (Tre) Trehalose; (Man) Mannitol; (Raf) Raffinose; (Suc) Sucrose; (Ala) L-alanine; (Arg) L-arginine; (Leu) L-leucine; (Lys) L-lysine. *Melting curves did not allow to calculate the T_m. Assays were performed in triplicate and data represents mean ± standard deviation.*

For Cat a similar trend was observed (Table 5.6) with L-lysine contributing for a less stable enzyme in the presence of mannose and raffinose. For Cat the SUG:AA ratios of 80:20 maintained the enzyme T_{m2}, while T_{m1} was less impacted in the presence of 20:80 SUG:AA ratios.

Table 5.6 – *T_m values determined for* catalase (Cat), *in the absence of excipients (buffer) and combined with sugar:amino acid (SUG:AA) combos at 20:80, 50:50 and 80:20, using differential scanning fluorimetry (DSF).*

	Sug:AA (20:80)		Sug:AA (50:50)		Sug:AA (80:20)	
	T_{m1} (ºC)	T_{m2} (ºC)	T_{m1} (ºC)	T_{m2} (ºC)	T_{m1} (ºC)	T_{m2} (ºC)
Tre:Ala	40 ± 0.6	57 ± 0.0	41 ± 0.6	57 ± 0.0	41 ± 0.6	57 ± 0.6
Tre:Arg	40 ± 0.6	57 ± 0.0	40 ± 0.0	57 ± 0.0	41 ± 0.0	56 ± 0.0
Tre:Leu	40 ± 1.5	57 ± 0.0	40 ± 0.0	57 ± 0.0	43 ± 1.2	57 ± 0.6
Tre:Lys	42 ± 0.6	57 ± 1.0	41 ± 0.0	53 ± 0.0	43 ± 1.0	56 ± 1.0
Man:Ala	40 ± 0.6	57 ± 0.0	41 ± 0.0	57 ± 0.0	41 ± 1.0	57 ± 0.0
Man:Arg	41 ± 0.0	57 ± 0.0	41 ± 0.0	57 ± 0.0	41 ± 0.6	56 ± 0.6
Man:Leu	41 ± 0.0	57 ± 0.0	41 ± 0.0	57 ± 0.0	41 ± 0.0	56 ± 0.6
Man:Lys	43 ± 0.6	-	42 ± 0.6	55 ± 1.7	42 ± 0.6	57 ± 0.6
Raf:Ala	*	*	44 ± 0.0	57 ± 0.0	43 ± 0.6	57 ± 0.0

Raf:Arg	43 ± 0.0	57 ± 0.0	43 ± 0.0	57 ± 0.0	43 ± 0.0	57 ± 0.0
Raf:Leu	43 ± 0.0	57 ± 0.0	42 ± 0.6	57 ± 0.0	44 ± 0.0	57 ± 0.0
Raf:Lys	45 ± 0.0	-	44 ± 0.0	57 ± 0.0	*	*
Suc:Ala	43 ± 0.6	57 ± 0.0	43 ± 0.0	56 ± 0.6	43 ± 0.0	57 ± 0.0
Suc:Arg	43 ± 0.0	57 ± 0.0	42 ± 0.6	56 ± 0.0	44 ± 0.0	56 ± 0.0
Suc:Leu	43 ± 0.6	57 ± 0.6	43 ± 0.0	56 ± 0.6	44 ± 0.0	56 ± 0.0
Suc:Lys	43 ± 0.0	57 ± 0.0	44 ± 0.0	57 ± 0.0	43 ± 0.6	56 ± 0.0
			Absence of excipients			
			T_{m1} (ºC)	T_{m2} (ºC)		
Buffer			44 ± 2.0	57 ± 2.0		

Note: (*Tre*) *Trehalose;* (*Man*) *Mannitol;* (*Raf*) *Raffinose;* (*Suc*) *Sucrose;* (*Ala*) L-*alanine;* (*Arg*) L-*arginine;* (*Leu*) L-l*eucine;* (*Lys*) *L-lysine. *Melting curves did not allow to calculate the T_m. Assays were performed in triplicate and data represents mean ± standard deviation.*

Interestingly, the melting curve profiles consisted of a merge between each single excipient profile, according to their ratio in the formulation as depicted in Figures 5.5 for the particular case of Trehalose:L-leucine and Trehalose:L-lysine. Overall, no significant stabilization effect induced by the tested combinations could be noticed, regardless of the ratio. As previously observed, Lysine had a destabilizing effect on all enzymes, the higher its concentration. In the case of GOx, however, the presence of sugar managed to neutralize Lysine effect, regardless of its concentration (Tables 5.4, 5.5 and 5.6).

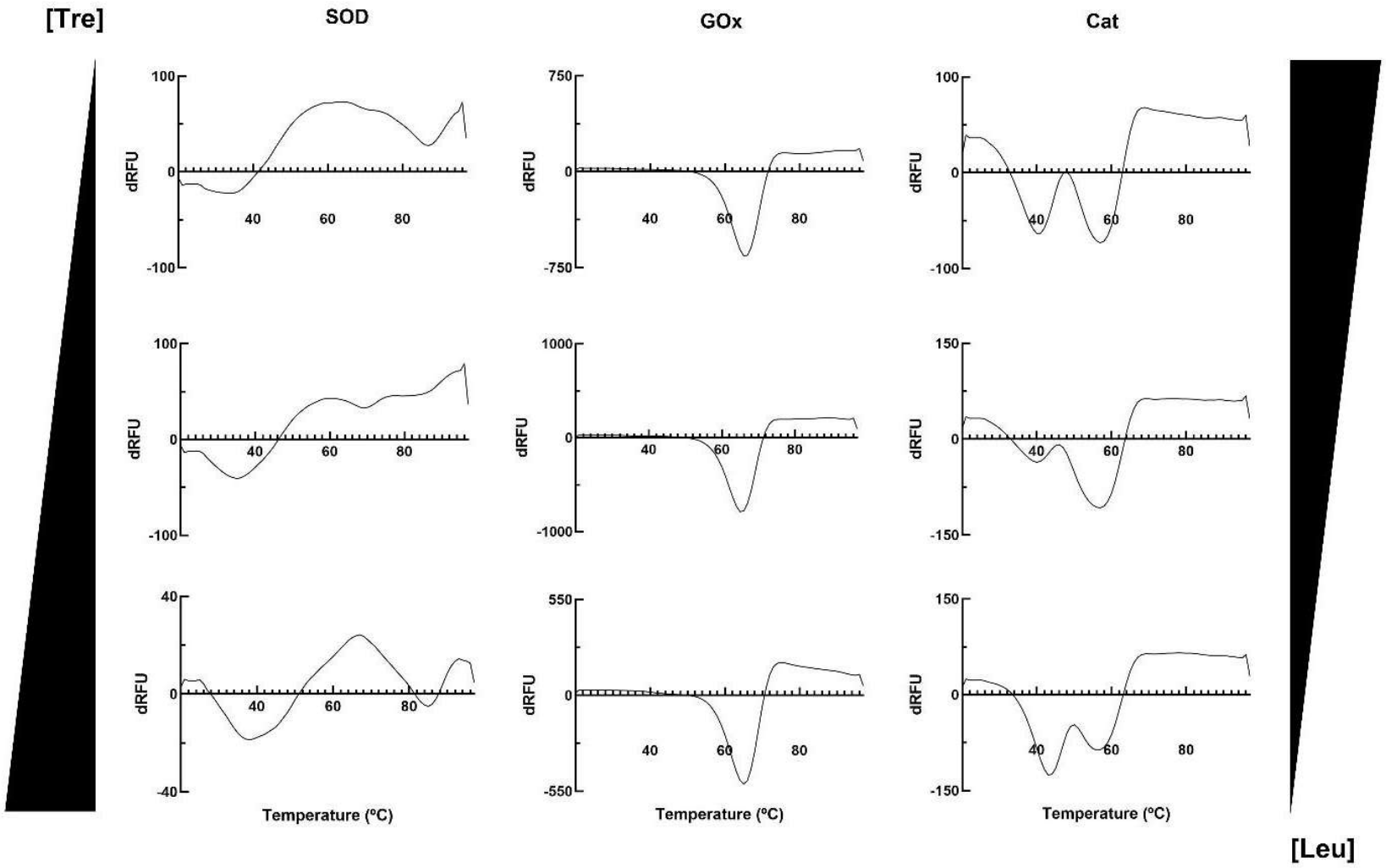

Figure 5.5 **-** First derivatives of the melting curves for Cu.Zn superoxide dismutase (SOD), glucose oxidase (GOx) and catalase (Cat), using differential scanning fluorimetry (DSF), when combined with trehalose and L-leucine (Tre:Leu) and trehalose and L-lysine (Tre:Lys) at 20:80, 50:50 and 80:20. Melting curves represent the mean of three assays.

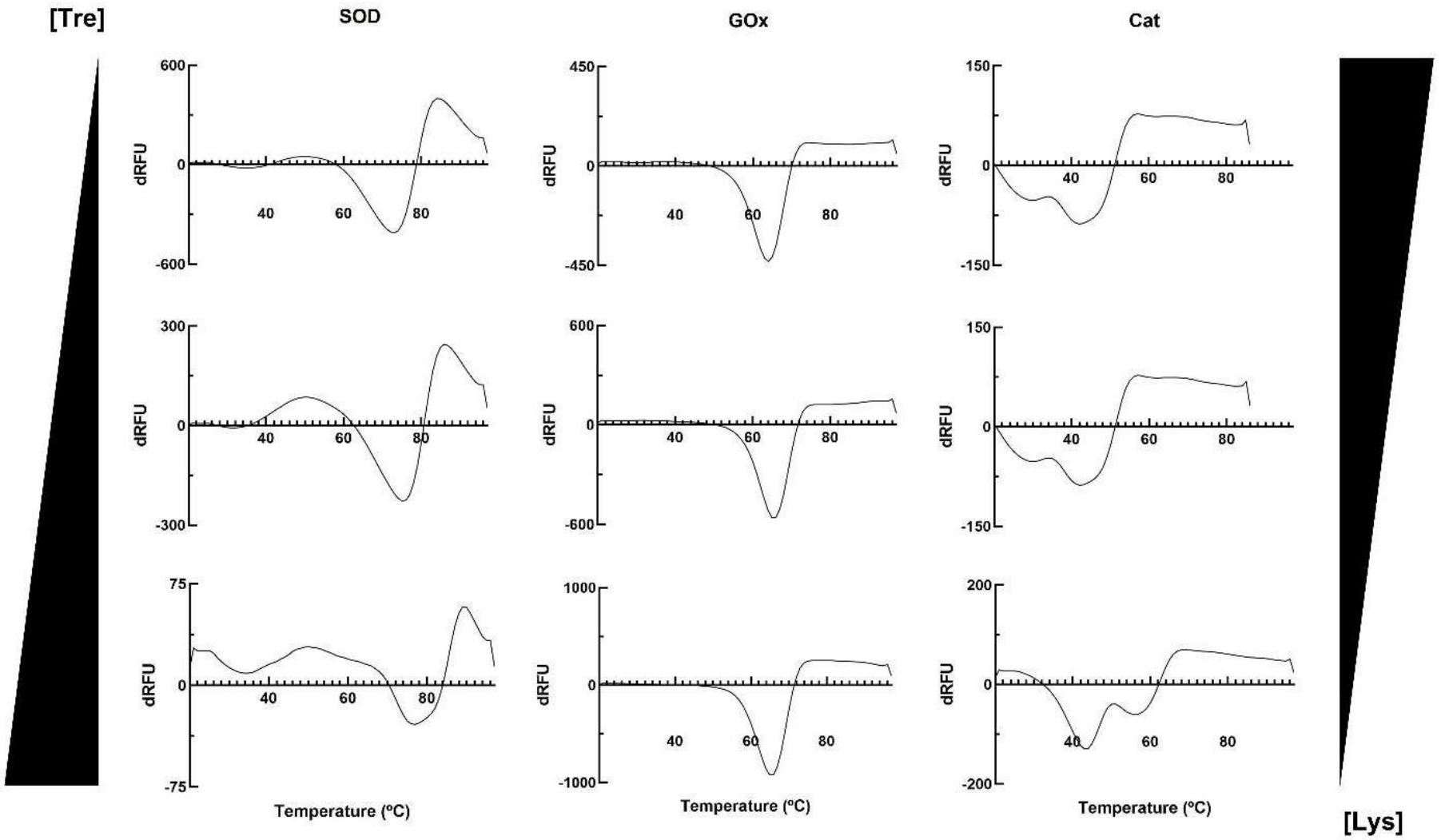

Figure 5.5 (cont.) **-** First derivatives of the melting curves for Cu.Zn superoxide dismutase (SOD), glucose oxidase (GOx) and catalase (Cat), using differential scanning fluorimetry (DSF), when combined with trehalose and L-leucine (Tre:Leu) and trehalose and L-lysine (Tre:Lys) at 20:80, 50:50 and 80:20. Melting curves represent the mean of three assays.

5.5 CONCLUSIONS

Herein, high-throughput differential scanning fluorimetry (HT-DSF) was used to examine the thermal stability of three model enzymes – SOD, GOx and Cat - under a range of different conditions comprising pH, NaCl concentration, single and combo excipients to narrow down formulations prior to spray drying. The DSF protocol allowed the fine-tuning of pH and [NaCl] optimum values, despite the tested excipients did not show a strong stabilizing effect on the model enzymes. From these, L-lysine, more specifically, impacted the stability of the model enzymes indicating that its use should be avoided for protein formulation. To further narrow down the formulations to be tested in the spray drying, high-throughput isothermal denaturation fluorimetry (HT-ITDF) is explored as a complement in the next chapter.

REFERENCES

[1] A. Ziaee *et al.*, “A rational approach towards spray drying of biopharmaceuticals: The case of lysozyme,” *Powder Technol.*, vol. 366, pp. 206–215, Apr. 2020, doi: 10.1016/j.powtec.2020.02.057.

[2] G. A. Ledet, R. A. Graves, L. A. Bostanian, and T. K. Mandal, “Spray-Drying of Biopharmaceuticals,” in *Lyophilized Biologics and Vaccines*, Springer New York, 2015, pp. 273–297.

[3] D. J. A. Crommelin, G. Storm, R. Verrijk, L. De Leede, W. Jiskoot, and W. E. Hennink, “Shifting paradigms: Biopharmaceuticals versus low molecular weight drugs,” *Int. J. Pharm.*, vol. 266, no. 1–2, pp. 3–16, 2003, doi: 10.1016/S0378-5173(03)00376-4.

[4] U. Angkawinitwong, G. Sharma, P. T. Khaw, S. Brocchini, and G. R. Williams, “Solid-state protein formulations,” *Ther. Deliv.*, vol. 6, no. 1, pp. 59–82, 2015, doi: 10.4155/tde.14.98.

[5] M. A. H. Capelle, R. Gurny, and T. Arvinte, “High throughput screening of protein formulation stability: Practical considerations,” *Eur. J. Pharm. Biopharm.*, vol. 65, no. 2, pp. 131–148, 2007, doi: 10.1016/j.ejpb.2006.09.009.

[6] R. Nayar and M. C. Manning, “High throughput formulation: strategies for rapid development of stable protein products.,” *Pharm. Biotechnol.*, vol. 13, pp. 177–198, 2002, doi: 10.1007/978-1-4615-0557-0_8.

[7] J. Pellaud, U. Schote, T. Arvinte, and J. Seelig, “Conformation and self-association of human recombinant transforming growth factor-β3 in aqueous solutions,” *J. Biol. Chem.*, vol. 274, no. 12, pp. 7699–7704, 1999, doi: 10.1074/jbc.274.12.7699.

[8] G. A. Senisterra and P. J. Finerty, “High throughput methods of assessing protein stability and aggregation,” *Mol. Biosyst.*, vol. 5, no. 3, pp. 217–223, 2009, doi: 10.1039/b814377c.

[9] J. Sloth, P. Bach, A. D. Jensen, and S. Kiil, “Evaluation method for the drying performance of enzyme containing formulations,” *Biochem. Eng. J.*, vol. 40, no. 1, pp. 121–129, May 2008, doi: 10.1016/j.bej.2007.11.024.

[10] H.-K. Chain and I. Gonda, “Solid State Characterization of Spray-Dried Powders of Recombinant Human Deoxyribonuclease (RhDNase)†,” *J. Pharm. Sci.*, vol. 87, no. 5, pp. 647–654, May 1998, doi: 10.1021/js9504292.

[11] J. A. Roe, A. Butler, D. M. Scholler, J. S. Valentine, L. Marky, and K. J. Breslauer, “Differential Scanning Calorimetry of Cu,Zn-Superoxide Dismutase, the Apoprotein, and Its Zinc-Substituted Derivatives,” *Biochemistry*, vol. 27, no. 3, pp. 950–958, 1988, doi: 10.1021/bi00403a017.

[12] T. Ye, J. Yu, Q. Luo, S. Wang, and H. K. Chan, “Inhalable clarithromycin liposomal dry

powders using ultrasonic spray freeze drying," *Powder Technol.*, vol. 305, pp. 63–70, Jan. 2017, doi: 10.1016/j.powtec.2016.09.053.

[13] A. I. Bourbon, A. C. Pinheiro, M. G. Carneiro-da-Cunha, R. N. Pereira, M. A. Cerqueira, and A. A. Vicente, "Development and characterization of lactoferrin-GMP nanohydrogels: Evaluation of pH, ionic strength and temperature effect," *Food Hydrocoll.*, vol. 48, pp. 292–300, 2015, doi: 10.1016/j.foodhyd.2015.02.026.

[14] L. M. Ellerby, D. E. Cabelli, J. A. Graden, and J. S. Valentine, "Copper - Zinc Superoxide Dismutase : Why Not pH-Dependent ?," no. 11, pp. 6556–6561, 1996.

[15] M. Luisa Corvo, J. C. S. Jorge, R. Van't Hof, M. E. M. Cruz, D. J. A. Crommelin, and G. Storm, "Superoxide dismutase entrapped in long-circulating liposomes: Formulation design and therapeutic activity in rat adjuvant arthritis," *Biochim. Biophys. Acta - Biomembr.*, vol. 1564, no. 1, pp. 227–236, 2002, doi: 10.1016/S0005-2736(02)00457-1.

[16] J. A. Tainer, E. D. Getzoff, K. M. Beem, J. S. Richardson, and D. C. Richardson, "Determination and analysis of the 2 Å structure of copper, zinc superoxide dismutase," *J. Mol. Biol.*, vol. 160, no. 2, pp. 181–217, 1982, doi: 10.1016/0022-2836(82)90174-7.

[17] L. G. Wood, D. a Fitzgerald, P. G. Gibson, D. M. Cooper, and M. L. Garg, "Increased plasma fatty acid concentrations after respiratory exacerbations are associated with elevated oxidative stress in cystic fibrosis patients.," *Am. J. Clin. Nutr.*, vol. 75, no. 4, pp. 668–75, 2002, [Online]. Available: http://www.ncbi.nlm.nih.gov/pubmed/11916752.

[18] A. Ahmad, S. Akhtar, and V. Bhakuni, "Monovalent cation-induced conformational change in glucose oxidase leading to stabilization of the enzyme," *Biochemistry*, vol. 40, no. 7, pp. 1945–1955, 2001, doi: 10.1021/bi001933a.

[19] E. Costa, F. Neves, and C. Moura, "Design of composite particles via spray drying for DPI formulations," *ONdrugDelivery*, no. 53, pp. 16–23, 2014.

[20] D. A. Fernandes, P. Leandro, E. Costa, and M. L. Corvo, "Dry powder inhaler formulation of Cu,Zn-superoxide dismutase by spray drying: A proof-of-concept," *Powder Technol.*, vol. 389, pp. 131–137, 2021, doi: 10.1016/j.powtec.2021.05.008.

[21] S. Focaroli *et al.*, "A Design of Experiment (DoE) approach to optimise spray drying process conditions for the production of trehalose/leucine formulations with application in pulmonary delivery," *Int. J. Pharm.*, vol. 562, no. November 2018, pp. 228–240, 2019, doi: 10.1016/j.ijpharm.2019.03.004.

[22] S. Ohtake, Y. Kita, and T. Arakawa, "Interactions of formulation excipients with proteins in solution and in the dried state," *Advanced Drug Delivery Reviews*. 2011, doi: 10.1016/j.addr.2011.06.011.

[23] T. Sou *et al.*, "Designing a multi-component spray-dried formulation platform for pulmonary delivery of biopharmaceuticals: The use of polyol, disaccharide,

polysaccharide and synthetic polymer to modify solid-state properties for glassy stabilisation," *Powder Technol.*, vol. 287, pp. 248–255, Jan. 2016, doi: 10.1016/j.powtec.2015.10.008.

[24] A. L. Feng, M. A. Boraey, M. A. Gwin, P. R. Finlay, P. J. Kuehl, and R. Vehring, "Mechanistic models facilitate efficient development of leucine containing microparticles for pulmonary drug delivery," *Int. J. Pharm.*, vol. 409, no. 1–2, pp. 156–163, 2011, doi: 10.1016/j.ijpharm.2011.02.049.

[25] N. K. Jain and I. Roy, "Effect of trehalose on protein structure," *Protein Sci.*, vol. 18, no. 1, pp. 24–36, 2009, doi: 10.1002/pro.3.

[26] S. K. Singh, *Sucrose and trehalose in therapeutic protein formulations*, vol. 38. Springer International Publishing, 2018.

[27] Y. F. Maa *et al.*, "Effect of spray drying and subsequent processing conditions on residual moisture content and physical/biochemical stability of protein inhalation powders," *Pharm. Res.*, vol. 15, no. 5, pp. 768–775, 1998, doi: 10.1023/A:1011983322594.

[28] H. K. Chan, A. Clark, I. Gonda, M. Mumenthaler, and C. Hsu, "Spray dried powders and powder blends of recombinant human deoxyribonuclease (rhDNase) for aerosol delivery," *Pharm. Res.*, vol. 14, no. 4, pp. 431–437, 1997, doi: 10.1023/A:1012035113276.

[29] A. Ajmera and R. Scherließ, "Stabilisation of proteins via mixtures of amino acids during spray drying," *Int. J. Pharm.*, vol. 463, no. 1, pp. 98–107, 2014, doi: 10.1016/j.ijpharm.2014.01.002.

[30] C. P. Quan, S. Wu, N. Dasovich, C. Hsu, T. Patapoff, and E. Canova-Davis, "Susceptibility of rhDNase I to Glycation in the Dry-Powder State," *Anal. Chem.*, vol. 71, no. 20, pp. 4445–4454, Oct. 1999, doi: 10.1021/ac9900580.

CHAPTER 6

Formulation of spray dried enzymes for dry powder inhalers: an integrated methodology

Running heads:

- *How to integrate biopharmaceutical formulation and spray drying process development towards a dry powder inhaler of a biologic*

This chapter has been published as:

Fernandes DA, Costa E, Leandro P, Corvo ML: *Formulation of spray dried enzymes for dry poder inhalers: An integrated methodology* (ready for submission)

Fernandes D A, Costa E, Corvo M L, Leandro P: *Spray Drying of Inhalable Biopharmaceuticals of Increasing Size and 3D Structure Complexity: From 30 to 250 kDa,* Respiratory Drug Delivery 2019, Vol 2, pp. 283-288, April 2019, Cascais, Portugal. (Awarded podium presentation)

Fernandes D A, Pereira J, Leandro P, Corvo M L, Costa E: *How to Successfully Spray Dry Biopharmaceuticals Targeting the Lungs: A Novel Integrated Methodology,* 22nd Congress International Society for Aerosols in Medicine (ISAM) 2019, Vol 32, Issue 3, Montreaux, Switzerland.

Fernandes D A, Pereira J, Leandro P, Corvo M L, Costa E: *How to Successfully Spray Dry Biopharmaceuticals Targeting the Lungs: A Novel Integrated Methodology,* 11th iMED.Ulisboa Postgraduate Students & 4rd i3DU Meeting 2019, Lisboa, Portugal.

6.1 OVERVIEW

Herein, based on previous outcomes, an integrated methodology combining high-throughput differential scanning fluorimetry (DSF), high-throughput isothermal differential scanning fluorimetry and Andersen cascade impaction (ACI), is presented towards an appropriate excipient selection for a dry powder inhaler formulation, based on enzyme stabilization, inhalation precedence and spray drying (SD) process development.

Goals: To develop and validate the previously mentioned integrated methodology, testing four non-reducing sugars and four amino acids (two hydrophobic and two hydrophilic) to formulate three model enzymes of increasing molecular mass and structural complexity, belonging to the oxidoreductase class and often implicated in oxidative stress: superoxide dismutase, glucose oxidase and catalase.

Results: For each tested enzyme, it was possible to identify the sugar and amino acid showcasing a superior stabilizing effect on the tested enzymes and powders aerodynamic performance. Also, the spray drying outlet temperature to generate the powders could be determined. After SD, using the selected conditions, all powders displayed 65-85% of aerodynamic performance while each enzyme kept its quaternary structure (oligomeric state).

Conclusions: The present integrated methodology proved to be successful, allowing to narrow down 48 potential formulations (four sugars x four amino acids x three ratios) to only one for each enzyme, within few hours, while requiring sample amounts in the μg range.

6.2 INTRODUCTION

Enzymes have been increasingly regarded as effective biologics for the treatment of a wide spectrum of human diseases. Their ability to bind and act on their substrates with high affinity, specificity, and rates of product synthesis render them potent drugs when compared to other large and small molecules [1]. As therapeutic agents, inhalable enzyme formulations hold great promise as the pulmonary administration route lacks inactivating agents, is more permeable when compared to other routes, and allows for needle-free treatment of local and systemic diseases due to lungs highly vascularized surface area [2]–[4].

Enzymes can be delivered to the lungs using three main platforms: nebulizers, pressurized metered dose inhalers (pMDIs) and dry powder inhalers (DPIs). Enzymes have already been successfully formulated in nebulizers (Dornase alfa, rhDNase,) [5], [6]. Nevertheless, the liquid nature of its dosage forms results in the early stability loss upon storage. Moreover, nebulization involves long dosing periods due to inefficient drug deposition, leading to drug wastage and may require sterilization of the nebulizer between uses. On the other hand, pMDIs require the use of propellants that hinder the formulation process from a biocompatibility standpoint [7]. Alternatively, DPIs seem to address these shortcomings, taking advantage of increased stability and propellant-free dry powder dosage forms [8]–[12].

To formulate safe and effective dry powder dosage forms of enzymes for DPIs, at least two criteria must be met: (i) protein 3D structure must be maintained until deposition and absorption in the site of action, not only to avoid immunogenic responses but also to maintain the protein biological function; (ii) the aerodynamic particle size distribution (aPSD) of the dry powder dosage form should be within 1 and 5 μm size range, so it reaches the deep lung.

Different powder processing technologies such as lyophilization/freeze drying, spray drying (SD), supercritical CO_2 and spray freeze drying have been described in the literature [13], [14] to produce dry powder dosage forms meeting the above criteria. Among the described approaches, SD is a powder processing technology consisting of a single drying step driven by a temperature gradient (evaporation) of an atomized liquid feed solution that yields a

powder. The SD relative simplicity, with increased control over key aerosol features that impact powder aerodynamic performance (particle size, shape, internal structure and surface), together with cost effectiveness and scalability [15] render it a potential candidate to generate powders meeting the above criteria. The SD is also considered suitable for biologics like enzymes, due to the mild temperature exposure through evaporative cooling and short residence times. In addition, the wide range of SD scales commercially available, including miniaturized set-ups with low volume requirements, make it an encouraging option when working with these molecules, often quite expensive. The SD also fits continuous manufacturing systems, widely recognized as part of the future of pharmaceutical and biopharmaceutical industries [16].

Spray dried powder dosage forms for DPIs may comprise the active pharmaceutical ingredient (API) alone or combined with excipients. Non reducing sugars and amino acids are the standard, most safe and simple excipients used to formulate spray dried powder dosage forms for DPIs featuring an enzyme or any other biologic as API [8], [17]. The stabilizing effect exerted by non-reducing sugars involves the replacement of hydrogen bonds that otherwise would be formed between water molecules and the enzyme in the dry solid state (promoting aggregation). In addition, non-reducing sugars tackle the Maillard reaction, in which reducing sugars react with the protein's amino groups forming a carbohydrate adduct (protein glycosylation), a reaction that may be promoted by temperature. Spray-dried non-reducing sugars entrap the enzyme into an amorphous glass matrix, displaying a metastable non-crystalline structure. Such amorphous glass matrices present a higher risk of conversion to the more stable crystalline form over time once their glass transition Temperature (T_g) is reached. At T_g, the spray dried powder dosage form showcases a rubbery behavior that allows it to reorganize into a more stable crystalline structure. This could not only reduce its solubility and bioavailability but also impact the enzyme conformational structure, posing an immunogenicity risk. Hence, the selected non-reducing sugars should have high T_gs to mitigate this risk.

The water replacement theory, previously described for non-reducing sugars, was also proposed to explain the stabilization induced by the amino acids. Amino acids possessing hydrophobic groups can orient their side chains towards the air at the air/liquid interface of the feed droplets during the drying process, avoiding adsorption to this interface and denaturation of the enzyme. Moreover, the hydrophobic surface to the spray dried particles helps improve the aerodynamic performance [18, 19].

The enzyme:non-reducing sugar:amino acid (ENZ:SUG:AA) combination and ratio should be fine-tuned targeting enzyme stabilization and improved aerodynamic performance. Despite previous work concerning spray dried enzymes has already been described in the literature [16], [20, 21], an integrated formulation methodology for the choice of the better operational parameters to achieve enzyme stabilization and powder aerodynamic properties is still not available. Considering the great number of possible excipients and range of process parameters, this integrated methodology would be advantageous to shorten development time and sample requirements, lowering the optimization costs [22]–[24]. Herein, to address this gap, we propose combining a high-throughput (HT) screening platform, namely differential scanning fluorimetry (HT-DSF) and isothermal denaturation fluorimetry (HT-ITDF), followed by Andersen Cascade Impaction (ACI). The HT-DSF and HT-ITDF are commonly used to assess the stability of protein conformation, under different assay conditions (e.g. presence of ligands and stabilizers, different buffers etc), through the determination of the protein melting temperature (T_m; HT-DSF) and half time ($t_{1/2}$; HT-ITDF) to thermal denaturation. These parameters correspond to the temperature (T_m) and time ($t_{1/2}$) at which half of the protein molecules are unfolded upon thermal denaturation [23]. Positive shifts in the T_m and $t_{1/2}$ of a protein in the presence of a specific condition indicates an increase in the protein conformational stability. Hence, HT-DSF and HT-ITDF could help narrow down the ENZ:SUG:AA combination to then be tested by ACI, aiming to define the ratio, while only requiring a few hours and micrograms of a biological sample.

To validate this integrated methodology, three enzymes, belonging to the oxidoreductase class and often implicated in oxidative stress, of increasing size (from 32.5 to 250 kDa) and

structural complexity (from homodimer to homotetramer), were studied: Superoxide Dismutase (SOD), Glucose Oxidase (GOx), and Catalase (Cat).

6.3 MATERIALS AND METHODS

6.1.1 Materials

Copper, Zinc SOD from bovine erythrocytes (S7571-300KU, 32.5 kDa), Aspergillus niger GOx (G2133-250KU, 140 kDa), bovine liver Cat (C40-500MG, 250 kDa) and Sypro Orange 5000x stock solution were purchased from Sigma (St. Louis, MO, USA). D-trehalose dihydrate and L-leucine were purchased from EMD Millipore Corp. (Billerica, MA USA), Mannitol from SPI Pharma (Wilmington, USA), Raffinose from AMRESCO (Solon, Ohio, USA), Sucrose, L-alanine, L-arginine and L-lysine from MERCK (Darmstadt, Germany).

6.1.2 Methods

6.3.2.1 Spray Drying

Spray drying was performed in a customized Mini Spray Drier BUCHI, model B-290 (Büchi Labortechnik AG, Flawil, Switzerland) in open-loop, equipped with a two-fluid-nozzle (orifice 0.7 mm, core/cap 1.5 mm) refrigerated by external water bath re-circulation. Outlet temperature (T_{out}) was defined based on the minimum suitable temperature for evaporating water, each excipient T_g and on SOD, GOx and Cat T_{ms} determined by DSF (T_m – 5 ºC). Atomization (Rot_{atom}), feed (F_{feed}) and Nitrogen drying gas (F_{drying}) flowrates were kept constant at 60 mm in the rotameter (~ 2.1 $kg.h^{-1}$), 1.7 $g.min^{-1}$ and 35 $kg.h^{-1}$, respectively. These process parameters were defined so that particle properties would sit within the inhalation range.

The atomization flow rate is expressed in mm unit of the spray drying rotameter that controls this process parameter. The placebo feed solutions for SD comprised three different SUG:AA ratios (80:20; 50:50; 20:80), at 2 % (w/w) of solids content in water. For the active feed solutions, SOD, GOx and Cat were added at 2.5 % (w/w) concentration at the selected ratio determined in the placebo trials.

6.3.2.2 Powder and Protein Characterization

6.3.2.2.1 Andersen Cascade Impaction

Powders aerodynamic performance was assessed using an eight-stage gravimetric Andersen Cascade Impactor (Copley 88 Scientific Ltd., Nottingham, UK), as previously described [25]. All powders were hand-filled inside a glovebox at controlled relative humidity below 10%, in HPMC size 3 capsules (Capsugel, Basel, Switzerland) with 20 ± 0.4 mg of each formulation, in triplicate. These were actuated for 4 s, using a Plastiape device HR model 7 at 60 $L.min^{-1}$, (pressure drop of 4 kPa). The filter from each stage was weighted before and after each actuation. The fine particle fraction (FPF) was determined as the percentage of the powder mass emitted from the capsule displaying an aerodynamic diameter below 5 µm. The mass median aerodynamic diameter (MMAD) and the geometric standard deviation (GSD) were retrieved from CITDAS software (Copley 88 Scientific Ltd., Nottingham, UK).

6.3.2.2.2 Differential Scanning Fluorimetry and Isothermal Denaturation Fluorimetry

The DSF and ITDF were performed using a CFX96 Touch™ Real-Time PCR (BIO-RAD). The T_m of each enzyme, in the absence of excipients, was determined by DSF on a 96-well plate format, in a final volume of 50 µL containing SYPRO® Orange at 2000x final concentration and 10 µg of each enzyme in the respective reconstitution buffer, recommended by the supplier (for GOx and Cat) namely sodium citrate 10 mM, NaCl 145 mM, pH 6 (SOD) [26], [27], sodium acetate 50 mM, pH 5.1 (GOx) and potassium phosphate 50 mM, pH 7.0 (Cat). After an initial step at 20 °C for 10 minutes, thermal denaturation was performed by increasing the temperature up to 97 °C at a 1 $°C.min^{-1}$ rate, while taking a fluorescence reading every 0.2 °C, using the FRET channel. To calculate the T_m, the obtained temperature scan curves were fitted to a sigmoidal dose-response function or to a biphasic equation, and the T_m values retrieved from the midpoint of the plotted transitions.

The ITDF assay was performed to determine enzyme's $t_{1/2}$ (kinetic thermal stability) in the absence and presence of single excipients. Assays were also performed on a 96-well plate format, in a final volume of 50 µL containing 10 µg of each enzyme, 195.6 µg of single excipient (ratio Enzyme:Excipient adjusted to 5:97.8, required in the spray dried powder), SYPRO®

Orange at a final concentration of 2000x, in the above enzyme reconstitution buffers. The kinetic assays were performed at the previously calculated T_m – 5 ± 1 ºC for 2.5 h, while taking a fluorescence reading every 0.2 min, using the FRET channel. The $t_{1/2}$ values were mathematically derived. The DFS and ITDF assays were performed in triplicate (n=3).

6.3.2.2.3 Size Exclusion Chromatography

To assess the impact of spray drying on the subunit's assembly of the tested proteins (quaternary structural level), size exclusion chromatography (SEC) was performed on a HiLoad 16/60 Superdex 200 1.6 cm x 60 cm column (GE Healthcare Healthcare Life Sciences; Uppsala, Sweden), coupled with an UV detector (λ_{280nm}). Mobile phases were pumped at a flow rate of 0.7 mL.min^{-1}, at 4 ºC, using enzymes reconstitution buffers previously described in 2.2.2.2. The relative molecular mass (MM) of the different oligomeric forms was estimated from a calibration curve obtained with standard proteins: cytochrome C (12.4 kDa), ribonuclease A (13.7 kDa), myoglobin (17.6 kDa), β-lactoglobulin (18.4 kDa), ovalbumin (45 kDa), BSA (66 and 132 kDa), alcohol dehydrogenase (150 kDa), β-amylase (200 kDa) and apoferritin (443 kDa). Blue Dextran 2000 and L-Tyr were used to determine the void volume (V_0 = 46.6 mL) and the total exclusion volume (V_T = 119.4 mL) of the column, respectively.

6.3.2.2.4 Protein Electrophoresis

To analyze the enzymes subunit integrity, proteins (1 μg) were loaded into a 10 % denaturant polyacrylamide gel (SDS-PAGE), separated by electrophoresis (Mini-PROTEAN® Tetra handcast; Bio-Rad) and visualized using the NzyBlue Safe dye (Nzytech; Portugal). The relative MM of the enzymes subunits was estimated by analysis of a calibration curve of relative migration *versus* Log MM of the NZYColour-II MM standard (NzyTech) which included proteins with MM ranging from 245 to 11 kDa.

6.4 RESULTS AND DISCUSSION

To develop and validate an experimental approach to screen for excipients that could efficiently stabilize proteins during spray drying, three model enzymes belonging to the oxidoreductase class with increasing size, conformational structure complexity and postulated to present increasing vulnerability to formulation, were selected: the 32.5 kDa homodimeric SOD (≈15.5 kDa/subunit), displaying Cu and Zn at the active site; the 160 kDa homodimeric GOx (≈64 kDa/subunit), with $FADH_2$ and Fe at the active site necessary for catalysis; and the 250 kDa homotetrameric Cat (≈60 kDa/subunit) presenting Fe complexed with Heme at the active site. Furthermore, the studied enzymes were selected as they comprise the mass range that not only encompasses other classes of biologics (Figure 6.1) but also display the ability to surpass lung epithelium and beyond that limit for local delivery [28].

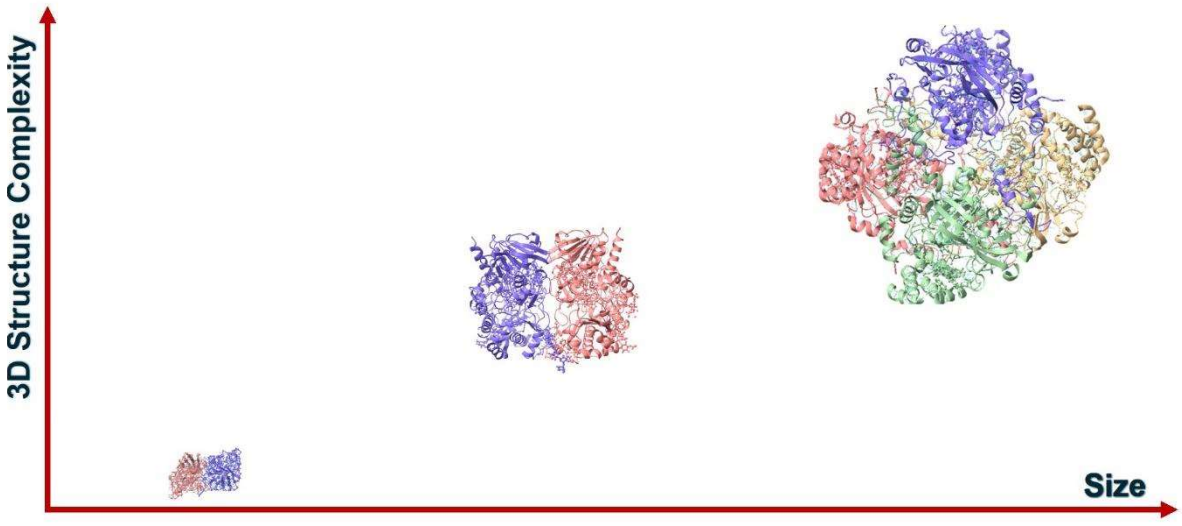

Figure 6.1 – *Rational for the selection of superoxide dismutase (SOD), glucose oxidase (GOx) and catalase (Cat) for spray drying (SD) excipient optimization. The 3D structures of SOD (32.5 kDa, homodimer), GOx (160 kDa, homodimer) and Cat (250 kDa, homotetramer) are represented, highlighting the different protein subunits (pink, blue, dark green and yellow). The size range of selected enzymes was defined as it covered the MM of other classes of biologics and based on the ability to surpass lung epithelium and beyond that limit for local delivery. SOD, GOx and Cat were also selected as they present complex and unstable quaternary structures (oligomeric assembly). Images were obtained using the UCSF Chimera software* [29] *and the PDB ID 2SOD (SOD), 1CF3 (GOx) and 5GKN (Cat).*

6.4.1 *Excipient screening and selection based on enzyme half-time stabilization by HT-ITDF*

For the screening and selection of stabilizing excipients, HT-ITDF was performed considering an initial pool of eight excipients, namely four non-reducing sugars (trehalose, mannitol, raffinose and sucrose), two hydrophobic amino acids (L-leucine and L-alanine), and two hydrophilic amino acids (L-arginine and L-lysine). Excipients were selected based on their spray drying process development (high glass transition temperatures), potential for enzyme stabilization and inhalation precedence (Table 6.1).

Table 6.1 – *Glass transition Temperature (T_g)* for the excipients included in this work

Excipient	T_g (ºC)	Ref
Trehalose	100	[30][19]
Mannitol	10	[31]
Raffinose	104	[32]
Sucrose	73.5	[30]
Leucine	126.85	[19][33]
Alanine	347.85	[33]
Arginine	136.85	[33]
Lysine	-15.15	[33]

Within the proposed integrated methodology, we hypothesized that when spray drying a biologic alone or embedded in an excipient matrix, as a conservative approach, the T_{out} should not exceed T_m to mitigate the risk of denaturation induced by this process parameter [34]. Hence, in this work the T_{out} was selected to correspond to T_m – 5 ºC for each of the enzymes used. In the cases where the enzyme displayed more than one T_m, the T_{out} was considered as the T_m average – 5 ºC (Table 6.2). On the other hand, T_g -T_{out} should be as large as possible, [16] preferably for T_{out} to be 10 to 20 ºC below the excipient system T_g to avoid powder stickiness, ultimately impacting physical properties, stability in the long run and process yield. Considering the excipient T_g (Table 6.1), mannitol was excluded due to its low T_g. Despite the same was observed for L-lysine, this was kept in the poll as a negative control.

Table 6.2 – *Superoxide dismutase (SOD), glucose oxidase (GOx) and catalase (Cat) melting temperatures (T_m) determined by differential scanning fluorimetry (DSF).*

	T_{m1} (ºC)	T_{m2} (ºC)	Mean T_m (ºC)
SOD	39 ± 2	85 ± 2	62 ± 2
GOx	66 ± 2	-	66 ± 2
Cat	44 ± 2	57 ± 2	51 ± 2

Note: Values represent the mean ± standard deviation (n=3)

SOD, GOx and Cat T_m were determined by DSF to set the temperature to be used on HT-ITDF. As the T_m corresponds to the temperature at which half of the protein molecules are denatured, it has been proposed that to better discriminate subtle differences in protein thermal denaturation kinetics (obtained by HT-ITDF), temperatures ≈ 4 to 6 ºC lower than the T_m should be used [23]. Therefore, the HT-ITDF assays were performed at temperatures corresponding to T_m –5 ± 1 ºC. As shown in Table 6.2, while GOx presented only a T_m of 62 ± 2 ºC, for SOD and Cat the thermal denaturation curves best fitted to a biphasic equation thus retrieving two T_m, 39 ± 2 ºC (T_{m1}) and 85 ± 2 ºC (T_{m2}) for SOD and 44 ± 2 ºC (T_{m1}) and 57 ± 2 ºC (T_{m2}) for Cat. The presence of more than one T_m is a frequent attribute of proteins presenting different structural domains that fold independently [23]. For the enzymes (SOD and Cat) displaying two T_{ms} (T_{m1} and T_{m2}), the ITDF temperature was selected based on the highest T_m namely, 80 ºC for SOD (T_{m2} – 5 ºC) and 53 ºC for Cat (T_{m2} - 5 ºC). For GOx, ITDF assays were performed at 62 ºC (T_m – 4 ºC). As shown in Figure 6.2, for each enzyme, a different kinetic denaturation profile was observed. At 80 ºC, SOD displayed a lag-phase (t_{lag}) before starting to unfold and one single plateau (Figure 6.2A); GOx (at 62 ºC) exhibited two plateaus ($t_{1/2\,1}$, $t_{1/2\,2}$) suggesting that denaturation takes places through two different processes (Figure 6.2B); Cat, on the other hand, at 53 ºC, presented one single plateau with no lag-phase (Figure 6.2C). Within each studied enzyme, the kinetic denaturation profiles were similar for the tested excipients, except for L-lysine. When combined with L-lysine, the kinetic profile of SOD and GOx exhibited one single plateau and absence of lag-phase. In the particular case of SOD a lower $t_{1/2}$ was yielded when compared to the enzyme alone ($t_{lag\ SOD}$ = 2.0 min, $t_{1/2\ SOD}$ = 9.4 min versus $t_{lag\ SOD+Lys}$ = 0.6 min, $t_{1/2\ SOD+Lys}$ = 3.3). The converse situation was observed despite Cat displaying the same kinetic profile. Its $t_{1/2}$ when combined with L-lysine

was slightly higher ($t_{1/2\ Cat}$ = 3.1 min versus $t_{1/2\ Cat+Lys}$ = 4.3 min). As previously mentioned, in the presence of a specific excipient, the higher the $t_{1/2,}$ the more resistant the enzyme structure to thermal stress. By analyzing the obtained data (Figure 6.2), and considering the pair SUG:AA, SOD is most stable when combined with raffinose:L-leucine ($t_{lag\ SOD}$ = 2.0 min, $t_{1/2\ SOD}$ = 9.4 min versus $t_{lag\ SOD+Raf}$ = 6.5 min , $t_{1/2\ SOD+Raf}$ = 18.2 min; $t_{lag\ SOD+Leu}$ = 10.8 min , $t_{1/2\ SOD+Leu}$ = 17.2 min), GOx with trehalose:L-alanine ($t_{1/2\ 1\ GOx}$ = 20.8 min, $t_{1/2\ 1\ GOx}$ = 85. 1 min versus $t_{1/2\ 1\ GOx+Tre}$ = 22.3 min; $t_{1/2\ 2\ GOx+Tre}$ = 98.4 min $t_{1/2\ 1\ GOx+Ala}$ = 23.2 min, $t_{1/2\ 2\ GOx+Ala}$ = 89.2 min) and Cat with sucrose:L-leucine ($t_{1/2\ Cat}$ = 3.1 min versus $t_{1/2\ Cat+Suc}$ = 4.6 min, $t_{1/2\ Cat+Leu}$ = 4.2 min), and therefore these were the excipients combinations selected for the spray drying process. Accordingly, the selected T_{out} were 57 ºC (SOD), 62 ºC (GOx) and 46 ºC (Cat).

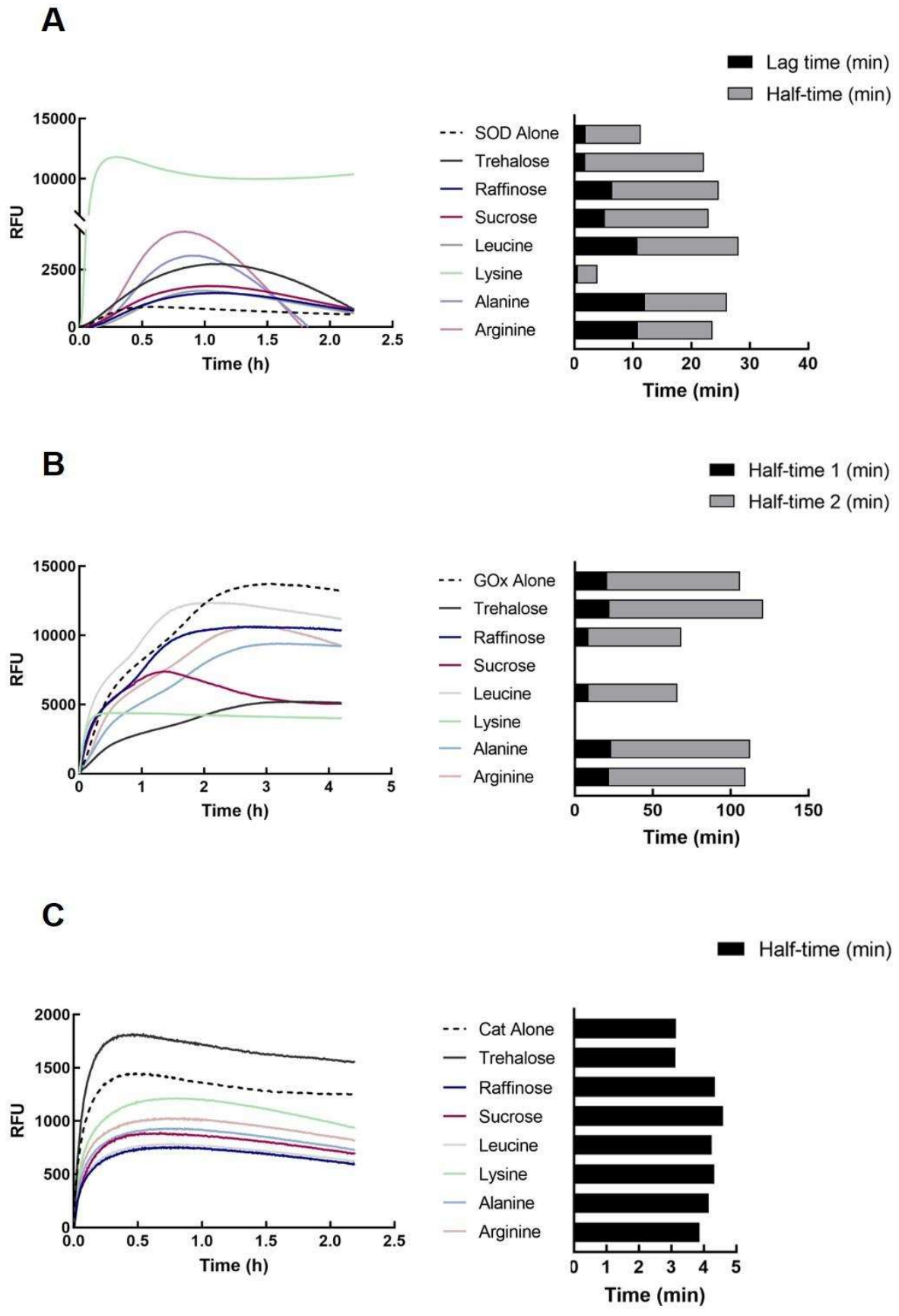

Figure 6.2 – *Isothermal Denaturation Fluorimetry (ITDF) profile of A - Superoxide Dismutase (SOD), B - Glucose*

Oxidase (GOx) and C - Catalase (Cat). The thermal denaturation kinetics of the enzymes were determined at 80 ºC for 2.5h (SOD; A), at 62 ºC for 5h (GOx; B) and at 53 ºC for 2.5h (Cat; C), alone and combined with the selected excipients.

6.4.2 Excipient ratio selection based on spray dried powder aerodynamic properties by ACI

After selecting the sugar and amino acid yielding the higher $t_{1/2,}$ when individually assayed (HT-ITDF) with the studied enzymes, and the T_{out} to be used, these enzymes were spray dried for three different SUG:AA ratios (80:20, 50:50 and 20:80) at the process conditions from Table 6.3.

Table 6.3 – *Placebo prototypes: feed solution and solids composition and spray drying process parameters.*

Feed Solution [deionized water:solids - 98:2 %(w/w)] **Solid's composition %(w/w)**	**Spray Drying process parameters**			
	T_{out} (˚C)	**Rot_{atom} (mm)**	**F_{feed} ($g.min^{-1}$)**	**F_{drying} ($kg.h^{-1}$)**
Raffinose:Leucine (80:20; 50:50; 20:80)	57	60	1.7	35
Trehalose:Alanine (80:20; 50:50; 20:80)	62	60	1.7	35
Sucrose:Leucine (80:20; 50:50; 20:80)	46	60	1.7	35

Note: Tout – Outlet temperature; Rot_{atom} – Atomization flow rate; F_{feed} – Feed flow rate; F_{drying} – Drying flow rate

The spray dried placebo prototype exhibiting the best aerodynamic performance (highest FPF) was then selected for the methodology validation with the respective enzyme. Figure 6.3 showcases the FPF observed for each tested ratio. When combined with raffinose (Figure 6.3A) a trade-off seems to be required for L-leucine concentration as an intermediate value (SUG:AA; 50:50) seemed to have resulted in the highest FPF. On the other hand, when combined with sucrose, a lower ratio of L-leucine (SUG:AA; 80:20) resulted in a higher FPF (Figure 6.3C). These results are in line with data described in the literature [19] as increased fine particle fractions could be achieved for a lower L-leucine concentration when combined with trehalose. Concerning L-alanine (when combined with trehalose) the higher the concentration, the higher the FPF (Figure 6.3B).

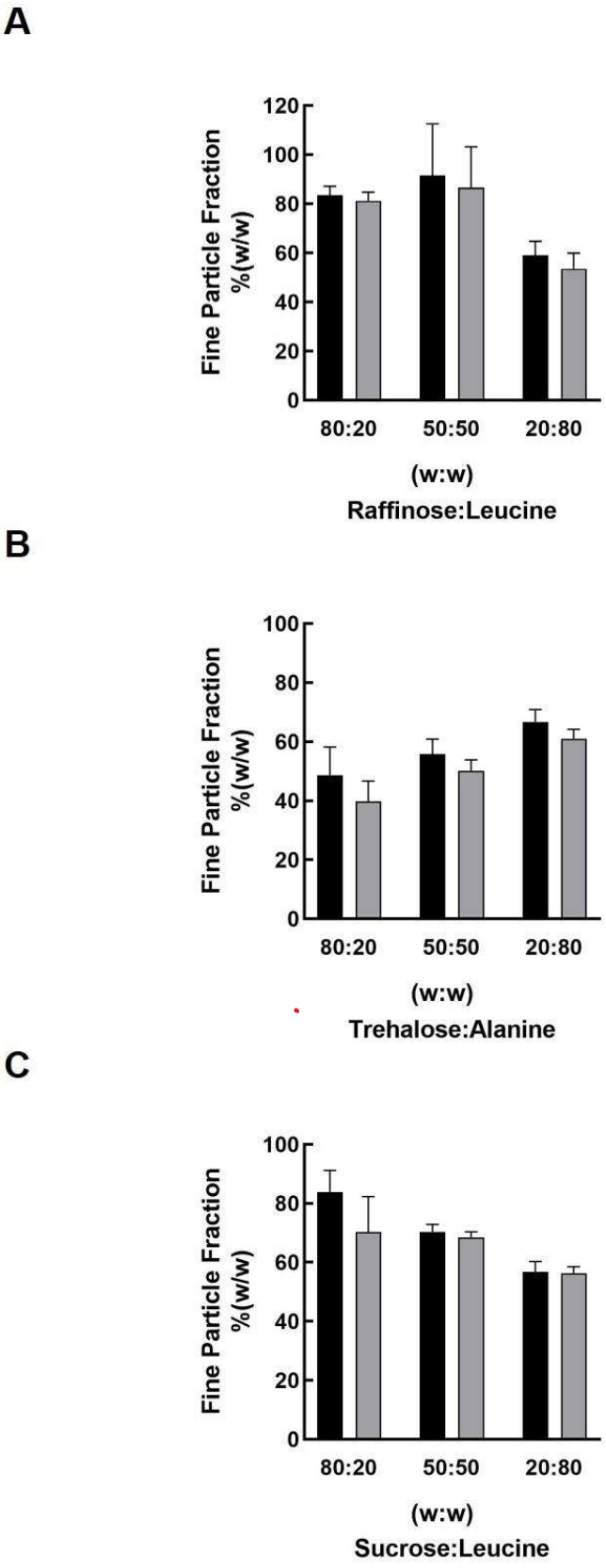

Figure 6.3 *– Fine Particle Fraction (FPF) based on Emitted Dose and Filled Weight of the placebo prototypes featuring the selected excipients at different SUG:AA ratios (80:20; 50:50 and 20:80) for Superoxide Dismutase (A), Glucose Oxidase (B) and Catalase (C).*

Based on the aerodynamic performance tests of the placebo prototype ratios, the selected conditions to be used in the active prototypes were raffinose:L-leucine at 50:50 for SOD, trehalose:L-alanine at 20:80 for GOx and sucrose:L-leucine at 80:20 for Cat.

6.5 Methodology Validation

To validate the prosed integrated approach, the model enzymes were spray dried using the selected conditions (excipient composition; T_{out} and excipient ratio; Table 6.4). The maintenance of the proteins quaternary structure after SD was monitored by SEC which also allowed to follow the presence of protein aggregates. Integrity of enzymes subunits (absence of proteolysis) was also monitored by SDS-PAGE.

Table 6.4 - *Active prototypes: feed solution composition and spray drying process parameters.*

Feed solution [deionized water:solids - 98:2 %(w/w)]	**Spray drying process parameters**			
Solid's composition %(w/w)	**T_{out} (°C)**	**Rot_{atom} (mm)**	**F_{feed} ($g.min^{-1}$)**	**F_{drying} ($kg.h^{-1}$)**
SOD:Raffinose:Leucine (2.5: 48.8 :48.8)	57	60	1.7	35
GOx:Trehalose:Alanine (2.5: 19.5 :78)	62	60	1.7	35
Cat:Sucrose:Leucine (2.5: 78 :19.5)	46	60	1.7	35

Note: Tout – Outlet temperature; Rot_{atom} – Atomization flow rate; F_{feed} – Feed flow rate; F_{drying} – Drying flow rate

The SEC chromatograms are shown in Figure 6.4. For each assay (before and after SD) the MM of the obtained separated protein was determined using an appropriate calibration curve (see material and methods section). The relative amount of the different oligomeric forms was computed by the ratio of the area beneath each peak and the total peaks area (Table 6.5). A good overlay of SEC chromatograms before and after SD was observed (Figure 6.4) for all tested enzymes. It should be emphasized that the high molecular mass (HMM) forms detected after SD for SOD (12.4%), GOx (1.9%) and Cat (6.6%) did not result from the drying process as they were already observed before SD (19.9, 3.0 and 5.9%, respectively). Importantly, the relative amount of the biological active oligomeric forms was maintained: 64.2, 79.2 and 82.8% of SOD dimer, GOx dimer and Cat tetramer, respectively.

Table 6.5 – *Molecular mass (MM) and relative amount (%) of oligomeric forms of superoxide dismutase (SOD), sglucose oxidase (GOx) and catalase (Cat) determined by size exclusion chromatography (SEC) and estimated MM of enzymes subunits determined by denaturant gel electrophoresis (SDS-PAGE), before (B_SD) and after (A_SD) Spray-Drying (SD).*

		SEC				SDS-PAGE	
		B_SD		A_SD		B_SD	A_SD
		MM (kDa)	%	MM (kDa)	%	MM (kDa)	
SOD	HMM[1]	> 600	19.9	> 600	12.4	14 (16)[4]	14 (16)[4]
	Dimer[3]	33	65.7	33	64.2		
	Monomer	-	-	-	-		
	LMM[2]	3.9	14.4	3.9	23.4		
GOx	HMM[1]	362	3.0	329	1.9	65 (73)[4]	65 (73)[4]
	Dimer[3]	147	92.3	147	79.2		
	Monomer	-	-	-	-		
	LMM[2]	4.2	4.6	4.2	18.9		
Cat	HMM[1]	> 400	5.9	>400	6.6	52 (46)[4]	52 (46)[4]
	Tetramer[3]	184	88.5	185	82.8		
	Dimer	70	5.6	70	7.1		
	Monomer	-	-	-	-		
	LMM[2]	-	-	4	3.5		

Note: [1](HMM) High molecular mass forms; [2](LMM) Low molecular mass forms. [3]Biological active oligomeric forms. [4]The MM of each subunit/monomer estimated by SEC was computed by the ratio of the MM of the active oligomeric form determined by SEC before and after SD and the expected number of subunits/monomers for each enzyme as described in the Methods.

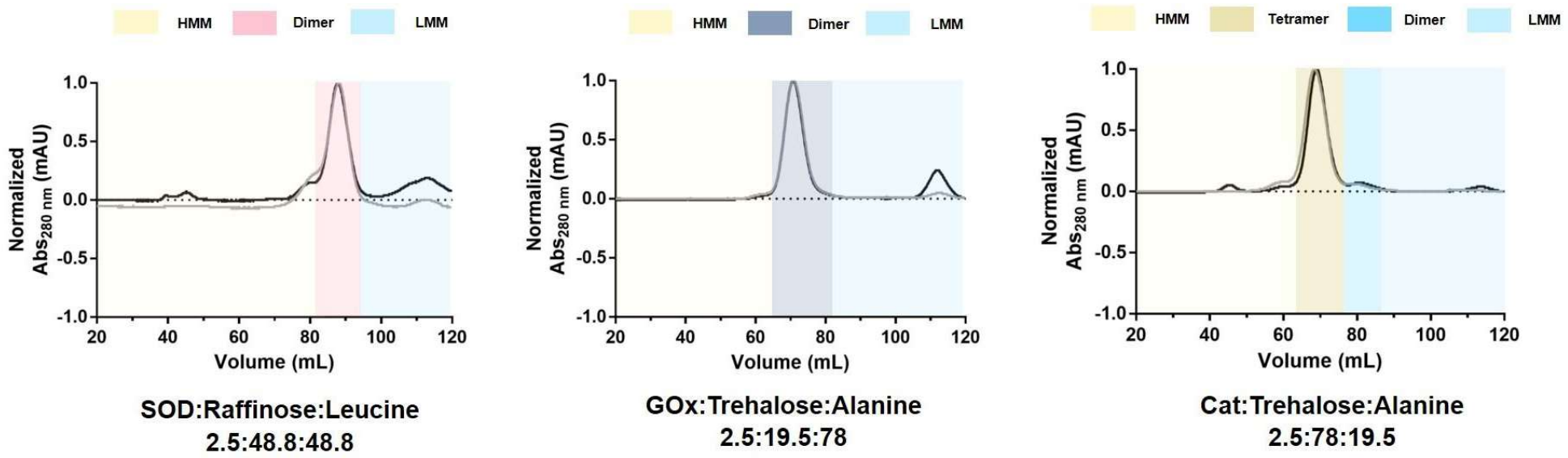

Figure 6.4 – Oligomeric profile of Superoxide Dismutase (SOD), Glucose Oxidase (GOx) and Catalae (Cat) before and after spray drying, monitored by size exclusion chromatography (SEC). The chromatograms for each tested conditions before (grey line) and after (black line) spray drying are shown. (HMM) high molecular mass forms; (LMM) low molecular mass forms.

Moreover, dissociation into the respective protein subunits/monomers did not occur upon SD since no peak corresponding to these forms was observed in the SEC chromatograms. Thus, the conditions selected for SD contributed to the maintenance of the fragile non-covalent interactions responsible for the necessary functional oligomeric species (SOD and GOx homodimers and Cat homotetramers). Furthermore, the SD selected conditions avoided the presence of potentially non-functional and immunogenic HMM forms. The analysis of the tested enzymes by SDS-PAGE, before and after SD (Figure 6.5) allowed the estimation of the MM of each enzyme subunit/monomer, indicating that no proteolysis occurred during the SD process. This observation was also in line with the subunit/monomer values estimated by SEC (Table 6.5). Moreover, the SDS-PAGE profile for each enzyme was the same before and after SD.

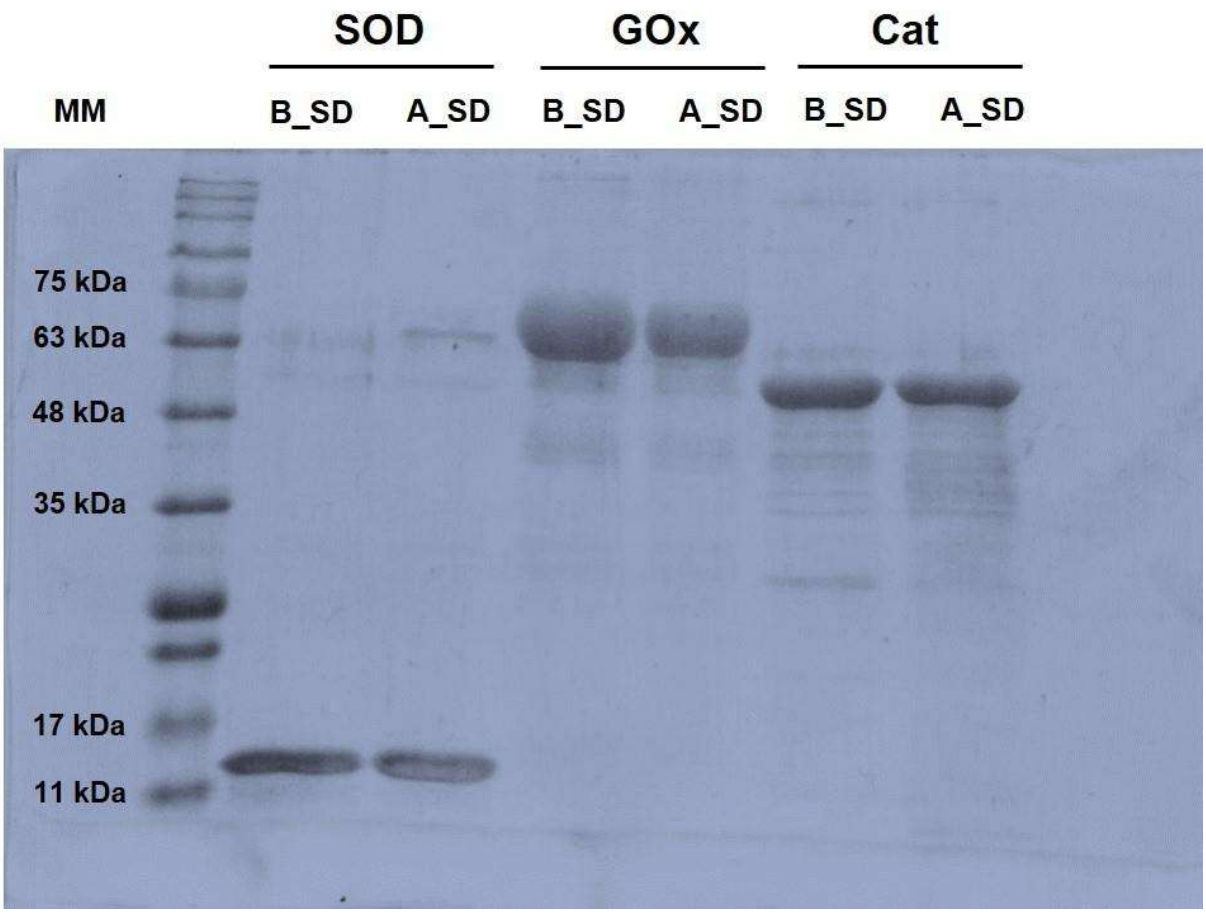

Figure 6.5 – *Analysis of superoxide dismutase (SOD), glucose oxidase (GOx) and catalase (Cat) before (B_SD) and after (A_SD) spray drying, by denaturant gel electrophoresis. (MM) molecular mass marker (Nzycolour-II MM standard).*

6.5 CONCLUSIONS

Herein, an integrated methodology to formulate and expedite spray dried DPI formulations featuring enzymes as APIs is proposed based on DSF followed by HT-ITDF and ACI. Three enzymes of increasing size and 3D structure complexity aiming to cover other classes of biopharmaceuticals were selected as models to develop and validate this strategy. DSF proved to be a valuable technique to identify the temperature at which ITDF screens should be performed and the T_{out} to be used. In addition, ITDF allowed to identify the most suitable excipients as all three enzymes displayed 65-85% of aerodynamic performance while keeping their functional oligomeric assembly (quaternary structural level) after SD with no significant presence of potentially non-functional and immunogenic HMM forms. Thus, the present integrated methodology proved to be successful in narrowing down 48 potential formulations (four sugars x four amino acids x three ratios) to only one for each enzyme, within few hours, while requiring µg range of sample amount.

REFERENCES

[1] M. Vellard, “The enzyme as drug: Application of enzymes as pharmaceuticals,” *Current Opinion in Biotechnology*, vol. 14, no. 4. Elsevier Ltd, pp. 444–450, 2003, doi: 10.1016/S0958-1669(03)00092-2.

[2] S. P. Newman, “Drug delivery to the lungs: Challenges and opportunities,” *Therapeutic Delivery*, vol. 8, no. 8. Future Medicine Ltd., pp. 647–661, Jul. 01, 2017, doi: 10.4155/tde-2017-0037.

[3] S. Mitragotri, P. A. Burke, and R. Langer, “Overcoming the challenges in administering biopharmaceuticals: Formulation and delivery strategies,” *Nature Reviews Drug Discovery*, vol. 13, no. 9. Nature Publishing Group, pp. 655–672, Sep. 01, 2014, doi: 10.1038/nrd4363.

[4] H. Okamoto, H. Todo, K. Iida, and K. Danjo, “Dry powders for pulmonary delivery of peptides and proteins,” *KONA Powder Part. J.*, vol. 20, no. March, pp. 71–83, 2002, doi: 10.14356/kona.2002010.

[5] H. K. Chan, A. Clark, I. Gonda, M. Mumenthaler, and C. Hsu, “Spray dried powders and powder blends of recombinant human deoxyribonuclease (rhDNase) for aerosol delivery,” *Pharm. Res.*, vol. 14, no. 4, pp. 431–437, 1997, doi: 10.1023/A:1012035113276.

[6] J. S. Wagener and O. Kupfer, “Dornase alfa (Pulmozyme),” *Curr. Opin. Pulm. Med.*, vol. 18, no. 6, pp. 609–614, 2012, doi: 10.1097/MCP.0b013e328358d51f.

[7] I. Ashurst, A. Malton, D. Prime, and B. Sumby, “Latest advances in the development of dry powder inhalers,” *Pharm. Sci. Technolo. Today*, vol. 3, no. 7, pp. 246–256, 2000, doi: 10.1016/S1461-5347(00)00275-3.

[8] S. A. Shoyele and A. Slowey, “Prospects of formulating proteins/peptides as aerosols for pulmonary drug delivery,” *Int. J. Pharm.*, vol. 314, no. 1, pp. 1–8, 2006, doi: 10.1016/j.ijpharm.2006.02.014.

[9] S. Ferrati, T. Wu, S. R. Kanapuram, and H. D. C. Smyth, “Dosing considerations for inhaled biologics,” *Int. J. Pharm.*, vol. 549, no. 1–2, pp. 58–66, Oct. 2018, doi: 10.1016/j.ijpharm.2018.07.054.

[10] K. Berkenfeld, A. Lamprecht, and J. T. McConville, “Devices for dry powder drug delivery to the lung.,” *AAPS PharmSciTech*, vol. 16, no. 3, pp. 479–90, 2015, doi: 10.1208/s12249-015-0317-x.

[11] N. Islam and E. Gladki, “Dry powder inhalers (DPIs)-A review of device reliability and innovation,” *Int. J. Pharm.*, vol. 360, no. 1–2, pp. 1–11, 2008, doi: 10.1016/j.ijpharm.2008.04.044.

[12] A. R. Clark, J. G. Weers, and R. Dhand, “The Confusing World of Dry Powder Inhalers:

It Is All about Inspiratory Pressures, Not Inspiratory Flow Rates," *Journal of Aerosol Medicine and Pulmonary Drug Delivery*, vol. 33, no. 1. Mary Ann Liebert Inc., pp. 1–11, Feb. 01, 2020, doi: 10.1089/jamp.2019.1556.

[13] F. Emami, A. Vatanara, E. J. Park, and D. H. Na, "Drying technologies for the stability and bioavailability of biopharmaceuticals," *Pharmaceutics*, vol. 10, no. 3. MDPI AG, Sep. 01, 2018, doi: 10.3390/pharmaceutics10030131.

[14] A. Langford, B. Bhatnagar, R. Walters, S. Tchessalov, and S. Ohtake, "Drying technologies for biopharmaceutical applications: Recent developments and future direction," *Dry. Technol.*, vol. 36, no. 6, pp. 677–684, 2018, doi: 10.1080/07373937.2017.1355318.

[15] A. Ziaee, A. B. Albadarin, L. Padrela, T. Femmer, E. O'Reilly, and G. Walker, "Spray drying of pharmaceuticals and biopharmaceuticals: Critical parameters and experimental process optimization approaches," *European Journal of Pharmaceutical Sciences*, vol. 127. Elsevier B.V., pp. 300–318, Jan. 15, 2019, doi: 10.1016/j.ejps.2018.10.026.

[16] J. T. Pinto *et al.*, "Progress in spray-drying of protein pharmaceuticals: Literature analysis of trends in formulation and process attributes," *Dry. Technol.*, 2021, doi: 10.1080/07373937.2021.1903032.

[17] E. Bodier-Montagutelli, A. Mayor, L. Vecellio, R. Respaud, and N. Heuzé-Vourc'h, "Designing inhaled protein therapeutics for topical lung delivery: what are the next steps?," *Expert Opin. Drug Deliv.*, vol. 15, no. 8, pp. 729–736, 2018, doi: 10.1080/17425247.2018.1503251.

[18] J. G. Weers and D. P. Miller, "Formulation Design of Dry Powders for Inhalation," *Journal of Pharmaceutical Sciences*, vol. 104, no. 10. John Wiley and Sons Inc., pp. 3259–3288, Oct. 01, 2015, doi: 10.1002/jps.24574.

[19] S. Focaroli *et al.*, "A Design of Experiment (DoE) approach to optimise spray drying process conditions for the production of trehalose/leucine formulations with application in pulmonary delivery," *Int. J. Pharm.*, vol. 562, no. November 2018, pp. 228–240, 2019, doi: 10.1016/j.ijpharm.2019.03.004.

[20] A. Ziaee *et al.*, "A rational approach towards spray drying of biopharmaceuticals: The case of lysozyme," *Powder Technol.*, vol. 366, pp. 206–215, Apr. 2020, doi: 10.1016/j.powtec.2020.02.057.

[21] J. Sloth, P. Bach, A. D. Jensen, and S. Kiil, "Evaluation method for the drying performance of enzyme containing formulations," *Biochem. Eng. J.*, vol. 40, no. 1, pp. 121–129, May 2008, doi: 10.1016/j.bej.2007.11.024.

[22] M. A. H. Capelle, R. Gurny, and T. Arvinte, "High throughput screening of protein formulation stability: Practical considerations," *Eur. J. Pharm. Biopharm.*, vol. 65, no. 2,

pp. 131–148, 2007, doi: 10.1016/j.ejpb.2006.09.009.

[23] G. A. Senisterra and P. J. Finerty, “High throughput methods of assessing protein stability and aggregation,” *Mol. Biosyst.*, vol. 5, no. 3, pp. 217–223, 2009, doi: 10.1039/b814377c.

[24] R. Nayar and M. C. Manning, “High throughput formulation: strategies for rapid development of stable protein products.,” *Pharm. Biotechnol.*, vol. 13, pp. 177–198, 2002, doi: 10.1007/978-1-4615-0557-0_8.

[25] D. A. Fernandes, P. Leandro, E. Costa, and M. L. Corvo, “Dry powder inhaler formulation of Cu,Zn-superoxide dismutase by spray drying: A proof-of-concept,” *Powder Technol.*, vol. 389, pp. 131–137, 2021, doi: 10.1016/j.powtec.2021.05.008.

[26] M. Luisa Corvo, J. C. S. Jorge, R. Van’t Hof, M. E. M. Cruz, D. J. A. Crommelin, and G. Storm, “Superoxide dismutase entrapped in long-circulating liposomes: Formulation design and therapeutic activity in rat adjuvant arthritis,” *Biochim. Biophys. Acta - Biomembr.*, vol. 1564, no. 1, pp. 227–236, 2002, doi: 10.1016/S0005-2736(02)00457-1.

[27] P. Marcelino *et al.*, “Therapeutic activity of superoxide dismutase-containing enzymosomes on rat liver ischaemia-reperfusion injury followed by magnetic resonance microscopy,” *Eur. J. Pharm. Sci.*, vol. 109, no. July, pp. 464–471, 2017, doi: 10.1016/j.ejps.2017.09.008.

[28] F. Depreter, G. Pilcer, and K. Amighi, “Inhaled proteins: Challenges and perspectives,” *International Journal of Pharmaceutics*, vol. 447, no. 1–2. pp. 251–280, Apr. 15, 2013, doi: 10.1016/j.ijpharm.2013.02.031.

[29] E. F. Pettersen *et al.*, “UCSF Chimera - A visualization system for exploratory research and analysis,” *J. Comput. Chem.*, vol. 25, no. 13, pp. 1605–1612, 2004, doi: 10.1002/jcc.20084.

[30] A. Simperler *et al.*, “Glass transition temperature of glucose, sucrose, and trehalose: An experimental and in silico study,” *J. Phys. Chem. B*, vol. 110, no. 39, pp. 19678–19684, 2006, doi: 10.1021/jp063134t.

[31] P. Ye and T. Byron, “Characterization of d-mannitol by thermal analysis, FTIR, and raman spectroscopy,” *Am. Lab.*, vol. 40, no. 14, pp. 24–27, 2008.

[32] A. Saleki-Gerhardt, J. G. Stoweell, S. R. Byrn, and G. Zografi, “Hydration and dehydration of crystalline and amorphous forms of raffinose,” *J. Pharm. Sci.*, vol. 84, no. 3, pp. 318–323, 1995, doi: 10.1002/jps.2600840311.

[33] Y. I. Matveev, V. Y. Grinberg, I. V. Sochava, and V. B. Tolstoguzov, “Glass transition temperature of proteins. Calculation based on the additive contribution method and experimental data,” *Food Hydrocoll.*, vol. 11, no. 2, pp. 125–133, 1997, doi: 10.1016/S0268-005X(97)80020-3.

[34] G. A. Ledet, R. A. Graves, L. A. Bostanian, and T. K. Mandal, “Spray-Drying of Biopharmaceuticals,” in *Lyophilized Biologics and Vaccines*, Springer New York, 2015, pp. 273–297.

CHAPTER 7

Summary, final remarks and future work

The present research had as primary goal the proposal of a methodology to produce dry powder inhaler formulations featuring biologics as API, namely therapeutic enzymes, while preserving their conformational stability, using spray drying (SD) as the core particle engineering technology.

To attain this, five main research questions were posed along the way. The answers to each one of them is briefly overviewed, herein.

- *Is it possible to spray dry a model therapeutic enzyme of a biologic while keeping its conformation and functional activity?*

Despite literature on spray drying of enzymes is available, data on therapeutic enzymes intended for inhalation is often absent or scattered. In addition, the great majority of the studies lacks the analysis to the enzyme conformational stability, without each, immunogenic events can take place. As such, a comprehensive study correlating and assessing the impact of spray drying process parameters and biopharmaceutical functional attributes felt required. A proof-of-concept study was thus conducted, assessing the impact of SD outlet temperature, atomization and feed flow rates on the conformational stability and enzymatic activity of Cu,Zn-SOD while embedded in a standard DPI formulation of trehalose:leucine. Cu,Zn-SOD:trehalose:leucine spray dried powders were successfully generated upon different processing conditions, displaying fine particle fractions of ≈60%, no loss of protein conformational stability and EAR ranging from 50–80%. Hence, SD proved to be suitable to prepare Cu,Zn-SOD based DPI powders within the considered working ranges, showcasing its potential as an alternative particle engineering technology.

- *Two-fluid versus Ultrasonic nozzles: Which one is the most suitable to produce biopharmaceutical dry powder inhaler formulations in a spray drying process?*

After the positive outcome observed from the proof-of-concept, focus was put on rendering spray drying even milder from a biologic standpoint. Atomization was one of the factors

pinpointed as a possible source of shear stress, so a different atomizing system, a high-frequency ultrasonic (US) nozzle with a low velocity profile when compared to conventional two-fluid (2F) nozzle, was considered. However, the US nozzle failed to generate spray dried powders within the orally inhalable size range with FPF below 17%, rendering it a poor candidate from an orally inhalation standpoint for biopharmaceutical delivery, when using the tested excipient system. In addition, the cooling system of the US nozzle as is, causes overheating at higher SD temperatures which could potentially impair the biopharmaceutical conformation. On the contrary and as expected, 2F nozzle displayed a PS within the inhalable size range with good FPF. Thus, 2F nozzle was the atomizing system selected to conduct the alternative spray drying set-up study and further work that followed. It is important to point out, though, that there were also some positive features to the US nozzle, such as a narrower PS span and maintenance of solid-state properties, that showcased its potential to target biopharmaceutical delivery through other alternative routes such as nasal where PS should be outside the inhalable size range to prevent deposition in the lungs.

- *Is it possible to increase recovery yields via spray drying set-up improvement?*

Besides the atomization system, an alternative spray drying set-up featuring a mesh gas distributor, a drying chamber with reduced length and surface area and direct powder discharge was tested as way to render the spray drying process more efficient, allowing to increase the relative amount of biopharmaceutical within the formulation with an acceptable yield.

By implementing a metallic mesh gas distributor and a drying chamber with reduced length and surface area, it was possible to reduce the minimum batch size of a conventional lab-scale spray dryer from ~5 g to 100 mg (50-fold) for the tested excipient system with yield > 50%. As such, an increase of the relative fraction of the biologic within the formulation from 0.1% to 5% (50-fold) becomes possible, while maintaining its nominal mass and within an acceptable yield. Ultimately, this allows more representative results of the process to be obtained in an economically viable way

- *Is it possible to use high-throughput screening platforms to expedite biopharmaceutical formulation prior to spray drying?*

Herein, high-throughput differential scanning fluorimetry (HT-DSF) was used to examine the thermal stability of three model enzymes – SOD, GOx and Cat - under a range of different conditions comprising pH, NaCl concentration, single and combo excipients (non-reducing sugars, hydrophobic and hydrophilic amino acids) to narrow down formulations prior to spray drying. The DSF protocol allowed the fine-tuning of pH and [NaCl] optimum values, despite the tested excipients did not show a strong stabilizing effect on the model enzymes. From these, L-lysine, more specifically, impacted the stability of the model enzymes indicating that its use should be avoided when formulating the target enzymes. To further narrow down the formulations to be tested in the spray drying, high-throughput isothermal denaturation fluorimetry (HT-ITDF) was explored as a complement.

- *How to integrate biopharmaceutical formulation and spray drying process development towards a dry powder inhaler of a biologic*

Based on the previous results, an integrated methodology to formulate and expedite spray dried DPI formulations featuring enzymes as model therapeutic biopharmaceutical APIs could be drawn. Three enzymes of increasing size and 3D structure complexity aiming to cover other classes of biopharmaceuticals were selected as models to develop and validate this strategy. On the other hand, four non-reducing sugars – Mannitol, Trehalose, Raffinose, Sucrose – two hydrophobic amino acids – L-leucine and L-alanine – and two hydrophilic amino acids – L-arginine and L-lysine were selected as excipients. HT-DSF proved to be a valuable technique to identify the temperature at which HT-ITDF screens should be performed and the T_{out} to be used. In addition, ITDF allowed to identify the most suitable excipients as all three enzymes displayed 65-85% of aerodynamic performance while keeping their functional oligomeric assembly (quaternary structural level) after SD with no significant presence of potentially non-functional and immunogenic HMM forms. This integrated methodology proved to be successful

in narrowing down 48 potential formulations (four sugars x four amino acids x three ratios) to only one for each enzyme, within few hours, while requiring µg range of sample amount. These features render this methodology a relevant and useful tool to reduce the gap between drug product development and the patient while doing so in an economically viable way. To strengthen the outcomes of this methodology, as part of future work, stability tests should be performed, and enzymatic activity results included. A representative study comparing the same dry powder inhaler formulations of other biologics in terms of powder and aerodynamic performance properties and biological function obtained by spray drying and freeze drying, while accounting for run time and economic burden analysis would also help to demonstrate the advantage of going for this particle engineering technology over a well-established and implemented one such as freeze-drying. Also, the extension of this methodology to other delivery routes and biologics displaying a folding structure would also be of benefit to widen the spectrum of therapeutic targets.